8-2-2018 1:00 PM

Characterization of interleukin (IL)-1β regulatory elements and chromatin conformation in macrophage activation

Woohyun Cho, *The University of Western Ontario*

Supervisor: Kim, Sung O., *The University of Western Ontario*

A thesis submitted in partial fulfillment of the requirements for the Master of Science degree in Microbiology and Immunology

Abstract

Rapid and potent expression of the pro-inflammatory cytokine, interleukin (IL)-1β, is a unique characteristic of macrophages. Enhancers are distal regulatory elements that promote gene expression in a cell-type specific manner. PU.1 is a lineage-determining transcription factor that regulates myeloid-specific genes by activating distal enhancers. To date, how macrophages rapidly and potently express IL-1β is not well understood. This study identifies a potential enhancer of IL-1β, and how PU.1 regulates its activity state in macrophages and non-myeloid cells. Enhancers are demarcated by unique histone modifications: high in H3K27Ac and H3K4me1, and low in H3K4me3. Based on the ChIP-seq data available from the ENCODE database, I found a genomic region located ~10 kbs upstream of the IL-1β TSS with these histone signatures. I hypothesize that the genomic region is an enhancer that regulates the expression of IL-1β mRNA in a PU.1-dependent manner in murine macrophages. A putative enhancer RNA (eRNA) was transcribed from the enhancer, and knock-down of the eRNAs with antisense oligonucleotides inhibited IL-1β production. Furthermore, through chromatin conformation capture (3C) analysis, enhancer-promoter interactions were detected in macrophages stimulated with the bacterial cell component lipopolysaccharide (LPS), confirming that the genomic element was an IL-1β enhancer. Overexpression of PU.1 in non-myeloid B16-BL6 cells induced IL-1β enhancer-promoter interaction, and promoted the expression of IL-1β mRNA and eRNAs upon LPS exposure. Enhancer knock-out by the CRISPR-Cas9 system reduced IL-1β expression in these cells. In summary, this study indicates that PU.1 alters the chromatin architecture which allows rapid and potent expression of IL-1β eRNAs and mRNA.

Keywords

Macrophages, Interleukin (IL)-1β, gene regulation, enhancers, enhancer RNAs, lineage-determining transcription factors, PU.1, chromatin architecture, chromatin conformation capture

Acknowledgments

First and foremost, I would like to express my thanks and gratitude to my supervisor, Dr. Sung Kim, for providing me the opportunity to be a member of the Kim lab, despite my lack of research experience in the field of immunology and epigenetics. Not only has Dr. Kim guided me academically with his expertise in the field, but has constantly encouraged me to strive for bigger goals in life.

Next, I would like to thank Dr. Soon-duck Ha who has trained me all the technical and analytical skills required to complete this thesis. Also, special thanks to present and past members of the Kim lab (Jeremy Wong, Justin Wang, Ori Solomon, Winnie Ong, Naomi Lewin) for all the entertaining and enjoyable discussions.

I would also like to thank my academic committee members, Dr. Rodney Dekoter and Dr. Joseph Mymryk, for their professional input, criticism, and words of encouragement. I would like to especially thank Dr. Dekoter and his lab for the collaboration.

Finally, I thank my family and friends for their unconditional love and support. To my dear parents and sister, thank you always for believing in me and motivating me to become a better person. To my friends, thank you all for always being by my side and sharing big moments in life.

Table of Contents

List of Tables

List of Figures

List of Appendices

CHAPTER 1

1 INTRODUCTION

1.1 Macrophage Differentiation

Macrophages are effector cells that have essential homeostatic and immunological roles in humans [1,2]. They are best known as sentinel innate immune cells that are responsible for detecting and killing foreign pathogens via phagocytosis [1-3]. Additionally, macrophages partake in generating rapid immune responses against invading microorganisms by producing various pro-inflammatory cytokines [4,5]. In addition to their immunological roles, their involvement in maintaining tissue homeostasis also needs recognition. Contribution to tissue and organ homeostasis is exemplified by their function as a janitorial cell that removes erythrocytes, cellular debris, and apoptotic and senescent cells [1]. Due to their anatomical location and physiological function, macrophages are often classified as a member of the mononuclear phagocytosis system (MPS) along with monocytes and dendritic cells [6]. Within this mononuclear phagocytic lineage, tissue-resident macrophages are considered as terminally differentiated cells that originate from circulating monocytes [2]. As circulating monocytes migrate into various tissues from the bloodstream, they undergo differentiation to become resident macrophages and perform specialized functions according to the microenvironment [2,5,7]. For example, osteoclasts are primarily involved in bone remodeling, and the absence of these specialized macrophages can result in osteoporosis and osteopetrosis [2,7]. Alveolar macrophages equipped with pattern recognition receptors (PRRs) and scavenger receptors on the surface are necessary for efficient clearance of microorganisms in the lung [7]. Thus, cells of the MPS, particularly macrophages, exhibit remarkable heterogeneity and plasticity [5,7]. Recently, the Immunological Genome (ImmGen) project (https://www.immgen.org/) has been launched to address whether or not the phenotypic and functional variance of tissue-resident macrophages are the result of unique gene expression profiles [8]. Analyses of the gene expression patterns of several populations of macrophages including peritoneal, splenic, and alveolar macrophages have shown that the expression levels of only a few selective genes, such as

MerTK, Toll-like receptor (TLR) 4, TLR7, TLR8, and TLR13, remained uniform across all populations [8]. These data indicated that the ability of macrophages to efficiently adapt to their surroundings and generate cell-type specific responses against external stimuli is a reflection of their variance in gene expression profiles.

1.1.1 Classically-activated vs. alternatively-activated macrophages

Macrophages express diverse classes of surface receptors such as PRRs, scavenger receptors, phosphatidyl serine receptors, integrins, and complement receptors that are required for their function [9]. Expression of such wide range of surface receptors allows macrophages to exhibit remarkable plasticity in nature. Based on their characteristics in producing inflammatory and immunoregulatory responses, a binary classification system is often used to distinguish macrophage activation states: classically-activated (M1) and alternatively-activated (M2) macrophages [1,5,10,11]. Microbial products such as lipopolysaccharide (LPS), and the inflammatory cytokines interferon (IFN)-γ, and tumor necrosis factor (TNF)-α induce macrophages to polarize toward M1 macrophages. M1 macrophages promote inflammation by secreting pro-inflammatory cytokines such as interleukin (IL)-1β, IL-6, and IL-23 and anti-microbial molecules such as reactive oxygen species (ROS) and nitrogen radicals [1,5,10]. In contrast, exposure of macrophages to IL-4, and IL-13 generates M2 macrophages that induce anti-inflammatory responses or have wound healing capabilities [1,5,10]. The contrasting characteristics of M1 and M2 macrophages are likely the result of unique gene expression profiles. Despite many genes that are co-upregulated or co-downregulated in macrophages of both activity states, there are multiple genes that are exclusively induced in one type of macrophages while suppressed in the other [11]. For example, it has been reported that N-formyl peptide receptor 2 (Fpr2) and cluster of differentiation 38 (CD38) are greatly enhanced in M1 macrophages [11]. Fpr2 is a G-protein coupled receptor that recognizes bacteria-derived N-formyl methionyl peptides, resulting in increased chemotaxis and ROS production by macrophages; whereas, CD38 is a glycoprotein that catalyzes the synthesis of key messengers of calcium signaling, cADP-ribose and ADP-ribose, from NAD^+ [11]. On the other hand, early growth response protein 2 (Egr2) is a gene that tends to be specifically upregulated in M2 macrophages [11]. Egr2 is a transcription factor (TF) that is closely

linked to cell proliferation, tumour suppression, and peripheral nerve myelination [12]. This particular TF also induces the generation of macrophage colony-stimulating factor (M-CSF) receptor, which is involved in the generation of anti-inflammatory macrophages [12,13].

1.1.2 Signaling pathway activated by LPS

LPS is a main constituent of the outer membrane of Gram-negative bacteria. LPS sledded from bacteria that enter the bloodstream of the host are detected by LPS-binding proteins (LBPs) [14,15]. LBP traffics LPS to CD14, which functions as a co-receptor that presents LPS monomers to the TLR4 and lymphocyte antigen 96 (MD2) complex [14,16,17]. Binding of phosphate and acyl groups of LPS to TLR4 and MD2, respectively, induces the dimerization of TLR4-MD2 complex that triggers intracellular signaling cascades through the toll/IL-1 receptor (TIR) domain [14]. TIR recruits one of the TIR containing adaptor proteins known as myeloid differentiation factor (MyD) 88, through interacting with another TIR containing adaptor protein, MyD88-adapter-like (Mal) [18]. Interaction between TLR4s and MyD88 initiates a cascade of signaling events that activates nuclear factor (NF)-κB [14]. At steady state, NF-κB is localized in the cytoplasm due to the cytosolic protein inhibitor κB (IκB) [19]. The signal transduction triggered by LPS causes degradation of IκB that leads to translocation of NF-κB to the nucleus and initiation of transcription [14]. In addition, TLR4 activates the MyD88-independent pathway, which is mediated by another TIR motif containing adaptors, known as TIR domain-containing adapter inducing interferon (TRIF) and TRIF-related adapter molecule (TRAM). The signaling cascade activated by these adaptors leads to the activation of NF-κB, IFN regulatory factor (IRF) 3 and IRF7 [17,20]. IRF3 and 7 promote the synthesis of IFN-α and -β that bind to their respective cognate receptors on the macrophages [20]. Activation of IFN receptors triggers the Janus kinases (JAKs)/ Signal transducer and activator of transcription (STAT) signaling cascade that induces expression of genes involved in anti-viral responses and caspase-11 [20,21]. Caspase-11 mediates NLRP3-induced cleavage of pro-caspase-1 into caspase-1 [21]. Caspase-1 is also known as the IL-1β-converting enzyme that converts biologically inactive pro-IL-1β to its active form [22].

1.2 IL-1β

The IL-1 family of cytokines are crucial elements of the innate immune system that can either initiate or suppress inflammation [22]. It comprises 11 members, which include IL-1α, -1β, -1Ra, -18, -1H4, -1H2, -1ε, -1HY2, -33, FIL1δ, and FIL1ε, with diverse roles in immune responses. For example, IL-1α and -1β are potent pro-inflammatory cytokines; whereas IL-1Ra, FIL1δ, and IL-1H4 have anti-inflammatory roles [22,23]. Amongst the IL-1 cytokines, IL-1β has been studied most thoroughly, and many reports highlight its role in various cellular processes such as cell differentiation, autophagy and apoptosis, and immune activation through T lymphocytes [24-27]. Despite the importance of IL-1β in the innate immune system, failure to control the intensity and duration of its expression can cause the development of autoinflammatory diseases, as it is closely associated with local and systemic inflammation [22,28]. Autoinflammatory diseases are a class of clinical disorders that arise due to dysregulation of the innate immune system, often resulting in chronic inflammation [22,29]. Most notably, familial cold autoinflammatory syndrome (FCAS), gout, type 2 diabetes, and Muckle-Wells syndrome are examples of IL-1β-associated autoinflammatory diseases [22,29]. Thus, IL-1β serves as a good therapeutic target to treat atherosclerosis and type 2 diabetes, as well as other inflammatory diseases [30-32].

1.3 Gene Regulation

1.3.1 Regulatory Elements

It is well established that each cell has a unique gene expression profile that determines its phenotype and allows to perform biological functions. Also the expression of genes must be tightly controlled, as dysregulation can give rise to various diseases. There are multiple regulatory elements that corporately regulate transcription. For example, core promoters are generally defined as nucleosome-depleted and DNaseI hypersensitive regions that encompass multiple elements such as the transcription start site (TSS) and the TATA box [33,34]. These proximal regulatory entities serve as the platform for the basal transcriptional machinery and the designated site of pre-initiation complex assembly [33,34]. Ultimately, promoters function in concert with distal regulatory

elements that either suppress or activate transcription of the target gene [35]. A large portion of mammalian genome is non-coding regions that were once considered as 'junk sequences' [36]. However, these non-coding regions contain functional distal regulatory elements which are now regarded as key players of gene regulation. Enhancers are distal regulatory elements that positively regulate and enhance transcription of cognate genes in a spatiotemporal manner [33]. Similar to promoters, enhancers also recruit the transcriptional machinery and produce transcripts commonly referred to as enhancer RNAs (eRNAs) [37]. In addition, silencers and insulators are regulatory elements that serve as negative regulators of gene expression [33]. Within the genome, silencers, which are docking sites for repressors, can be positioned either away from or within proximal promoters [33]. Insulators also serve as negative regulatory elements that are renowned for their two functions: barrier function (prevent decompaction of chromatin) and enhancer blocking [36,38]. Notably, insulators can block the activity of enhancers by preventing the formation of inter- and intra-chromosomal interaction between enhancers and irrelevant genes [36]. Altogether, the interplay of positive and negative regulatory elements as well as various transcription factors dictate the gene expression profile of a cell.

1.3.2 Epigenetics

Gene regulation is not limited to the activity of regulatory elements; but also controlled by epigenetics, which is defined as inheritable regulation of gene expression without changes in the DNA sequence [39]. Amongst many epigenetic processes, DNA methylation is one of the most thoroughly studied [39]. Generally, DNA methylation is known to have a robust inverse relationship with chromatin accessibility [40]. Methylation of DNA is mediated by DNA methyltransferases (DNMTs), a family of proteins that transfers methyl groups to cytosine in CpG dinucleotides (cytosine directly linked to guanosine via phosphodiester bond) in mammals [39,41]. Specifically, methyl groups are added to the C5 position of cytosine, forming 5-methylcytosine (5mC) [39]. It is widely accepted that 5mC is a methylation marker that has a repressive effect on gene expression [41,42]. For example, Hashimoto *et* al. demonstrated that chemical treatment (IL-1β or TNF-α ± oncostatin M or 5-aza-deoxycytidine) of human articular

chondrocytes induced the production of IL-1β mRNA and protein [43]. Intriguingly, they observed a significant reduction in the methylation of CpG sites in the promoter of IL-1β [43], suggesting that the methylation status of the gene is an epigenetic marker that regulates its production. Likewise, the methylation status of enhancers has also been shown to contribute in gene regulation; and ultimately be involved in disease progression and cancer development [44]. Monomethylation of histone (H) 3 lysine (K) 4 (H3K4me1), a unique chromatin signature of enhancers, is associated with DNA hypermethylation [45]. In addition, DNA methylation negatively correlates with acetylation of H3K27 (H3K27Ac), which demarcates active enhancers, [45]. Specifically, hypermethylation of DNA results in diminished levels of H3K27Ac at enhancers [45, 46], and essentially reduces the activity of these distal regulatory elements [47]. There are currently two mechanisms suggested for DNA demethylation. In passive DNA demethylation, loss of methyl groups occurs in cell replication-dependent manner, and daughter cells inherit less methylated DNA due to inhibition of DNMTs [41,48,49,50]. Active DNA demethylation occurs independently of cell replication and is a more rapid process that involves direct removal of the methyl groups. Initially, ten-eleven translocation (TET) protein converts 5mC to 5-hydroxymethylcytosine (5hmC), an intermediate form of oxidized 5mC [49]. 5hmC can be further oxidized into metabolites such as 5-formylcytosine (5fC) and 5-carboxylcytosine (5caC) by TET proteins, in which the resulting products are fixed via base excision repair facilitated by thymine DNA glycosylase [48,51,52].

Post-translational modification (PTM) of histones is another notable epigenetic mechanism that is essential for gene regulation [44]. Histones are positively charged nuclear proteins that closely associate with negatively charged DNA to form chromatin [53]. Initially, 147 base pairs of DNA are wrapped around histone octamers that consist of two H2A-H2B dimers and one H3-H4 tetramer [53]. Supercoiling of DNA around the histone octamer forms the basic unit of DNA compaction, nucleosomes [53,54]. The N-termini of H2B, H3, H4, and C-terminus of H2A, commonly referred to as histone tails, tend to protrude from nucleosomes, and are prone to various PTMs such as methylation, acetylation, phosphorylation, ubiquitination, SUMOylation, ADP ribosylation, and deamination [54]. Formation of nucleosomes for the purpose of DNA compaction is

undoubtedly important; however, such tight packaging of the DNA can limit accessibility by various TFs and interfere with proper gene expression [55]. Thus, remodeling of nucleosomes mediated by PTMs such as methylation, acetylation, and phosphorylation is necessary to overcome such structural complications [55].

Histone tails are enriched in positively charged K and arginine (R), which are subject to methylation [55,56]. Histone methylation involves the transfer of methyl groups from S-adenosylmethionine to the ε-amino group of K and ϖ-guanidino group of R by lysine methyltransferases and arginine methyltransferases, respectively [56]. Although both amino acids can be methylated, K4, 9, 27, and 36 of H3 and K20 of H4 are considered as the most common substrates for methylation [57]. Lysine residues can be methylated to varying degrees (mono-, di-, tri-), which affect the hydrophobic and steric properties of the amino acid [58]. The three degrees of methylation marks at specific K residues serve as docking sites for various effector proteins, and can dictate the role of lysines as either activators or repressors of gene expression [58]. For example, monomethylation of H3K4 H3K4, H3K36, and H3K79 are associated with transcriptional activation, whereas higher degrees of methylation at H3K9, H3K27, and H4K20 are involved in repressive gene expression [59]. Interestingly, methylated lysine residues may have further contributions in gene regulation by serving as specific markers of proximal and distal regulatory elements. For example, combination of H3K4me1 and H3K4me3 are characteristics that are considered when defining proximal promoters and distal enhancers, as unique ratios of these epigenetic signatures are conserved at these regulatory elements across the genome [47,60,61]. High and low levels of H3K4me1 and H3K4me3 ($H3K4me1^{hi}$, $H3K4me3^{low}$) are recruited at distal enhancers while the inverse ratio ($H3K4me1^{low}$, $H3K4me3^{hi}$) of these histone modifications are observed at proximal promoters [60,61].

Histone acetylation is a reversible PTM that correlates with active gene expression by promoting the formation of euchromatin and increasing DNA accessibility [62]. Unlike histone methylation, acetylation of K residues neutralize the charge of the histone tails [63]. Acetylation-mediated loss of charge can disrupt the interaction between histones and DNA, essentially causing the chromatin to take on an ‘open’ conformation [44,63]. The transfer of acetyl group from acetyl Coenzyme A (acetyl-CoA) to the ε-amino group

of K is catalyzed by histone acetyltransferases (HATs) [63]. HATs are multisubunit protein complexes that can be classified as either cytoplasmic proteins that acetylate newly synthesized histones prior to nuclear translocation or nuclear proteins that promotes addition of acetyl groups to histone tails [63]. There are five subclasses of HATs: general control nonderepressible 5 (Gcn5)-related acetyltransferases (GNATs); MOZ, Ybf2/Sas3, Sas2, Tip60 (MYST)-related HATs; p300/CREB-binding protein (CBP) HATs; general transcription factor HATs (TFIID subunit TAF250); nuclear hormone-related (steroid receptor coactivator 1/3) HATs [64]. Although the HAT domain responsible for interacting with CoA is conserved in all subclasses, substrate specificity of HATs still varies between and within subclasses, as each HAT complex comprises distinct combinations of domains and subunits [64]. For example, GNATs that contain Gcn5 alone preferentially acetylates H3K14, while the accessory protein, Ada, modifies H3K9, 14, and 18 [64]. Similar to histone methylation marks, acetylation of specific K residues can also be utilized as markers of regulatory elements. p300/CBP HATs are homologous proteins that serve as transcriptional co-activators [65]. These histone modifiers are often recruited to enhancers, and can acetylate all four types of histones [65]. Specifically, previous studies reported that p300/CBP are capable of catalyzing the acetylation of H3K27 (H3K27Ac), a unique marker of active enhancers [66,67].

The level of histone acetylation is maintained by the interplay of HATs and histone deacetylases (HDACs) [63]. HDACs are responsible for the removal of acetyl group from the K residues, resulting in hypoacetylation of histone tails that strengthens the interaction between histones and DNA [63]. HDACs can be classified into either the classical (Zn^{2+}-dependent) or SIR2 (silent information regulator 2; NAD^{+}-dependent) families [63]. The classical HDACs are subdivided into Class I (HDAC 1, 2, 3, 8), Class II (HDAC 4-7, 9, 10), and Class IV (HDAC 10) [63]. These metal-dependent deacetylases have activation sites that require Zn^{2+} as the cofactor [63]. Class I HDACs are primarily localized and active in the nucleus, whereas most class II HDACs exist within the cytoplasm [63,68]. Although HDAC10 (class IV) is the least studied amongst all HDACs, the current understanding is that it has roles in both nuclear and cytoplasmic compartments [68]. There are 7 Sir2 family members (SIRT1-7) that belong in class III of deacetylases [68]. Sir2 HDAC-mediated deacetylation of K residues involves the

transfer ADP-ribose from NAD^+ to acetyllysine [68]. This particular class of HDACs are distributed throughout the entire cell and are localized in the nucleus, cytoplasm, as well as mitochondria [68]. In general, HDACs do not repress gene expression alone, but rather work in concert with other repressor proteins like DNA methyltransferases [63].

1.3.3 Chromatin Organization

All cellular activities that govern physiological and homeostatic events in the body are dictated by the genetic information stored in the DNA. The entire human genome, which can span 2 meters in length, must be tightly organized in order to be packed in the nucleus of a single cell (Fig. 1.1). The formation of nucleosomes is the initial step of DNA compaction that reduces the length of the genome by approximately 7-fold [54]. Then, the chromosomes are segregated into distinct chromosome territories, which allow intra-chromosomal interactions to form while communication between chromosomes becomes less preferred [54,69]. Within the chromosome territories, the chromosomes are partitioned into either open ("A") or closed ("B") regions [54]. The open compartment is occupied by DNA segments that are enriched in genes, regulatory elements, and various features that mark active transcription, whereas closed compartments consist of transcriptionally repressive genomic regions [54]. The DNA in A and B compartments are then further segregated into topologically associating domains (TADs), which organize co-expressed genes into distinct regions [54,70]. Despite being positioned in different chromosomes, genes within TADs can be subjected to transcriptional activation mediated by *trans*-acting enhancers that exist in the same TADs via intermolecular interactions [54]. The DNA segments in TADs tend to be on average ~800 kb in length, and these genomic entities are retained throughout cell differentiation [70-72]. Interestingly, the nuclear positions of these TADs tend to be conserved across species including humans, mouse, and fruit flies [71]. Finally, TADs can be partitioned into sub-TADs, in which these subdomains tend to vary between cell types [54].

Figure 1.1. Packaging of the genome in the nucleus occurs in a hierarchical manner. At the top of the hierarchy, chromosomes are initially organized into distinct regions in the nuclear space (chromosome territories – different coloured regions in the nucleus), where the genome is further partitioned into transcriptionally active (A) or repressive (B) compartments. Within each compartment, TADs (red circular region) and sub-TADs (small green circular regions within TADs) are formed, allowing chromatin looping-mediated interaction between regulatory elements such as enhancers, silencers, and insulators with the promoters of target genes to occur.

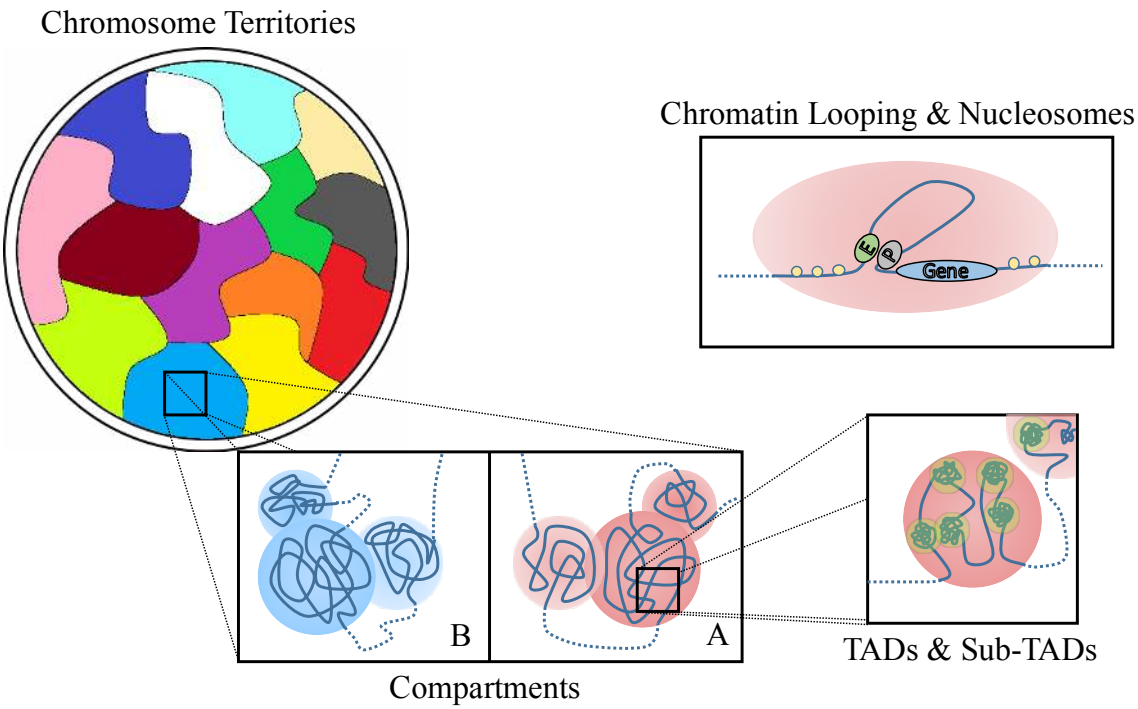
Chromosome Territories
Chromatin Looping & Nucleosomes
Gene
B
A
Compartments
TADs & Sub-TADs

1.4 Distal regulatory element: Enhancers

Enhancers are *cis*- and *trans*-acting regulatory elements that engage with promoters over long distances to promote gene transcription in a cell-type specific manner [42,73,74]. As above-mentioned, unique gene expression profiles are determined by combinatory activities of different regulatory elements [75]. Recent studies showed that more than 1 million putative enhancers, which greatly exceeds the number of coding genes, have been identified in the human genome [76,77]. These enhancers are hypersensitive to DNases, indicating euchromatin status of their chromatin landscapes. The lineage-determining transcription factors (LDTFs) are crucial proteins that bind specific motifs within enhancers and promote a shift in chromatin architecture from heterochromatin to euchromatin via ATP-dependent nucleosome remodelers [42,73,74,76]. Subsequently, co-activators, p300/CBP, are recruited to the readily accessible enhancers [42,74]. These histone modifiers induce epigenetic reprogramming of nucleosomes that flank the enhancer domains [73]. When enhancers are activated, TFs and RNA polymerase II (RNAPII) are recruited to the enhancers, resulting in dynamic transcription of eRNAs [42,73,77-81]. However, the mechanisms of how enhancers promote gene transcription are not fully understood. It is speculated that enhancers promote transcription by recruiting the pre-initiation complex and releasing RNAPII from the promoter to move along the DNA [74].

1.4.1 Epigenetic signatures of enhancers

DNA segments with chromatin signatures H3K4me1^{hi} and H3K4me3^{low} were originally defined as enhancers, whereas higher levels of H3K4me3 compared to H3K4me1 were recruited at active promoters [42,60,82]. Dissimilar to the invariant binding patterns of an insulator protein CCCTC-binding factor (CTCF), the locations of H3K4me1-marked enhancers are different across many cell types [60]. Additionally, cells also display highly distinct distribution patterns of DNase-hypersensitive and p300-binding sites [60,83]. These results indicate that the association of nucleosome-depleted genomic regions with H3K4me1 and p300 is a marker for cell-type specific enhancers. It was also shown that H3K4me1 is deposited at potential enhancers prior to nucleosomal depletion and enrichment of H3K27Ac [84]. In some cases, H3K4me1 remains bound to enhancers

following the dissociation of H3K27Ac, a unique histone modification of active enhancers [85]. The difference in the dynamics of these histone modifications suggest that H3K4me1 is an epigenetic marker of both active and poised enhancers [60,86].

As previously mentioned, co-activators like p300 and CBP are HATs that are recruited to enhancers and acetylate H3K27 [42,66,67,87]. Further studies confirmed that H3K27Ac demarcates active enhancers [82,85]. HAT-mediated acetylation of H3K27 plays a central role in promoting the release of RNAPII. Upon acetylation, bromodomain-containing protein (Brd) 4, a member of the bromodomain and extra terminal domain (BET) family of proteins, binds to acetylated K residues of histone H3 and H4 [88,89]. The association of Brd4 with acetylated histones is followed by the recruitment of the positive transcription elongation factor (P-TEFb) and the Mediator complex [90]. Brd4 converts P-TEFb into an active form that leads to the phosphorylation of negative elongation factor (NELF) complex and DRB sensitivity inducing factor (DSIF), which directly interact with RNAPII to hold the polymerase at the promoter region [91,92]. Furthermore, P-TEFb also phosphorylates Serine 2 (Ser2) of carboxy terminal domain (CTD) of RNAPII, a modification that indicates the transition of a polymerase from the pause to the elongation phase [91,93]. Kaikkonen *et al.* demonstrated this phenomenon in macrophage enhancers as elevated levels of Ser2P RNAPII are observed near the nucleosome free regions post stimulation with the TLR4 agonist Kdo2-Lipid A [91]. Therefore, a method in identifying active enhancers is through examining the H3K4me1, H3Kme3, and H3K27Ac markers.

1.4.2 Lineage-determining transcription factors of macrophage enhancers

The plastic nature of macrophages that allows the cells to achieve diverse functional states in response to various microenvironments is mediated by enhancers, which promote the expression of specific genes [94]. Amongst several hematopoietic TFs, PU.1 plays a central role in the development of macrophages and B cells [95]. PU.1 is a member of the Ets family of proteins that specifically recognize and bind to purine-rich motifs of DNA [96,97]. PU.1 has four domains with distinct characteristics and functions [98,99]. The acidic domain and the adjacent glutamine (Gln)-rich domain make up the N-

terminus half of PU.1. These domains are essential for PU.1's capacity to transactivate genes [98,100]. The C-terminus consists of the DNA-binding domain which is homologous across the entire Ets family of proteins [98]. The PEST domain spans the middle of PU.1 and is necessary for interaction with other proteins like PU.1-interacting partner (Pip) in B cells [98,101]. The role of PU.1 in rendering B cell- or macrophage-lineage commitment is dependent on the intracellular concentration of PU.1, where a high level of PU.1 is required for macrophage differentiation [102]. It was shown that PU.1 drives progenitor cells toward the macrophage lineage by selectively binding to macrophage-specific enhancers [103]. Furthermore, studies discovered that PU.1 bound H3K4me1-marked genomic regions in macrophages, whereas the binding pattern of PU.1 differed in B cells of various developmental stage [103,104]. PU.1-bound regions are also occupied by p300, fulfilling a criterion that is often used for identifying enhancers [103]. Thus, PU.1 shapes cellular identity of macrophages via selectively binding to enhancers that promote expression of macrophage-specific genes. However, gene expression profiles of macrophages are not dictated by PU.1 alone, but rather in concert with other TFs including CCAAT/enhancer binding protein (C/EBP) family of proteins and AP-1 [104-106]. It has been shown that PU.1-bound enhancer regions also contained binding motifs for C/EBP and AP-1, resulting in co-localization of these TFs with PU.1 [104,105]. Moreover, despite the importance of graded concentration of PU.1 in macrophage differentiation, the ratio of PU.1 to C/EBPα concentrations should also be taken into account, as high levels of C/EBPα can drive granulocyte and neutrophil development [107,108]. Therefore, macrophage differentiation is not determined solely by PU.1 but also its association and cooperation with other TFs.

1.4.3 eRNAs

Transcripts produced from active enhancers, eRNAs, are another considerable factor of gene regulation. eRNAs are a subclass of non-coding RNAs that are uni- or bi-directionally transcribed by RNAPII and other components of the transcriptional initiation complex, which have been recruited to readily accessible enhancers [42]. Dissimilar to mRNA, majority of eRNAs do not acquire a poly(A) tail; hence, half-life of eRNAs tends to be shorter than that of mRNAs [42,73]. Regardless, rapid and dynamic

production of eRNAs by extracellular stimuli prompted investigators to examine the functional importance of eRNAs in gene regulation. Li *et al.* showed that knock-down of eRNAs with small interfering (si)RNAs and LNAs resulted in diminished levels of *TFF1, FOXC1, and CA12* in 17β oestradiol-exposed MCF-7 cells [80]. Although the functional importance of eRNAs has been demonstrated, the mechanisms by which eRNAs regulate gene expression remain elusive. A potential mechanism of eRNA is its ability to promote RNAPII release from its pause phase by interacting with the NELF-DSIF complex [109]. NELF-DSIF complexes associate with nascent RNA through RNA recognition motif (RRM) in NELF, which accounts for the repressive function of the protein [109]. *Schaukowitch et al.* demonstrated that NELF is readily released from *Arc* and *Gadd45b* promoters in depolarized neurons; however, knock-down of eRNAs transcribed from enhancers located ~7 kilobases (kbs) upstream and downstream of *Arc* and *Gadd45b*, respectively, inhibited NELF dissociation from the promoters [109]. Subsequently, they also showed that NELF-E, a subunit of NELF that carries the RRM sequence, directly bound to *Arc* and *Gadd45b* eRNAs through pull-down assay [109]. This suggested that eRNAs compete with nascent RNA to interact with NELF via RRM, causing it to dissociate from RNAPII [109]. Moreover, another mechanism by which eRNAs affect the transcriptional output is through the recruitment of the Mediator complex at the promoter region of target genes [110,111]. It was shown that eRNAs physically interact with the Mediator complex subunit (MED) 1 and MED12 subunits of the Mediator complex, and siRNA-mediated knock-down of eRNAs directly reduced the co-localization of the Mediator and RNAPII at the respective promoter region [110,111]. Furthermore, as enhancer-promoter interactions have been detected in many studies, the functional role of eRNAs in facilitating chromatin looping between enhancers and promoters was examined. Studies have shown that the frequency of spatial interactions between enhancers and promoters is significantly reduced upon depletion of eRNAs [80,110,111]. In line with eRNA-mediated formation of enhancer-promoter interactions, the Mediator complex behaves in a similar manner, as knock-down of MED1 and MED12 subunits inhibits chromatin looping between regulatory elements [110].

1.4.4 Physical association of enhancers and promoters

Enhancers are remotely positioned from their cognate genes. The distance between these genomic elements can extend as far as 2-3 Mbs. In order for enhancers to positively regulate gene expression, they must be in proximity with their target promoters [42,74,112]. Chromatin looping is a proposed model describing the interaction between distal regulatory elements and promoters in the nuclear space by extruding the intervening DNA [42,74]. In addition to eRNAs and the Mediator complex discussed above, major structural remodelers of the genome include CTCF and cohesin [113-116]. CTCF is an insulator protein that is largely deposited at borders of TADs [117]. Not only does this protein segregate active genetic segments from the inactive by sorting them into different compartments, it also has the ability to either activate or repress gene expression via enhancer blocking activities [117]. Notably, CTCF is a strong determinant of enhancer-promoter interactions along with cohesin, a protein complex structured like a ring [114,116,117]. Cohesin is primarily responsible for sister chromatid cohesion during DNA replication; however, it has been reported that cohesin associates with CTCF to remodel the chromatin landscape, and depletion of either protein attenuates the interaction frequency between enhancers and promoters [113,114,118,119]. In addition, cohesin is also known to co-localize with the Mediator complex [119]. Collectively, these findings infer that the interplay of various chromatin remodelers is crucial for the dynamic organization of the genome.

1.4.5 Detection of enhancer-promoter interactions via Chromosome Conformation Capture (3C) analysis

The most widely applied technology to analyze the genome architecture is 3C and its derivative high-throughput experiments such as 4C (circularized 3C-seq), 5C (3C-carbon copy) and Hi-C [120]. These techniques are favoured over other genome visualization techniques like light microscopy due to its sensitivity [121]. Additionally, another noteworthy advantage of 3C is that it can quantitate the interaction frequency of DNA segments in the nuclear space. Fig. 1.2 outlines the overall procedure of 3C analysis, which has been employed throughout this study to examine the intra-chromosomal interaction of the proposed enhancer and the IL-1β promoter. Initially, DNA regions in

proximity are crosslinked via formaldehyde fixation [120-123]. Following the isolation of the nuclei, fixed chromatins are exposed to restriction enzymes [120-123]. The choice of restriction enzyme should be carefully considered to obtain proper sizes of DNA fragments and avoid cleavage of the gene areas of interest [122]. Subsequently, ligation of digested DNAs is performed with preference of ligation between DNAs in close proximity [120-123]. Finally, the ligated products are de-crosslinked and purified to generate a collection of adjoined DNA segments commonly referred to as 3C library [122]. Quantification of 3C library is performed via real-time quantitative (q)PCR assays. Since a vast number of different combinations of ligated DNAs is generated in a given 3C library, a specific ligation event can be very rare and occur 1/2000 to 1/20000 of the time [122]. Therefore, utilization of a sequence specific double-dye qPCR methods, such as TaqMan probes, rather than dye-based methods (SYBR Green), will increases the specificity of 3C analysis [122].

Figure 1.2. Workflow of 3C analysis. The interacting DNA regions, particularly regulatory elements such as the promoter (orange box) and the enhancer (blue box) of a gene, are positioned in close proximity in the nuclear space via chromatin looping. The regulatory elements are crosslinked by formaldehyde (small red circles), followed by restriction enzyme digestion (black arrows) to cleave and remove any intervening DNA. The restriction enzyme-mediated cleavage of the DNA leaves either overhangs or blunt ends (represented as different coloured boxes at the ends of each DNA fragment), which are then re-ligated. Ligation of the crosslinked DNA regions generates target fragments in opposite orientations that can be amplified via qPCR.

Chromatin looping-mediated interaction of enhancer and promoter	
Formaldehyde crosslinking	
Restriction enzyme digest	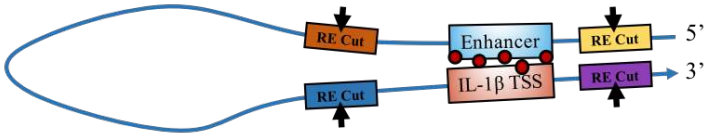
Intramolecular ligation	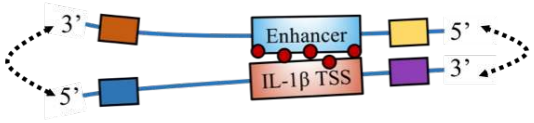
Taqman qPCR	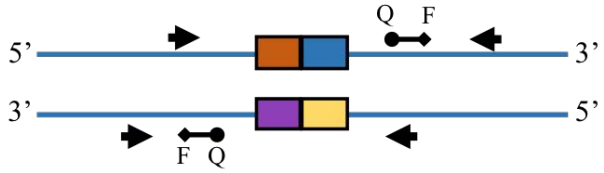

1.5 Rationale, Hypothesis, and Research Aims

Enhancers are genomic regulatory elements that determine the characteristics of each cell type. PU.1 is a LDTF that plays a key role in macrophage generation and differentiation by activating enhancers. Enhancers are often demarcated by unique histone modifications: H3K27Ac^{hi}, H3K4me1^{hi}, H3K4me3^{low}. Based on these histone signatures available from the Encyclopedia of DNA Elements (ENCODE: https://genome.ucsc.edu/encode/) database, I identified a genomic region located ~10 kbs upstream of the IL-1β TSS as a potential enhancer (Fig. 3.1). I hypothesize that the genomic region is an enhancer that regulates the expression of IL-1β mRNA in a PU.1-dependent manner in murine macrophages. Based on this hypothesis, I have proposed the following research aims:

Aim I – Identifying the active enhancer of IL-1β in murine macrophages

Aim II – Examining the role of PU.1 in the enhancer-promoter regulatory network of IL-1β

Aim III – Elucidating the role of PU.1 domains in the IL-1β regulatory network

Chapter 2

2 Materials and Methods

2.1 Reagents

Dulbecco's modified eagle medium (DMEM) and RPMI-1640 medium used to culture RAW264.7 macrophages and B16-BL6 melanoma cells, respectively, were purchased from Sigma Aldrich. Transfection reagents, Lipofectamine RNAiMAX and Polyjet, were obtained from Invitrogen and SignaGen Laboratories, respectively. PowerUP™ SYBR® Green Master Mix was from Applied Biosystems while dual-labeled Taqman probe (dye: JOE) and Hot Start Taq DNA polymerase were from Integrated DNA Technologies and New England Biolabs. Scrambled and eRNA-specific ASO were obtained from Exiqon. The primers used for qPCR assays were purchased from Eurofins genomics. QX200™ ddPCR™ EvaGreen supermix and droplet generation oil for EvaGreen were obtained from Bio Rad. The reagents utilized for 3C analysis include: Formaldehyde (VWR), DpnII, T4 DNA Ligase, and T4 DNA Ligase Buffer were from New England Biolabs, RNase (Qiagen), Proteinase K and Phenol:Chloroform:Isoamyl Alcohol (PCI) were purchased from Invitrogen.

2.2 Cell culture and Transfection

RAW264.7 macrophages were cultured in DMEM (high glucose) that contains 8% fetal bovine serum (Sigma – Aldrich), 10 mM MEM non-essential amino acids, 1 mM sodium pyruvate, 100 IU/mL penicillin, and 100 μg/mL streptomycin. B16-BL6 melanoma cells were cultured in RPMI-1640 medium that contains 10% fetal bovine serum (Sigma – Aldrich), 10 mM MEM non-essential amino acids, 1 mM sodium pyruvate, 100 IU/mL penicillin, and 100 μg/mL streptomycin. Throughout transfection of B16-BL6 cells with the transfection reagent, Polyjet, the cells were cultured in DMEM (high glucose, 10% FBS) containing all of the aforementioned components. All cells were cultured in an incubator with an optimal temperature of 37^{o}C and CO_2 level of 5%.

2.2.1 Transfection of RAW264.7 macrophages with ASO

In order to transfect RAW264.7 macrophages with ASO (sequence in Table 2.1), Lipofectamine RNAiMAX was used according to the manufacturer's instructions. Frozen (-80^{o}C) RAW264.7 macrophages were thawed and cultured for two days prior to transfection. On the day of transfection, 7.0 x 10^5 cells were plated on 6-well plates and stabilized for three hours. Briefly, 250 pmole of scrambled and eRNA-specific ASO were mixed with Opti-MEM (reduced serum medium – Gibco). Simultaneously, Lipofectamine RNAiMAX was mixed with Opti-MEM in a different vial. The two components were mixed and incubated for 15 mins. ASO-Lipofectamine complexes were then thoroughly deposited into respective wells, and the cells were transfected for 22 hours. Upon completion of transfection, the cells were divided into non-LPS vs LPS groups, and re-seeded on 6-well plates. The cells were then stimulated with LPS (100 ng/mL) for 90 mins.

2.2.2 Transfection of B16-BL6 cells

2.2.2.1 Reprogramming of melanoma cells with LDTFs

B16-BL6 cells cultured for two days before being transfected. Reprogramming of B16-BL6 cells initially requires transfection of the cells with LDTFs. Polyjet was employed to transfect B16-BL6 cells according to the manufacturer's instructions. 5.0 x 10^5 B16-BL6 melanoma cells were re-plated on 6-well plates and cultured in RPMI-1640 medium one day prior to transfection. On the following day, the RPMI medium was replaced with high glucose DMEM. 0.7 μg of control pcDNA3, pcDNA3-PU.1 and/or pBR322-C/EBPα plasmids, which were generously donated by Dr. Dekoter's lab (UWO), were thoroughly mixed with the Polyjet media (serum-free DMEM). In another vial containing Polyjet media, Polyjet was added and carefully mixed. The plasmid and Polyjet containing solutions were carefully mixed and incubated for 15 mins to form plasmid-Polyjet complexes. The complexes were then added into each well and incubated for 24 hours. After five hours of transfection, extra media was added into each well to lower cytotoxicity. For eRNA and IL-1β mRNA analysis, the transfected cells were divided into non-LPS vs LPS groups, re-plated on 6-well plates, and incubated in RPMI-1640 medium

for another 24 hours. The LPS group was then stimulated with 100 ng/mL of LPS for 6 hours.

2.2.2.2 Introduction of ASO

For the eRNA knock-down study, the melanoma cells initially transfected with LDTFs (post 24 hours) were divided into scrambled vs eRNA-specific ASO groups and re-plated on 6-well plates. On the next day (48 hours post transfection), identical protocol for transfection with LDTFs was performed to transfect the cells with 250 pmole of either scrambled or eRNA-specific ASO for 22 hours. Once the transfection was done, the melanoma cells were exposed to LPS (100 ng/mL) for 6 hours.

2.3 RT-qPCR

The cells were harvested upon completion of LPS stimulation for the indicated time points. 250 μL of TRIzol was used to extract the total cellular RNA from the harvested cells. cDNA was prepared in 20 μL reaction mixtures containing 1 μg of the isolated RNA, dNTPs, poly-N6 (random) primers, and Moloney murine leukemia virus reverse transcriptase. The following conditions were used for synthesis of cDNA: 65^{o}C for 5 mins (predenaturation),25^{o}C for 10 mins (extension), 42^{o}C for 1 hour (cDNA synthesis), 90^{o}C (termination). Subsequently, qPCR assays were performed with 10 μL qPCR reaction mixtures that consisted of 1 μL of cDNA, PowerUP^{TM} SYBR® Green Master Mix (1X), forward and reverse primers (500 nM), and distilled water. The following conditions were used for qPCR analyses: 50^{o}C for 2 mins, 95^{o}C for 2 mins, 40 cycles of 95^{o}C for 15 secs/ 58 - 60^{o}C for 30 secs/72^{o}C for 20 secs/83^{o}C for 15 secs. The Rotor-Gene 6 software was used to generate Ct values and analyze melting curves. Expression levels of IL-1β mRNA and eRNAs were normalized to the housekeeping gene, GAPDH, and quantified via ΔΔCt analysis. The sequences of GAPDH mRNA, IL-1β mRNA, and eRNAs are listed in Table 2.1. The amplicon size of the qPCR products was examined by gel electrophoresis.

2.4 Droplet Digital PCR

cDNA synthesized via RT-PCR was used to measure the absolute quantities of eRNAs. Reaction mixtures and oil droplets were generated with QX200™ ddPCR™ EvaGreen supermix and droplet generation oil for EvaGreen, respectively, according to manufacturer's instructions. Initially, 25 µL reaction mixtures comprised of 1.25 µL of cDNA, the EvaGreen supermix (1X), eRNA primer sets (100 nM), and water for molecular biology (EMD Millipore) were prepared. The prepared reaction mixture and the droplet generation oil were transferred into the respective wells of a DG8 cartridge. The cartridge was loaded in the QX200 droplet generator, and the generated oil droplets (number varies between 15,000 – 20,000 droplets) were then transferred onto a ddPCR 96-well plate, which was enclosed with heat-sealing aluminum foil. PCR was subsequently carried out. The following conditions were used for PCR: 95^{o}C for 5 mins (enzyme activation), 40 cycles of 95^{o}C for 30 secs (denaturation)/ 58^{o}C for 1 min (annealing/extension), 4^{o}C for 5 mins/90^{o}C for 5 mins (signal stabilization). Once PCR was finished, the 96-well plate was then loaded in the QX200 droplet reader. QuantaLife was used to analyze fluorescence measurements.

2.5 Culturing and isolating subpopulations of CRISPR cells

B16-BL6 melanoma cells were cultured for two days prior to transfection with CRISPR editing plasmids. Polyjet was the transfection reagent used, and the same protocol as described in section 2.2.2.1 was employed. The total amounts of CRISPR editing plasmids used were 1.0 µg and 1.5 µg. Each group of cells were pulled and genotyped. The remainder of the cells were frozen (-80^{o}C). The absence or presence of the enhancer was analyzed via gel electrophoresis. The sequences of the validation primers are listed in Table 2.1. Then, the frozen cells (1.0 µg group) were re-cultured, and a total of 100 cells were re-seeded on a 10 cm plate. Re-plated cells were cultured for nearly two weeks while checking for the growth of each subpopulation daily. Once the aggregates of cells could be seen with the naked eye, the 10 cm plate was thoroughly washed with fresh PBS, and 2 µL of trypsin was used to detach and pick out each subpopulation of cells. The cells were transferred onto a 24-well plate, and re-grown for another week. Once each well reached confluency of 70-80%, the cells were harvested, genotyped, and

analyzed for enhancer knock-out by gel electrophoresis. Single cell colonies of a subpopulation of interest was re-analyzed using the same protocol as described above.

2.6 Chromosome Conformation Capture (3C)

The general outline of sample preparation for 3C analysis is depicted in Fig. 1.1. Initially, a total of 1.2 x 10^7 cells of wild-type and LPS-stimulated RAW264.7 macrophages, and wild-type, pcDNA3-PU.1 and/or pBR322-C/EBPα-overexpressed B16-BL6 melanoma cells were prepared. 1.0 x 10^7 cells were then harvested, thoroughly washed with PBS two times, and resuspended in 12 mL of PBS (room temperature). Formaldehyde (2%) was added to crosslink the DNA for 10 mins at room temperature while tumbling. The tubes were immediately put on ice after formaldehyde fixation and 1 M glycine (0.125 M) was added to terminate crosslinking. The samples were spun at 805 x g for 8 mins at 4^{o}C. The collected pellet was washed with PBS. The samples were re-spun at 805 x g for 8 mins at 4^{o}C. PBS was removed and the cell pellet was resuspended in 3 mL of pre-made lysis buffer (ice cold). The cells were lysed for 15 mins at 4^{o}C. The lysis buffer contained the following components: NaCl (10 mM), Tris-HCL (10 mM; pH 8.0), NP-40 (0.2%), distilled water, and cOmplete^{TM}, EDTA-free protease inhibitor cocktail tablet (1X). Once finished, the lysed cells were spun down at 805 x g for 8 mins at 4^{o}C. The pellet of extracted nuclei was washed with PBS, and transferred to a new Eppendorf tube. The resuspended nuclei were spun down at maximum speed for 1 min at 4^{o}C. The supernatant was carefully removed, and the extracted nuclei was snap-frozen in liquid N_2 and stored in -80^{o}C. Simultaneously, 2.0 x 10^6 cells were also harvested and resuspended in TRIzol. In order to ensure that the prepared cells generated expected responses, IL-1β mRNA and eRNA expression levels were analyzed in these samples prior to digestion/ligation steps of the extracted nuclei.

Frozen nuclei were thawed and resuspended in 500 µL of 1.2x restriction enzyme (DpnII) buffer. 20% SDS was added (final: 0.3%), and incubated at 37^{o}C for 1 hour shaking at 1000 rpm. 20% Triton X-100 (final: 2.0%) was then added, and incubated again at 37^{o}C for 1 hour shaking at 1000 rpm. 10 µL of the undigested DNA was aliquoted and stored (-20^{o}C), which was used to determine the digestion efficiency. 400 U of DpnII was added to the remainder of undigested DNA, and incubated at 37^{o}C for 24 hours shaking at 1000

rpm. Afterwards, 10 µL of the digested DNA was also aliquoted and stored in -20^{o}C. Post digestion of the DNA, 20% SDS (final: 1.6%) was added to the tube. The mixture was incubated at 65^{o}C for 25 mins while shaking at 1000 rpm. The digested DNA was transferred into 50 mL falcon tubes, and 6.125 mL of the prepared ligase buffer (1.15x) and 20% Triton X-100 (final: 1.0%) were also added. The samples were incubated at 37^{o}C for 1 hour while tumbling. Following incubation, 800 U of T4 DNA ligase was added and incubated at 16^{o}C for 72 hours. Once done, the tubes were allowed to reach room temperature, and 160 µL of 0.5 M EDTA was added to inhibit the ligase activity. The ligated DNA was de-crosslinked with proteinase K (500 µg) at 65^{o}C overnight. On the following day, another 500 µg of proteinase K was added and incubated for another 2 hours. DNA was extracted with 7 mL of PCI twice and subsequently with 7 mL of chloroform once. The tubes were centrifuged for 10 mins at room temperature at 2465 x g. 7 mL of distilled water, 1 mL of 3M sodium acetate, and 19.25 mL of 100% EtOH were added to the retrieved aqueous phase (7 mL), and stored at -20^{o}C overnight. The samples were spun at 2465 x g for 1 hour at 4^{o}C. The pelleted DNA was washed with 70% EtOH, then briefly air-dried. 400 µL of 10 mM Tris-HCl (pH 8.0) was used to resuspend the pellet. RNase (300 µg) was added and incubated at 37^{o}C for 45 mins. DNA was extracted again with 400 µL of PCI and chloroform (once each). The samples were centrifuged at max speed for 5 mins at room temperature. Same ratio of each component was added to the retrieved aqueous phase, and stored at -20^{o}C for 2 hours. DNA was pelleted by centrifuging at max speed for 30 mins at 4^{o}C, washed with 70% EtOH, and re-spun at same speed for 5 mins. 3C library was finally prepared by resuspending the air-dried pellet in 200 µL of distilled water. Taqman qPCR was employed to analyze enhancer-promoter interactions in the samples. The sequences of the primers and dual-labeled Taqman probe are shown in Table 2.1. The following conditions were utilized for Taqman qPCR: 95^{o}C for 15 mins, 46 cycles of 95^{o}C for 10 secs/55-58^{o}C for 20 secs/65^{o}C for 40 secs.

2.6.1 Restriction Enzyme Digestion

Restriction enzyme digestion efficiency is a critical step in 3C sample preparation. In order to determine the digestion efficiency, extracted nuclei were digested with 100 U,

200 U, 400 U, and 600 U of DpnII. Moreover, the effect of freeze and thawing the nuclei was examined by either freeze and thawing the sample digested with 600 U of DpnII or immediately processing it. Instead of taking 10 μL aliquots of undigested and digested DNA, the samples were divided in half. Other than the fact that the ligation step was omitted, identical protocol as described above was used to prepare 3C library of undigested and digested DNA. SYBR Green-mediated detection of fluorescence was performed in this experiment with the same qPCR conditions used in section 2.3. The primer sets, shown in Fig. 2.1 (sequences are listed in Table 2.1), used to determine the digestion efficiency were designed to target either within a DNA fragment from the IL-1β promoter or the adjacent DpnII-mediated cleavage site.

2.7 Statistical Analysis

Data were analyzed with statistical tests indicated in the figure legends. GraphPad Prism 6.0 was used to perform statistical analysis. Data are expressed as means ± S.D. (n=3).

Table 2.1. List of sequences of ASO, qPCR primers, CRISPR validation primers, 3C analysis primers, and restriction enzyme digestion efficiency primer.

Experiment	Target	Primer Sequence
ASO	Scrambled	AACACGTCTATACGC
	eRNA	CAATCCTGGTTGATGA
qPCR/ddPCR	GAPDH	F: GCATTGTGGAAGGGCTCATG R: TTGCTGTTGAAGTCGCAGGAG
	IL-1β	F: GTGGACCTTCCAGGATGAGG R: GCTTGGGATCCACACTCTCC
	534 eRNA	F: CCTGACCCACACAAGGAAGT R: ATGTGCGGAACAAAGGTAGG
	1251 eRNA	F: TACTGCCTGCATCCATCTGC R: GGGAGCTCTTCTTGCTTGGA
	2258 eRNA	F: ATGTTGTGCAACTTGCCTGC R: AGGAGGTTTGTCTGGGAGGA
	2860 eRNA	F: ATGAGAGGGAAAGAACAGACCC R: GCTAAGCAATGACTGTCCTCA
	3236 eRNA	F: ACTTGGGGAGGAAAGGATGT R: ATGAGGAGCAAGCCAGTGAG
	4152 eRNA	F: AGTGCATGTTCCAACGTCAA R: GACCATCAAGAACAGCAGCA
	5370 eRNA	F: CTAGTCCCAGGGAGTTCTGC R: AGGGTTAGGCGCTATGGTCT
	6212 eRNA	F: CTATGGCCTATGGCTTCTGC R: TTTTGCCACATGGCTGATAA
	7182 eRNA	F: ACAGTCTCGCCACAGAAAGAA R: CCATCAAAAGGACAACTGCAT
	7951 eRNA	F: AATCACGAACAGACGACCATC R: GCCTCCCTATCTCCCTACCTT
	8453 eRNA	F: AGTAGTACCAGAGCCCCATGT R: GCTTCCCTTTGCATCTAGCA
	9013 eRNA	F: GGGTTTAAGGGTCTGGTCTTG R: CAGAAAGCTGGGAATTGGAG
	9236 eRNA	F: CATCAACCAGGATTGGACGTG R: GCACTGGGGATCCTATTAACC
	9486 eRNA	F: CGGGGAAGTGGCTGATAGTA R: TCAGGCTTCCTTCAGTGGAT
	10368 eRNA	F: ATGGAGCCCATCCCAGAG R: AGTTACCAGCAGGGCCACTC
	10841 eRNA	F: AGCCGGAGCTAAAATGGAGAC R: CCACCACCCCAAGGACTTATC
	11743 eRNA	F: AGACATTGCCCTCCAGATCC R: CTGGGGAAAAGATGGGCAAC
	13252 eRNA	F: CGCTTATGTTGGGAATTTGG R: TCACAGAAGCAGGCAAGATG

	14256 eRNA	F: CCCAGGAAAGTGACGTTGTT R: GACCTTGCTTCCACTCTTGC
	15232 eRNA	F: GGCCCAGGGAGTAGCTCTAT R: TGGAGGGGCTGAGAGTTCTA
CRISPR Validation	12001 CRISPR F	CCCCACCAGTTATGCTATACG
	11780 CRISPR R	CCAACAATTCAGCAAGAGCA
	5794 CRISPR R	ACTTCATCTCCAGTTAGCCTGC
3C	Dual-labeled Taqman probe	5'-JOE/TCGTTCACCACC/ZEN/ TTTGCACTGTGCAAC/BkFQ-3'
	Universal Forward	TGCTCATGAACAGGCAGATG
	Reverse #1	TTGTCTGGGAGGATTTGGAG
	Reverse #2	TCTGTAGGCAAGCCTGT
	Reverse #3	GATGCAAGTACCATGGGATG
	Reverse #4	AAAGGAAAGTGGTGTGTTTGTG
	Reverse #5	GCTGGTGGTTCTGGGTTCTA
	Reverse #6	AGGGCAACTTTGTGCAGATG
	Reverse #7	CCATCTCCTCACTCCCTTCC
	Reverse #8	GCCATCAAAAGGACAACTGC
	Reverse #9	CGACCATCAATGAGACCAAA
	Reverse #10	CTCTCCAGCACCCGTGAAT
	Reverse #11	AGACCAGACCCTTAAACCCT
	Reverse #12	TTCCGATTCACTTCCTCACC
	Reverse #13	TGCGTTGTAGTTGAAGCTGT
	Reverse #14	CTAACCCCTTCCAACACCT
	Reverse #15	GCTTACTCTGACTGCTTGCC
	Reverse #16	GTGTTCTCAGGCTGCCTTTC
Restriction Enzyme Digestion Efficiency	Undigested DNA	F: CCTGACCCACACAAGGAAGT R: ATGTGCGGAACAAAGGTAGG
	Digested DNA	F: TGCTCATGAACAGGCAGATG R: TATCCCTTTTCCAGGTCTCC

Figure 2.1. Visual representation of primer design for restriction enzyme digestion efficiency. The image displays two adjacent DNA fragments, which have been generated by DpnII-mediated digestion (red dotted lines), within the promoter of IL-1β. Two sets of primers have been designed to determine the digestion efficiency of the DNA in 3C samples. The digested (DIG F&R) primer set targets the DNA region that contains DpnII cleavage site (5'-GATC-3'), whereas the undigested (UND F&R) primer set amplifies a genomic region within a fragment. The PCR products produced by the DIG primers were compared to the amplicons produced by the undigested primers, which represent maximum amplification and were used as the control.

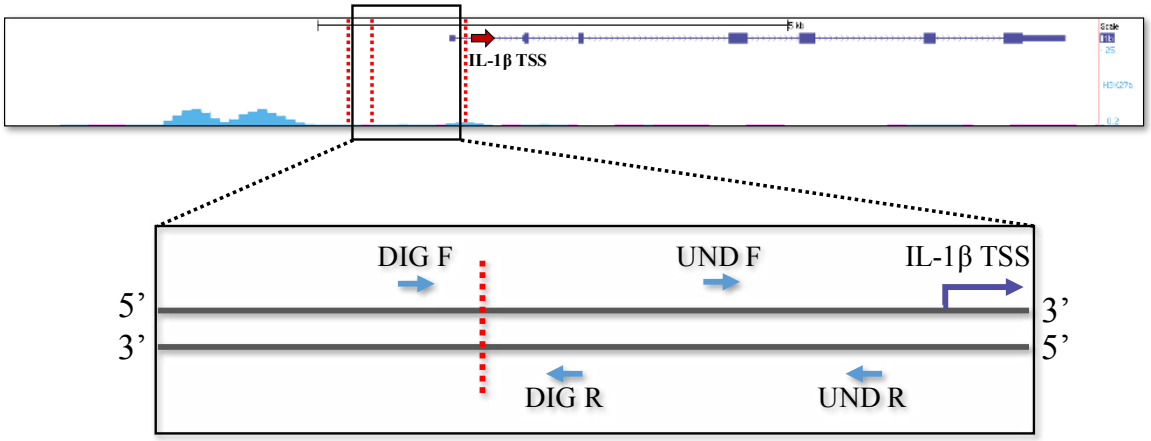
IL-1β TSS
DIG F
UND F
IL-1β TSS
5’
3’
3’
5’
DIG R
UND R

Chapter 3

3 Results

3.1 Identifying the active enhancer of IL-1β in murine macrophages

3.1.1 The genomic region with enhancer histone modifications is macrophage-specific

As a means to identify a potential active enhancer of IL-1β, I sought for a genomic region with enhancer-associated histone markers (H3K27Ac^{hi}, H3K4me1^{hi}, H3K4me3^{low}) in a 100 kilobase (kbs) frame of window (± 50 kbs from IL-1β TSS). Based on the chromatin immunoprecipitation sequencing (ChIP-seq) analysis of the chromatin markers available in the ENCODE database as illustrated in Fig. 3.1A, I located a potential active enhancer enriched in H3K27Ac, H3K4me1, and devoid of H3K4me3 approximately 10 kbs upstream of the IL-1β TSS in murine bone marrow-derived macrophages (BMDMs). Considering that enhancers are cell-type specific regulatory elements, histone modification profiles of other cell lines including B-cell lymphomas (CH12), liver, and brain cells were also analyzed. The non-myeloid cell lines lacked the unique histone markers at the potential enhancer region, suggesting that the genomic region serves as a macrophage-specific enhancer of IL-1β. Furthermore, two binding motifs of PU.1 (5'-GAGGAAGT-3'; core motif highlighted in red in Fig. 3.1B), which activates macrophage-specific enhancers in combination with other LDTFs, are located within the putative enhancer, indicating that PU.1 potentially recognizes and binds to this regulatory element in BMDMs.

Figure 3.1. A putative enhancer marked by H3K27Ac/H3K4me1/H3K4me3 within a 100 kbs window of IL1β locus in murine BMDMs. A) The ChIP-seq data from the ENCODE database shows a putative enhancer region, which recruits high levels of H3K27Ac and H3K4me1 and low levels of H3K4me3 in BMDMs, but not in CH12, liver, and brain cells. B) A zoomed in image of the highlighted region shown in (A). The highlighted region represents the position of the proposed enhancer (H3K27Ac^{hi}, H3K4me1^{hi}, H3K4me3^{lo}, RNAPII^{hi}) relative to the IL-1β TSS. The two arrows within the putative enhancer indicate the location of PU.1 binding motif (5'-GAGGAAGT-3').

A)

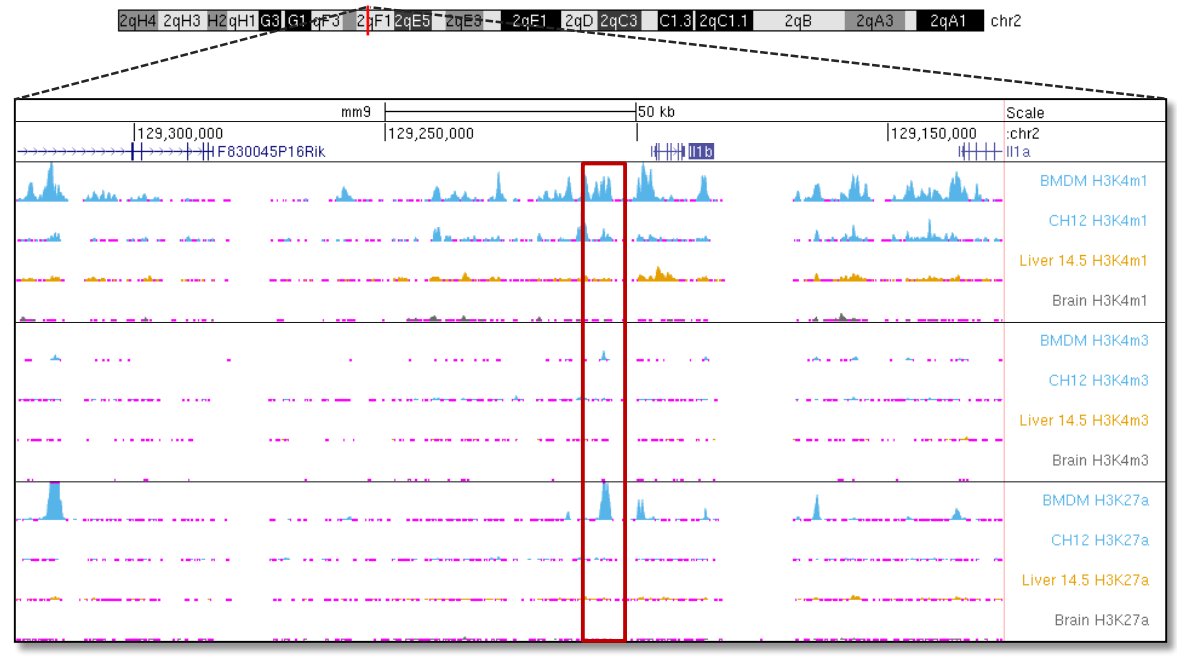
2qH4 2qH3 H2qH1 G3 G1 qF3 2qF1 2qE5 2qE3 2qE1 2qD 2qC3 C1.3 2qC1.1 2qB 2qA3 2qA1 chr2
mm9
50 kb
Scale
129,300,000
129,250,000
129,150,000
chr2
F830045P16Rik
Il1b
Il1a
BMDM H3K4m1
CH12 H3K4m1
Liver 14.5 H3K4m1
Brain H3K4m1
BMDM H3K4m3
CH12 H3K4m3
Liver 14.5 H3K4m3
Brain H3K4m3
BMDM H3K27a
CH12 H3K27a
Liver 14.5 H3K27a
Brain H3K27a

B)

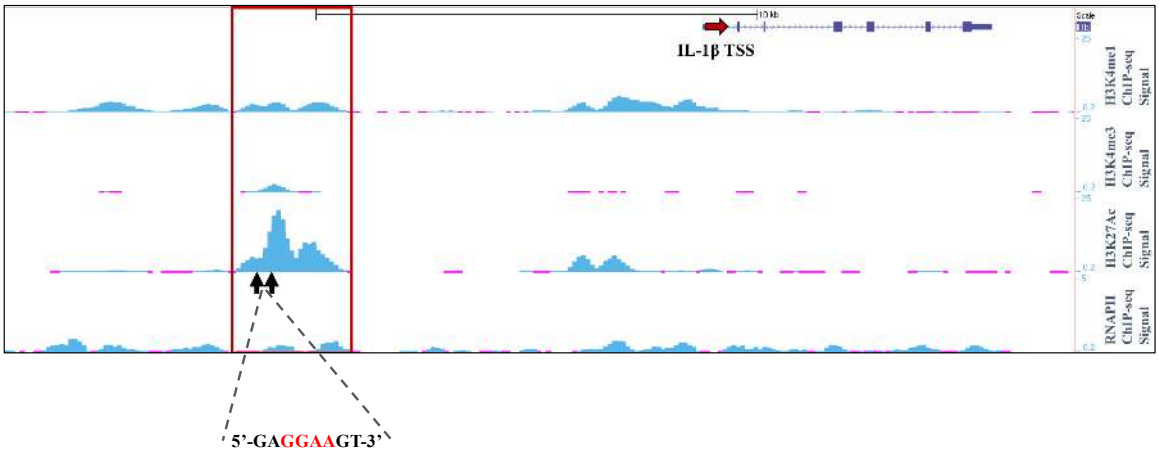
IL-1β TSS
H3K4me1 ChIP-seq Signal
H3K4me3 ChIP-seq Signal
H3K27Ac ChIP-seq Signal
RNAPII ChIP-seq Signal
5'-GAGGAAGT-3'

3.1.2 The putative genomic element produces eRNAs in response to LPS in murine macrophages

Active enhancers recruit RNAPII, along with other transcription factors and produce eRNAs [42,73]. As a means to examine whether eRNAs are generated from the proposed enhancer of IL-1β, 12 qPCR primer sets that target approximately every 500-1000 bps in genomic regions upstream, downstream, and within the putative enhancer were designed to quantitatively measure the production of non-coding transcripts in LPS-activated macrophages (Fig. 3.2A). Black horizontal bars show the positions of these eRNA primers relative to the IL-1β TSS. It was observed that the expression levels of eRNAs were dependent on the duration of macrophage exposure to LPS (Fig. 3.2B). Using 2 representative primer sets (9013, 11743), which produced greatest eRNA fold increase in Fig. 3.2B, to further analyze eRNA production, I found that eRNAs were rapidly induced and peaked at 90 mins post-stimulation of the macrophages, which then gradually decreased to a basal level after 720 mins (Fig. 3.2C). Then, the kinetics of IL-1β mRNA production in the same set of samples were examined to address whether the IL-1β mRNA was generated in a time-dependent manner upon LPS exposure (Fig. 3.2D). I observed a correlation between the eRNAs and IL-1β mRNA productions. The kinetics of IL-1β mRNA production was slightly delayed in comparison to the eRNAs and reached maximal production 180 mins after LPS stimulation.

Figure 3.2. The production of eRNAs and IL-1β mRNA by LPS in macrophages. A) A schematic presentation of H3K27Ac ChIP-seq peaks in BMDMs based on the the ENCODE database and eRNA primer sets. The black horizontal bars and numerical values indicate the location of eRNA primers and the number of base pairs upstream of the IL-1β TSS (red arrow). B - D) RAW264.7 cells were stimulated with LPS (100 ng/mL) for the time indicated. Expression of eRNAs (B, C) and IL-1β mRNA (D) were analyzed by RT-qPCR using GAPDH as the housekeeping gene. Fold inductions of eRNAs and IL-1β mRNA were compared between untreated and LPS-stimulated (each time point) RAW264.7 macrophages. The data are expressed as means ± S.D. (n=3); *, $P < 0.05$, **, $P < 0.05$, ***, $P < 0.05$, Student's *t* test.

A)

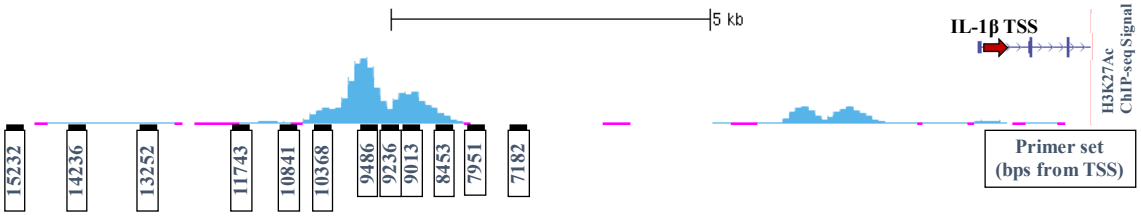
5 kb
IL-1β TSS
H3K27Ac ChIP-seq Signal
Primer set (bps from TSS)
15232
14236
13252
11743
10841
10368
9486
9236
9013
8453
7951
7182

B)

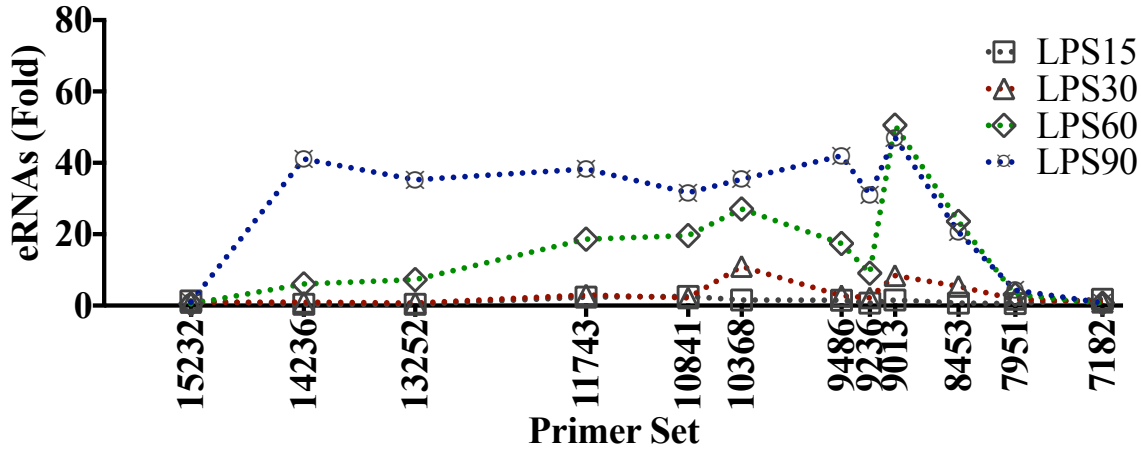
eRNAs (Fold)
80
60
40
20
0
LPS15
LPS30
LPS60
LPS90
15232
14236
13252
11743
10841
10368
9486
9236
9013
8453
7951
7182
Primer Set

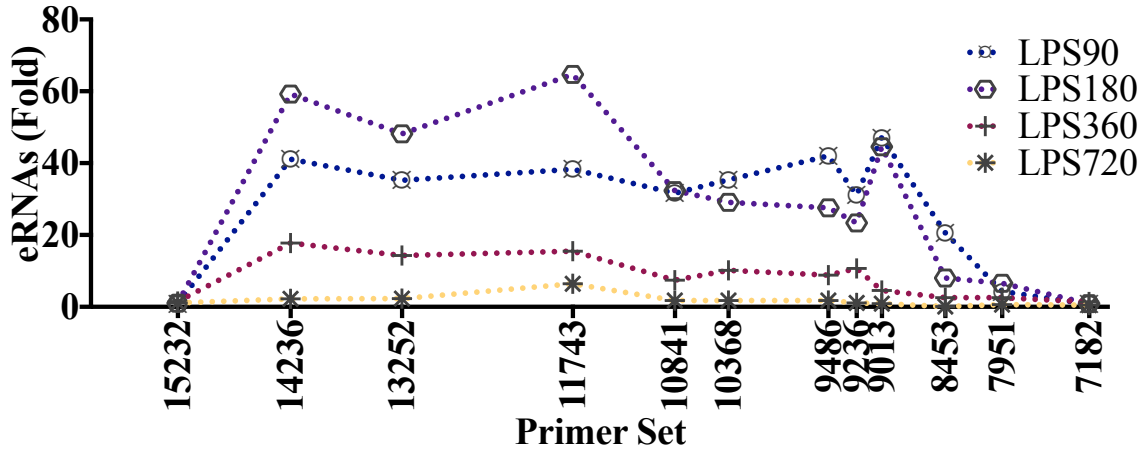
eRNAs (Fold)
80
60
40
20
0
LPS90
LPS180
LPS360
LPS720
15232
14236
13252
11743
10841
10368
9486
9236
9013
8453
7951
7182
Primer Set

C)

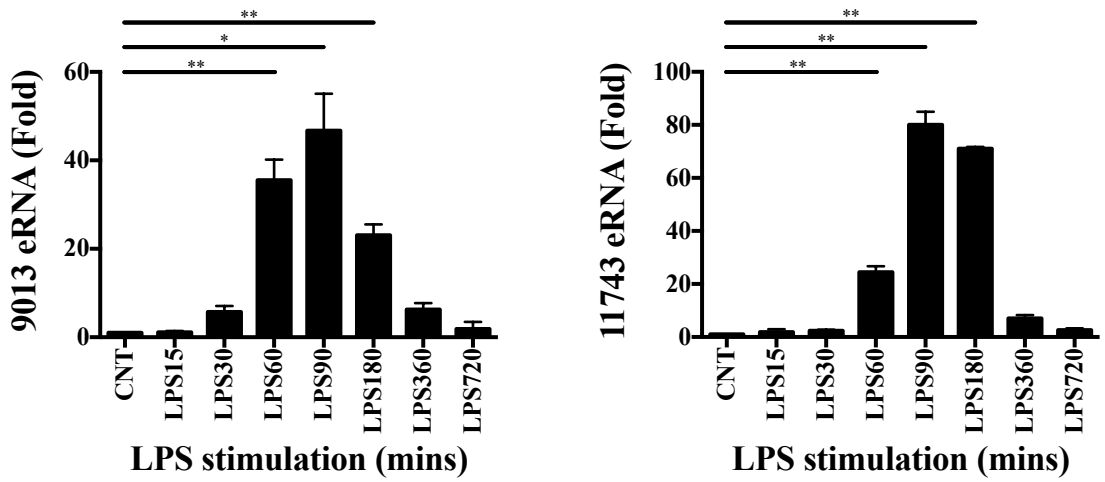
9013 eRNA (Fold)
60
40
20
0
**
*
**
CNT
LPS15
LPS30
LPS60
LPS90
LPS180
LPS360
LPS720
LPS stimulation (mins)
11743 eRNA (Fold)
100
80
60
40
20
0
**
**
**
CNT
LPS15
LPS30
LPS60
LPS90
LPS180
LPS360
LPS720
LPS stimulation (mins)

D)

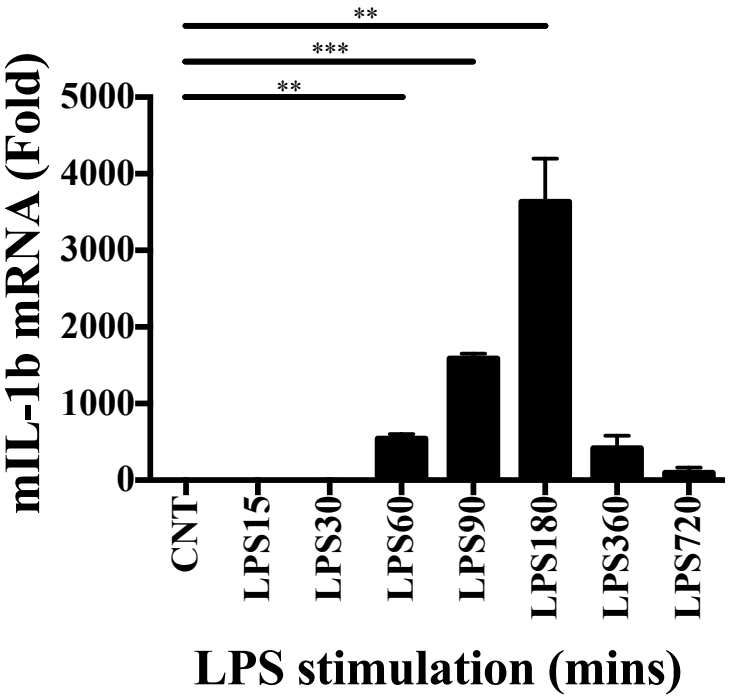
mIL-1b mRNA (Fold)
5000
4000
3000
2000
1000
0
**
***
**
CNT
LPS15
LPS30
LPS60
LPS90
LPS180
LPS360
LPS720
LPS stimulation (mins)

3.1.3 Measurement of LPS-induced eRNA production by droplet digital (dd)PCR

A notable limitation of real-time PCR approach is that it only measures a relative quantity (fold change) of template in a given primer set, and absolute quantities of template cannot be obtained. Taking this into consideration, I used the ddPCR to measure the absolute quantity of eRNAs (template), which allows comparison between different primer sets [124,125]. ddPCR utilizes the power of oil droplets by partitioning a sample of DNA into thousands of droplets. Each droplet contains all the necessary components to run a PCR assay [126]. Thus, as opposed to detecting the fluorescence signal of a single reaction in a standard qPCR, thousands of reactions are simultaneously carried out in a typical ddPCR [126]. Depending on whether a copy of the target DNA is allocated in the oil droplets or not, either a positive or a negative signal is generated, respectively [126]. Based on the ddPCR fluorescence data in Fig 3.3A, it is apparent that there was an increase in the number of positive droplets in LPS-stimulated macrophages. However, one factor that must be taken into consideration when analyzing a ddPCR fluorescence data is that the total number of oil droplets generated varies between samples. In order to overcome this issue, the concentrations of positive droplets (unit: fluorescent droplets/μL), which were generated via QuantaLife software, were used as the unit of measurement to make direct comparisons between untreated and LPS-treated RAW264.7 cells (Fig. 3.3B). Expectedly, elevated concentrations of eRNAs were observed in macrophages 60 mins post LPS exposure. Specifically, concentrations of eRNAs detected by 8453, 9013, 9236, 9486, 10368, and 10841 primer sets were induced up to ~20-folds in LPS-stimulated macrophages, whereas the amount of transcripts produced from the other regions remained similar to the basal level.

Figure 3.3. Measurement of copy numbers of eRNAs by ddPCR in macrophages activated by LPS. A) Illustration of ddPCR fluorescence graphs for eRNA production between wild-type and LPS-stimulated (60 mins) RAW264.7 macrophages. The blue dots that are positioned above the threshold line (pink) represent positive droplets whereas negative droplets are depicted as black dots. The standard RT-PCR was used to generate cDNA from the eRNAs produced in the cells. The fluorescence of each oil droplet has been detected via EvaGreen dye. B) Concentration of eRNAs in copies/μL (solid line) from each sample was derived from the number of positive droplets shown in (A). The concentration of eRNAs in LPS-stimulated macrophages was compared to the background eRNA concentration from wild-type macrophages, and was represented as fold changes. The dotted line represents the fold changes of eRNAs in LPS60 RAW264.7 macrophages quantified via qPCR.

A)

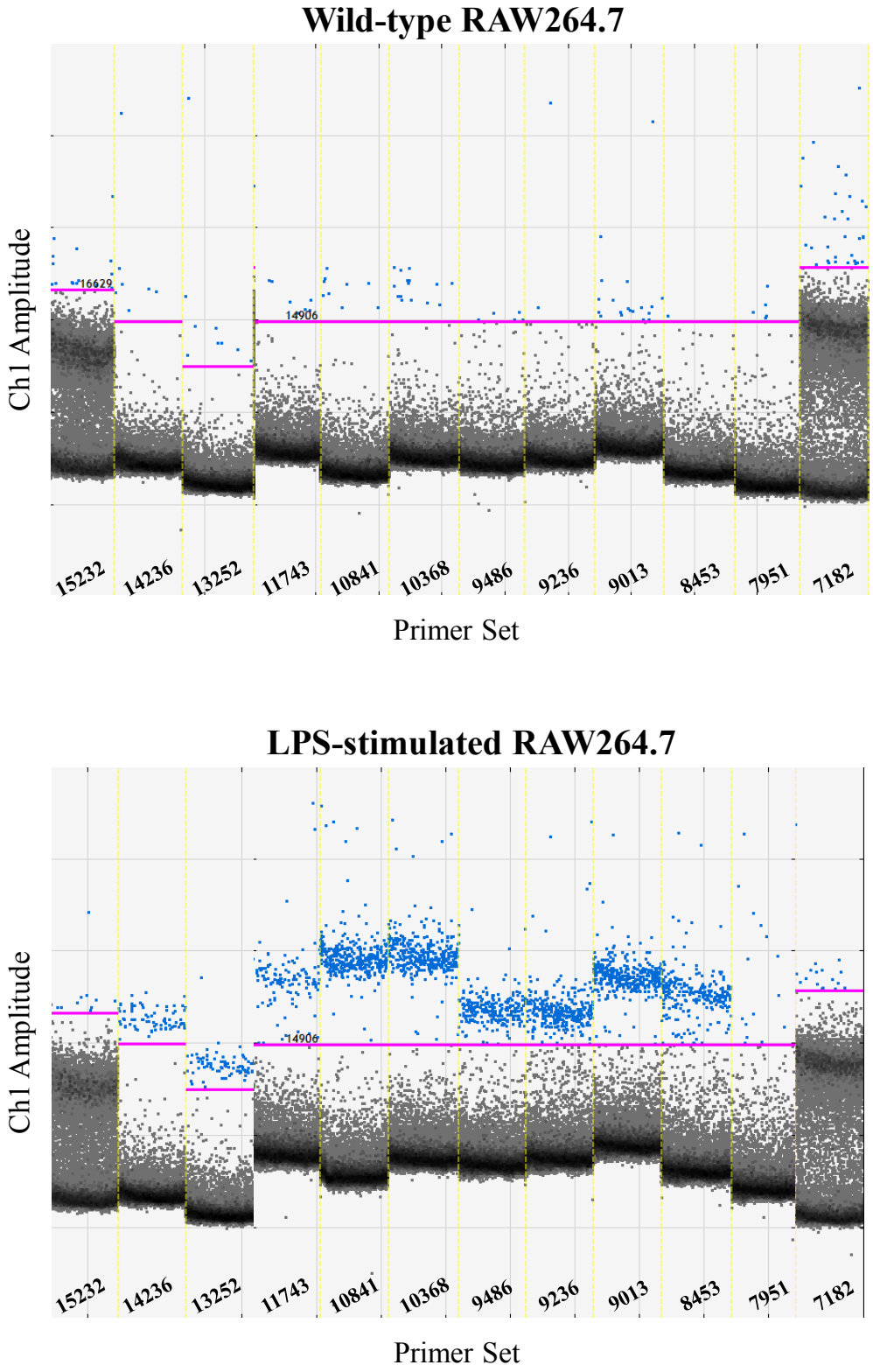
Wild-type RAW264.7
Ch1 Amplitude
16629
14906
15232
14236
13252
11743
10841
10368
9486
9236
9013
8453
7951
7182
Primer Set
LPS-stimulated RAW264.7
Ch1 Amplitude
14906
15232
14236
13252
11743
10841
10368
9486
9236
9013
8453
7951
7182
Primer Set

B)

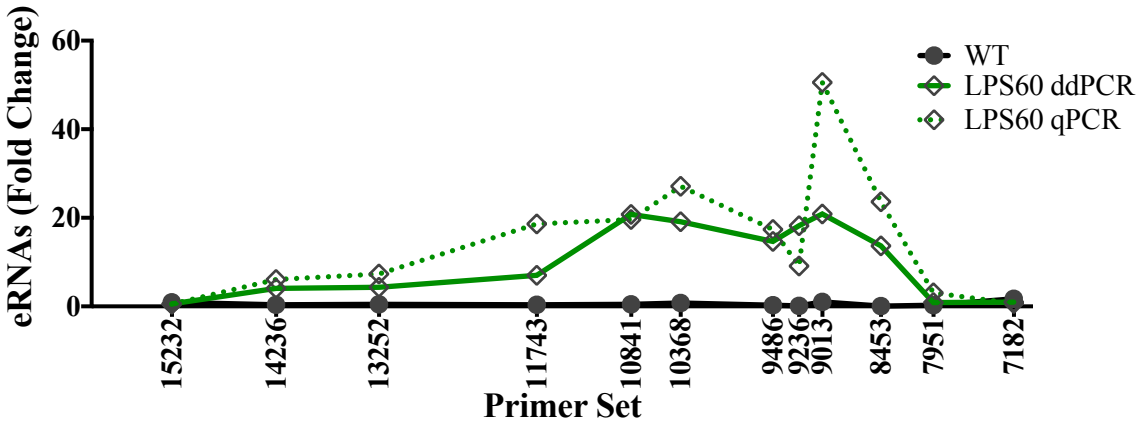
eRNAs (Fold Change)
60
40
20
0
15232
14236
13252
11743
10841
10368
9486
9236
9013
8453
7951
7182
Primer Set
WT
LPS60 ddPCR
LPS60 qPCR

3.1.4 Examining the role of the putative eRNA in IL-1β mRNA production

To address the role of the putative eRNA in promoting IL-1β transcription, a loss-of-function experiment was performed using the antisense locked nucleic acid (LNA™) GapmeR (herein termed ASO). Except for a few nucleotides along the middle stretch of the single-stranded ASO, 5' and 3' ends comprise LNAs, which are modified nucleotides with an oxymethylene bridge connecting the 2' oxygen and 4' carbon [127]. Such structural modifications increase the overall rigidity of the ASO [127]. Furthermore, the DNA(ASO):RNA heteroduplex are cleaved by RNase-H that are abundant in the nucleus [127]. Considering that eRNAs are localized in the nucleus, ASO forms a stable duplex with target RNAs and leads to the degradation of RNAs by RNase-H [127]. Transfection of RAW264.7 cells with the ASO targeting the putative anti-sense eRNA (eRNA-ASO; targeting 9237-9253 bps upstream of the IL-1β TSS) suppressed 64%, 52%, and 78% of amplicons produced from 10841, 10368, and 9486 primer sets, respectively, whereas random ASO (scrambled-ASO) had no effect (Fig. 3.4A). Also, cells transfected with eRNA-ASO decreased the production of IL-1β mRNA by ~50% compared to cells transfected with scrambled-ASO (Fig. 3.4B). These results indicate that the putative eRNA is required for optimal production of IL-1β mRNA.

Figure 3.4. Knock-down of the putative eRNA reduces IL-1β mRNA production in RAW264.7 macrophages. A and B) RAW264.7 macrophages were transfected with 250 pmole of scrambled-ASO or eRNA-ASO for 24 hours. These cells were then stimulated with LPS (100 ng/mL) for 90 mins. Productions of the putative eRNA (A) and IL-1β mRNA (B) were measured using RT-qPCR using GAPDH as the reference gene. The data are expressed as means ± S.D. (n=3); *, $P < 0.05$, ***, $P < 0.05$, ****, $P < 0.05$, Student's *t* test.

A)

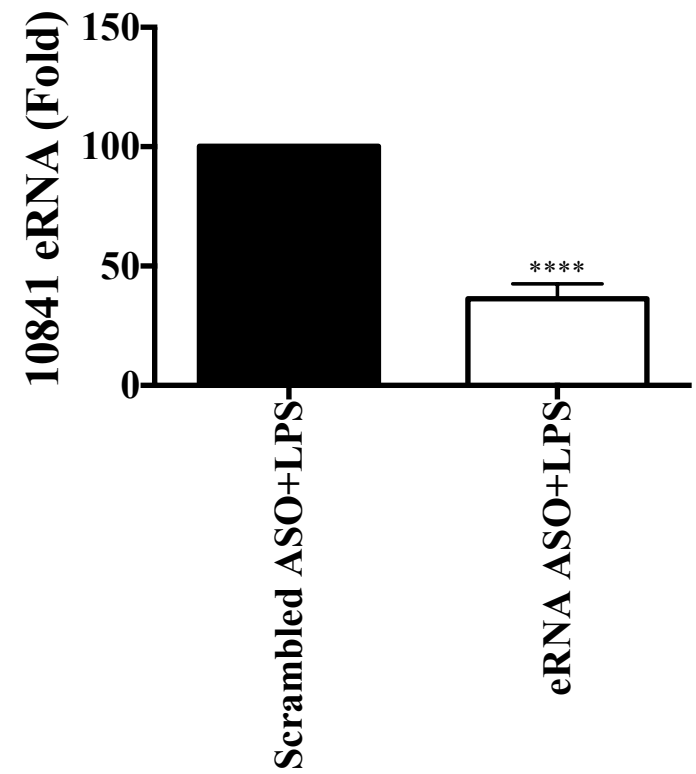
10841 eRNA (Fold)
150
100
50
0
****
Scrambled ASO+LPS
eRNA ASO+LPS

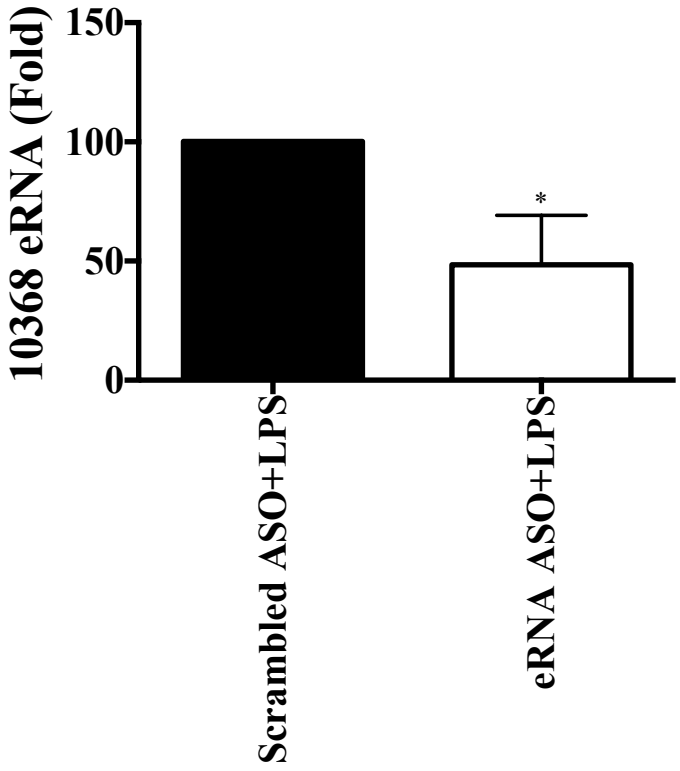
10368 eRNA (Fold)
150
100
50
0
*
Scrambled ASO+LPS
eRNA ASO+LPS

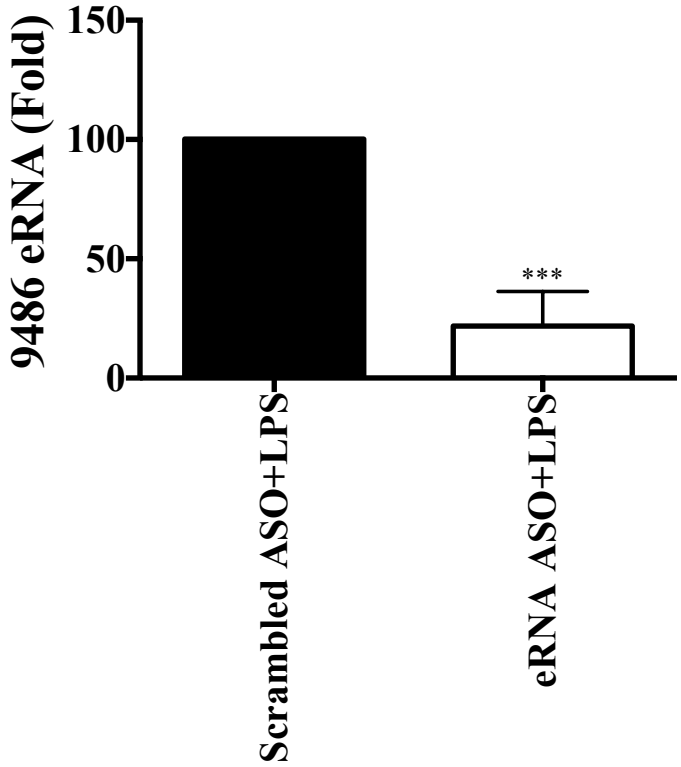
9486 eRNA (Fold)
150
100
50
0
***
Scrambled ASO+LPS
eRNA ASO+LPS

B)

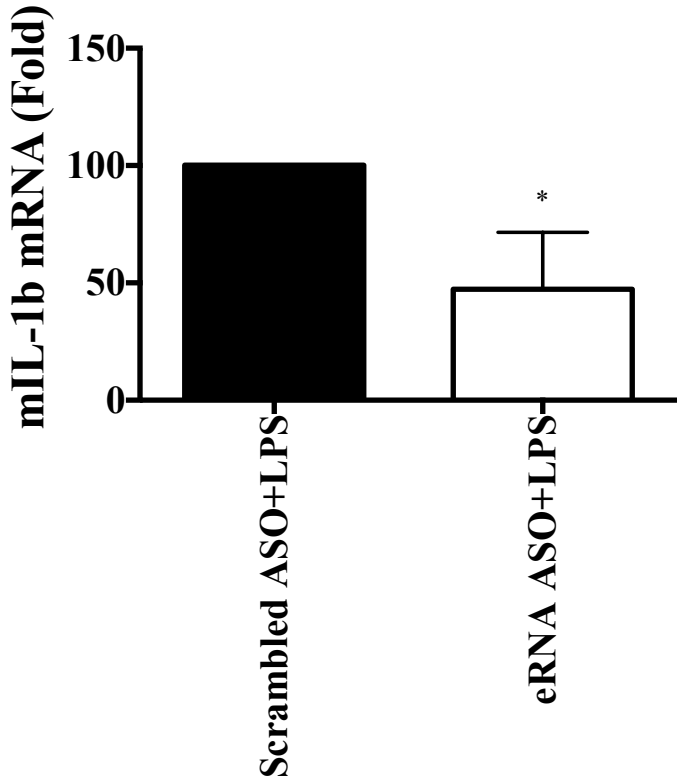
mIL-1b mRNA (Fold)
150
100
50
0
*
Scrambled ASO+LPS
eRNA ASO+LPS

3.1.5 LPS enhances the physical interaction between the putative enhancer and IL-1β promoter in macrophages

Enhancers are often distally positioned from the promoter region and these regulatory elements should be brought in close proximity via chromatin looping (i.e. looping out the intervening DNA) [128-131]. The physical interaction between these regulatory elements has been suggested to be mediated by the interplay of eRNAs and various transcription factors such as RNAPII and the Mediator complex [132]. Thus, I utilized the 3C technique to examine the interaction between the putative enhancer and IL-1β promoter in LPS-exposed RAW264.7 macrophages. Initially, the digestion efficiency of the restriction enzyme of choice had to be determined prior to 3C sample preparation. It has been suggested that the digestion efficiency of the chromatin should at least be 60-70%, as low digestion efficiency can generate inaccurate quantification results [122]. I decided to use the restriction enzyme DpnII, which recognizes 5'-GATC-3' and cleaves before G, that renders ~500 bp size genomic DNA fragments. First, I optimized the digestion condition by testing varying amounts of DpnII to yield ≥ 70% digestion efficiency (Fig. 3.5) [133,134]. I found that the minimum amount of DpnII required to reach ~70% digestion efficiency was 400 U. Next, I found that the crosslinked DNA should go through a round of freeze (-80^{o}C) and thaw cycle prior to digestion to increase the digestion efficiency by ~25%.

Through 3C-TaqMan qPCR analysis, I found that the interaction between the IL-1β promoter and proximal fragments occurred in both non-treated and LPS-treated (180 min) macrophages (Fig. 3.6 B, C). As the DNA is not in linear form and is densely packaged in the nucleus, the promoter and the proximal fragments are likely situated in proximity in the nuclear space. Since 3C measures the ligation frequencies between fragments based on their proximity, the ligation between the promoter and the proximal fragments in untreated and LPS-stimulated RAW264.7 cells likely occurred by chance and was considered as background interaction. However, we observed that the ligation between the promoter of IL-1β with both 3'- and 5'-ends of the putative enhancer occurred upon stimulation of macrophages with LPS for 180 mins (Fig. 3.6C), which was absent in wild-type cells (Fig. 3.6B). The grey upright bars represent the frequency of

interaction between the IL-1β promoter and the crosslinked genomic fragment. It is important to note that Fig. 3.6C only displays new enhancer-promoter interactions detected upon LPS challenge. Overall, these results are a clear indication that enhancer-promoter interactions are stimulus-dependent in murine macrophages.

Figure 3.5. Optimization of restriction enzyme digestion for 3C analysis. RAW264.7 cells (1.0×10^7) were fixed with formaldehyde for crosslinking of interacting DNA regions and then the genomic DNAs were extracted. Extracted DNAs were digested with varying amounts of DpnII (100, 200, 400, 600 U), and the DNAs digested with 600 U of DpnII underwent a round of freezing and thawing (FT; NFT: No FT). Digested DNA fragments were de-crosslinked with proteinase K and subsequently extracted. Digestion efficiency was measured via qPCR with primer sets targeting undigested and digested genomic regions.

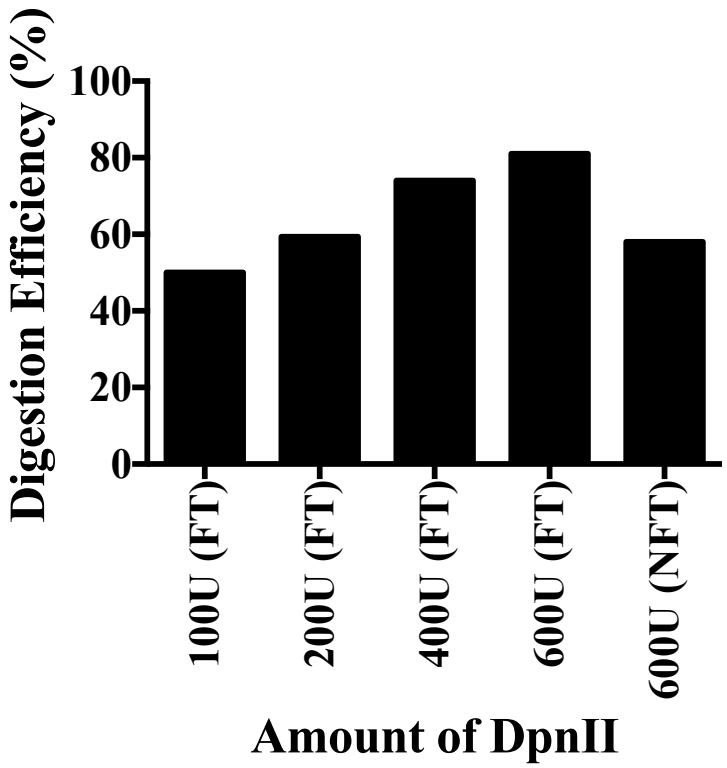
Digestion Efficiency (%)
100
80
60
40
20
0
100U (FT)
200U (FT)
400U (FT)
600U (FT)
600U (NFT)
Amount of DpnII

Figure 3.6. LPS stimulation induces enhancer-promoter interaction in macrophages. A) Dotted lines represent possible cleavage sites by DpnII (400 U), and arrows indicate the primers used to probe the digested DNA fragments. Each reverse primer (black) was utilized in combination with the promoter-recognizing universal forward primer (red). B and C) RAW264.7 cells were treated with none (A) or LPS for 180 mins (B) and fixed by formaldehyde. DNAs were then digested with DpnII (400 U) and ligated for 72 hours. The physical interaction between the regulatory elements were quantified via TaqMan qPCR. The arrows extending from the IL-1β promoter to the DNA fragments generated by DpnII indicate the occurrence of ligation. The upright bars represent the ligation frequencies between the promoter and interacting DNA fragments, which have been compared to the ligation frequency of two adjacent DNA fragments in the promoter region.

A)

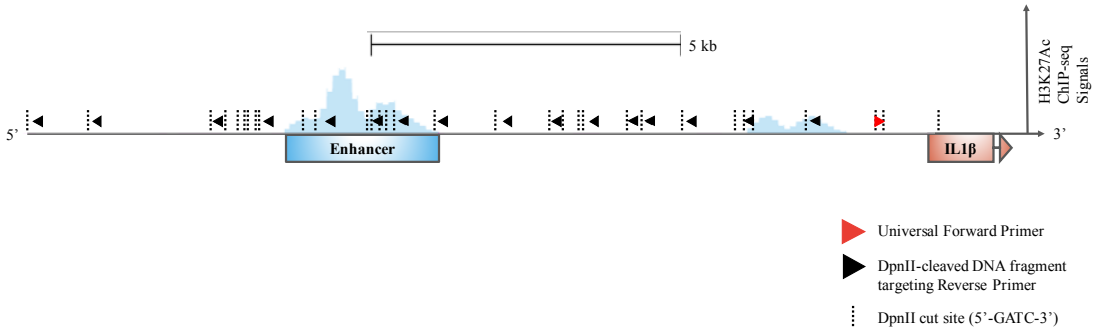
5 kb
H3K27Ac ChIP-seq Signals
5'
3'
Enhancer
IL1β
Universal Forward Primer
DpnII-cleaved DNA fragment targeting Reverse Primer
DpnII cut site (5'-GATC-3')

B)

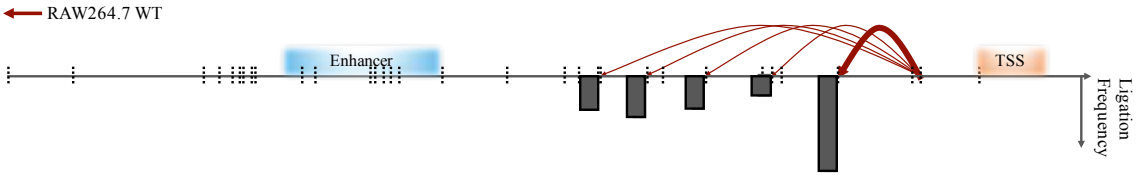
RAW264.7 WT
Enhancer
TSS
Ligation Frequency

C)

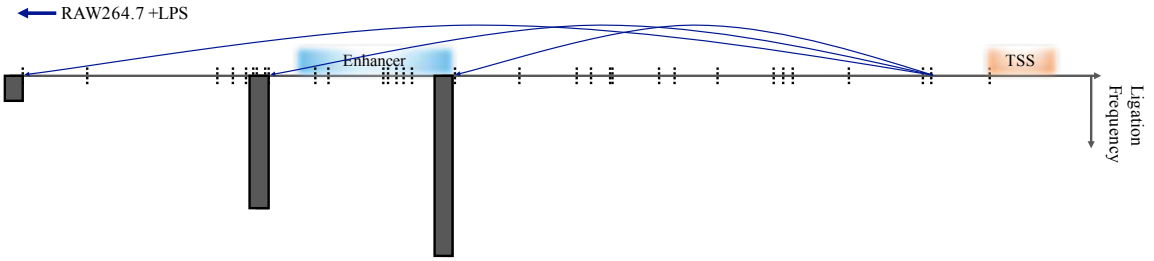
RAW264.7 +LPS
Enhancer
TSS
Ligation Frequency

3.2 Examining the role of PU.1 in the enhancer-promoter regulatory network of IL-1β

3.2.1 Overexpression of PU.1 is sufficient for inducing IL-1β mRNA expression in B16-BL6 murine melanoma cells

Rapid production of IL-1β in response to microbial infection is a feature of innate immune cells, such as macrophages, and this unique phenotype is likely due to regulatory elements that allow prompt transcriptional initiation triggered by extracellular signals. As shown in Fig. 3.1, the macrophages harbor an active enhancer (H3K27Ac^{hi}, H3K4me1^{hi}, H3K4me3^{low}), which is not detected in other cell lines. Since LDTFs play key roles in determining cell identities, I have examined the role of LDTFs involved in macrophage differentiation including PU.1 and C/EBPα in regulating the putative enhancer for IL-1β. As shown in Fig. 3.7A, transfection efficiency of B16-BL6 melanoma cells is very high, as mRNA expression levels of PU.1 and C/EBPα increased by ~40000- and ~500000-fold, respectively, compared to vector control (VC) transfected cells. Furthermore, B16-BL6 cells are able to activate the mitogen-activated protein kinases (MAPKs: extracellular regulated kinases (ERKS) and p38 MAPK) within 60 mins in response to LPS (Appendix A). Therefore, these cells could be an ideal system to examine the role of LDTFs in regulating IL-1β production. As shown in Fig. 3.7B, ectopic expression of PU.1 rendered these cells to express IL-1β mRNA in response to LPS. In contrast, C/EBPα overexpression did not induce the production of IL-1β mRNA. Concomitant expression of PU.1 and C/EBPα did not change IL-1β mRNA expression levels when compared to cells overexpressed with PU.1 alone. These results suggest that PU.1 alone is sufficient for rendering B16-BL6 melanoma cells to produce IL-1β in response to LPS.

Figure 3.7. The production of IL-1β mRNA in response to LPS is dependent on the overexpression of PU.1 in B16-BL6 melanoma cells. A) B16-BL6 cells were transfected with VC or PU.1 and/or C/EBPα (0.7 μg each) plasmids for 48 hours. The expression levels of PU.1 and C/EBPα were analyzed via qPCR, and normalized to GAPDH. Data are expressed as means ± S.D. (n=3); *, $P < 0.05$, **, $P < 0.05$, Student's *t* test. B) B16-BL6 cells were ectopically expressed with the same plasmids as described in (A) and stimulated with LPS (100 ng/mL) for 6 hours. IL-1β mRNA production was quantified via qPCR. Data are expressed as means ± S.D. (n=3); ***, $P < 0.05$, Student's *t* test.

A)

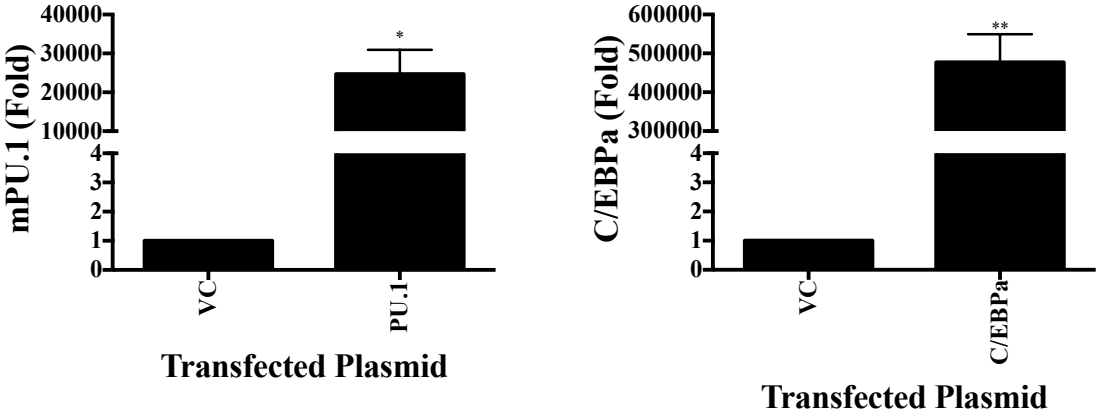
mPU.1 (Fold)
40000
30000
20000
10000
4
3
2
1
0
*
VC
PU.1
Transfected Plasmid
C/EBPa (Fold)
600000
500000
400000
300000
4
3
2
1
0
**
VC
C/EBPa
Transfected Plasmid

B)

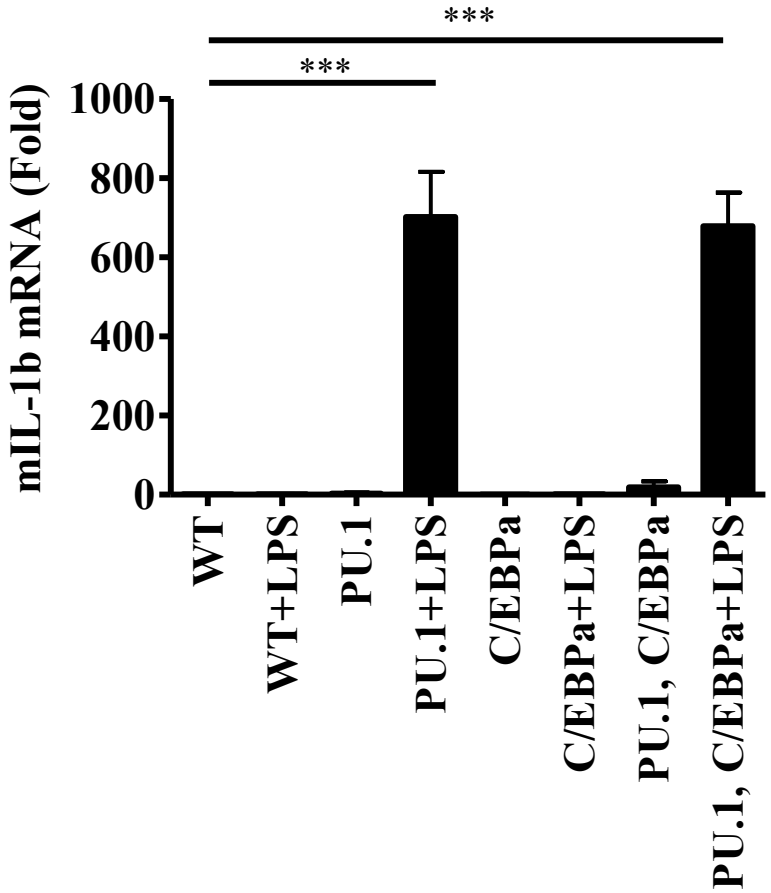
***
***
mIL-1b mRNA (Fold)
1000
800
600
400
200
0
WT
WT+LPS
PU.1
PU.1+LPS
C/EBPa
C/EBPa+LPS
PU.1, C/EBPa
PU.1, C/EBPa+LPS

3.2.2 Overexpression of PU.1 induces the activation of the putative IL-1β enhancer

Since overexpression of PU.1 rendered B16-BL6 cells to induce IL-1β mRNA expression (Fig. 3.7B), I have examined whether PU.1 overexpression also activated the putative enhancer found in macrophages (Fig. 3.1). As shown in Fig. 3.8A, overexpression of B16-BL6 cells with either PU.1 alone or PU.1 and C/EBPα induced basal level of eRNA transcription prior to LPS stimulation, whereas C/EBPα had a minimal effect. Subsequently, I investigated the effect of LPS stimulation on eRNA production in cells ectopically expressing either PU.1, C/EBPα or both PU.1 and C/EBPα. Fig. 3.8B displays that LPS increased the production of transcripts by approximately 3-fold from regions targeted by 14236, 13252, 9486, and 8453 primer sets. The greatest fold increase (~10-fold) in eRNA was detected by the 10841 primer set. Similar to IL-1β mRNA data, C/EBPα did not have much contribution in promoting transcription of eRNAs in response to LPS (Fig. 3.8C). Moreover, combination of PU.1 and C/EBPα generally increased the production of eRNAs upon LPS stimulation (Fig. 3.8D); however, most of these fold increases turned out to be statistically insignificant. Interestingly, LPS-induced eRNAs detected by 11743 and 10841 primer sets in PU.1- and C/EBPα-overexpressed cells elevated by ~4-fold.

Figure 3.8. eRNAs are readily produced in PU.1-overexpressed B16-BL6 melanoma cells in response to LPS. A-D) B16-BL6 cells were overexpressed with PU.1 and/or C/EBPα (0.7 μg each) for 48 hours, then either unstimulated or stimulated with LPS (100 ng/mL) for 6 hours. The production of eRNAs in cells transfected with VC, PU.1, C/EBPα, or both LDTFs was measured via qPCR prior to LPS stimulation (A). Fold changes in eRNA production were compared between unstimulated or LPS stimulated B16-BL6 cells overexpressed with PU.1 (B), C/EBPα (C), or both LDTFs (D). Production of eRNAs was quantified by qPCR. GAPDH was the housekeeping gene used to analyze eRNA expression. Data are expressed as means ± S.D. (n=3); **, $P < 0.05$, ***, $P < 0.05$, ****, $P < 0.05$, Student's *t* test.

A)

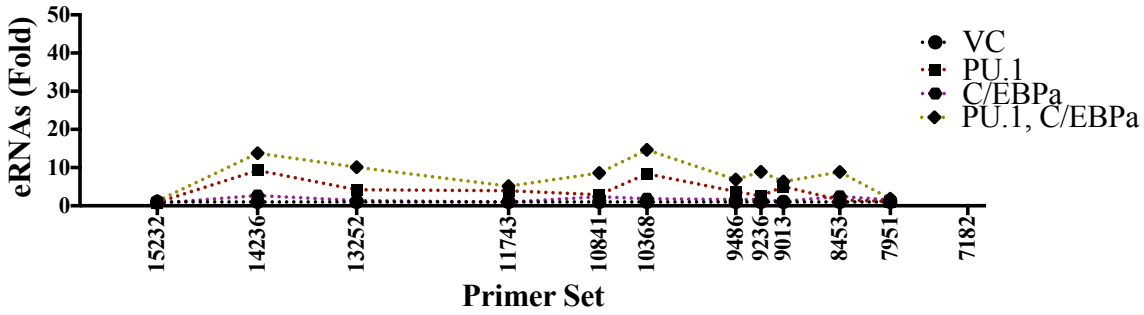
eRNAs (Fold)
50
40
30
20
10
0
VC
PU.1
C/EBPa
PU.1, C/EBPa
15232
14236
13252
11743
10841
10368
9486
9236
9013
8453
7951
7182
Primer Set

B)

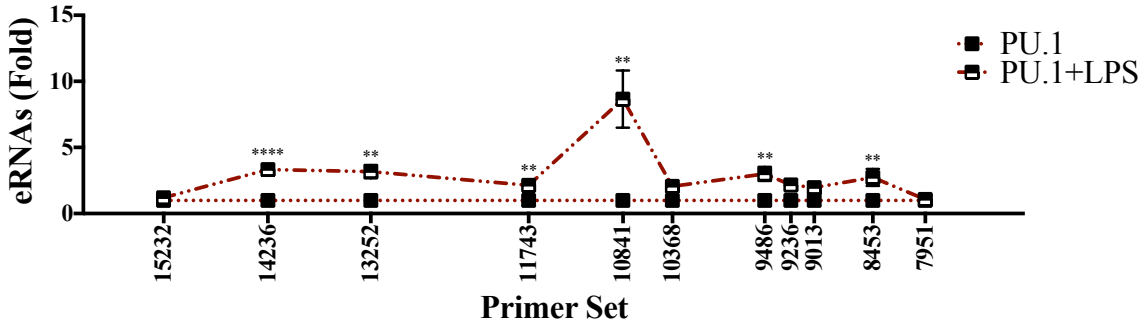
eRNAs (Fold)
15
10
5
0
PU.1
PU.1+LPS
****
**
**
**
**
**
15232
14236
13252
11743
10841
10368
9486
9236
9013
8453
7951
Primer Set

C)

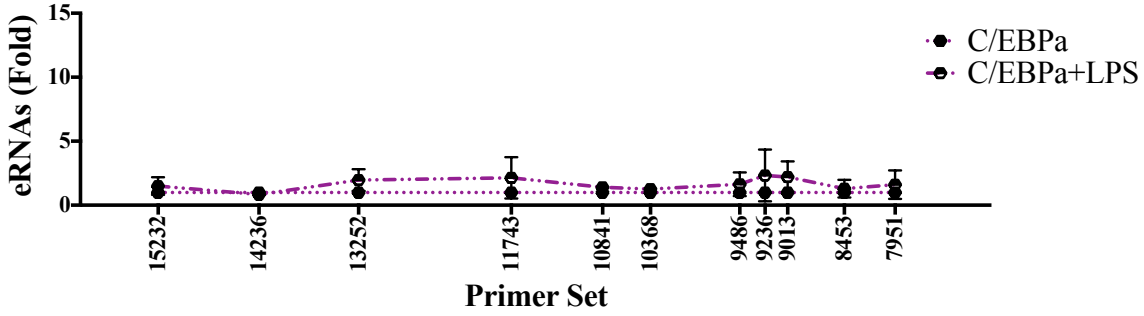
eRNAs (Fold)
15
10
5
0
C/EBPa
C/EBPa+LPS
15232
14236
13252
11743
10841
10368
9486
9236
9013
8453
7951
Primer Set

D)

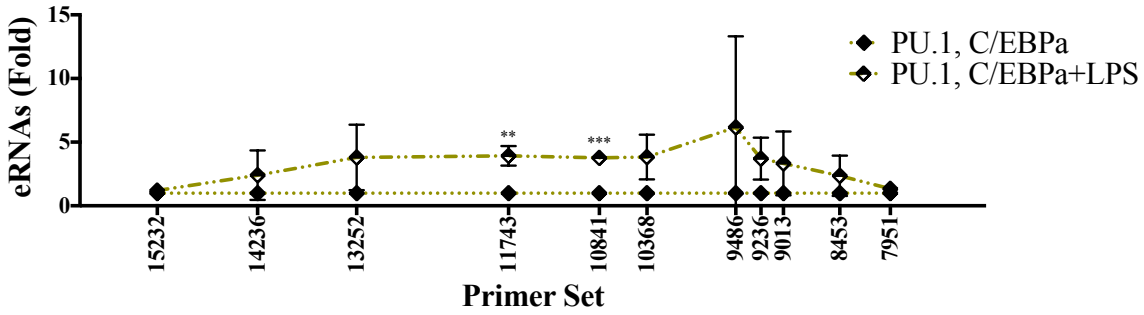
eRNAs (Fold)
15
10
5
0
PU.1, C/EBPa
PU.1, C/EBPa+LPS
**
***
15232
14236
13252
11743
10841
10368
9486
9236
9013
8453
7951
Primer Set

3.2.3 Examining the role of the putative IL-1β regulatory element by gene editing

To address the role of the putative enhancer identified through the ENCODE database, the regulatory element was edited out using the clustered regularly interspaced short palindromic repeats (CRISPR)-Cas9 system in B16-BL6 cells as shown in Fig. 3.9A. The two guide RNA sequences with the protospacer adjacent motif (PAM; 3 bases highlighted in red) in the 3'-ends were designed to be complimentary to genomic regions upstream and downstream of the putative enhancer. Cas9-mediated cleavage of the DNA was expected to yield two blunt ends that would be repaired via the non-homologous end joining (NHEJ) pathway. To confirm that the genome has been edited, the forward primer (Fig. 3.9A: red arrow), which is complimentary to the sequences of the 5'-side of the genomic NHEJ product, was used in combination with either the 11780 (inner) or 5794 (outer) reverse primers that target the un-edited or edited 3'-side of the genomic NHEJ products, respectively. The amplicons produced by the inner primer set (241 bps) indicates failure to generate DNA double strand breaks and intact enhancer region, whereas amplicons produced by the outer primer set (296 bps) infers successful knock-out of the enhancer and repairing of the genome. I initially analyzed the PCR products using these primer sets in wild-type and B16-BL6 cells transfected with two different amounts (1 and 1.5 μg; herein termed CR1 and CR1.5) of the CRISPR editing plasmids. I found that only the inner amplicons were detected in non-transfected wild-type cells (Fig. 3.9B), which was an expected finding as the genomic region that spans the enhancer targeted by the outer primer set is too large to be amplified under the same PCR conditions (6229 bps). In contrast, both of the inner and outer primer sets yielded amplicons with expected sizes in cells transfected with the CRISPR editing plasmids (Fig. 3.9B). These results indicated that the gene-edited cells were likely heterogeneous cell populations that consisted of cells harboring the genomic sequences of the edited and un-edited regulatory element. Therefore, I selected 9 single colonies from these cells and re-analyzed for the enhancer knock-out. Among them, one colony (#4) showed PCR products from both inner and outer primers while only PCR products from the inner primers were detected in all of the other colonies (Fig. 3.9C). To further examine if colony #4 originated from a single cell, cells were sub-cloned and re-analyzed for the

genome edition status. PCR amplicons from the inner and outer primers were detected in all the 8 sub-colonies examined (Fig. 3.9D), suggesting that the colony contains a homogenous cell population harboring only one allele with successful gene editing.

3.2.3.1 Monoallelic deletion of the putative regulatory element compromises the production of IL-1β eRNAs and mRNA

To examine the role of the putative regulatory element in eRNA and IL-1β mRNA production, cells harboring the monoallelic regulatory element and wild-type cells were transfected with PU.1 for 48 h, then stimulated with LPS for 6 h. Cells with the monoallelic regulatory element produced significantly lower amount of eRNAs than cells with intact regulatory element based on qPCR assays using the 11743, 10841, 10368, and 9486 primer sets (Fig. 3.10A). In line with these results, expression of IL-1β mRNA was significantly reduced by ~70% in cells with monoallelic regulatory element than control cells (Fig. 3.10B).

Figure 3.9. Genetic deletion of the putative regulatory element by a CRISPR-Cas9 vector in B16-BL6 cells. A) Visual representation of the relative locations of CRISPR-Cas9-mediated cleavage sites, and primer sets used to validate the deletion of the enhancer region in B16-BL6 cells. PCR products of 241 and 296 bp sizes using the combination of the forward primer (12001: red arrow) and the inner (11780: black arrow) or the outer (5794: black arrow) reverse primers suggest unsuccessful and successful deletion of the putative regulatory element, respectively. The sequences 5'-AAATGCCAGCGCCCTGAGAG-3' and 3'-AGGCAAATTCAATGGGAATG-5' are complimentary to the gRNAs used, and the 3 bp DNA sequences highlighted in red indicate the PAM sequence. B) The PCR products amplified by the inner and outer primer sets were analyzed in wild-type and B16-BL6 cells transfected with CRISPR editing plasmids (1, 1.5 μg). Detection of bands for inner primer and outer primer sets indicate the presence or absence of the putative regulatory element, respectively. C and D) Gel electrophoresis analyses of the PCR amplicons from CR1(C)- and colony #4(D)-derived single colonies. Identical validation system described in (A) and used in (B) were employed to confirm the success of genome edition.

A)

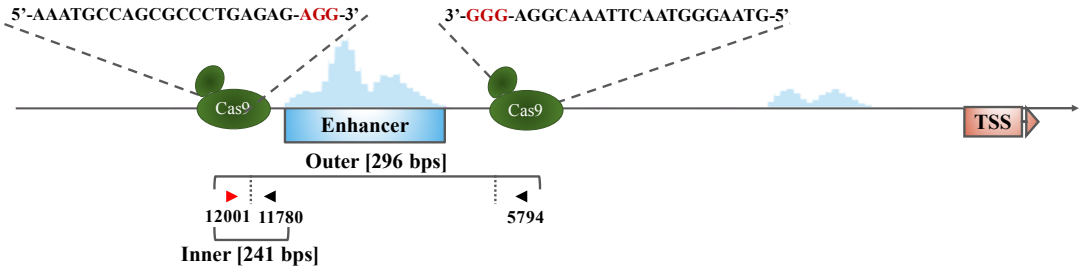
5'-AAATGCCAGCGCCCTGAGAG-AGG-3'
3'-GGG-AGGCAAATTCAATGGGAATG-5'
Cas9
Cas9
Enhancer
TSS
Outer [296 bps]
12001
11780
5794
Inner [241 bps]

B)

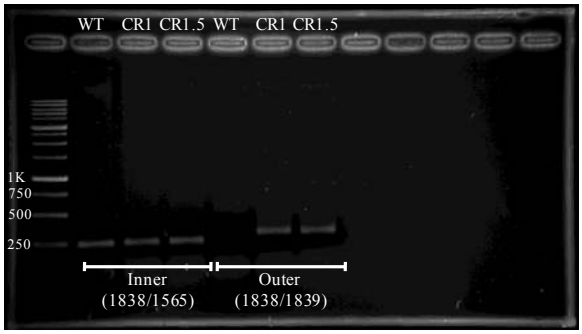
WT CR1 CR1.5 WT CR1 CR1.5
1K
750
500
250
Inner
(1838/1565)
Outer
(1838/1839)

C)

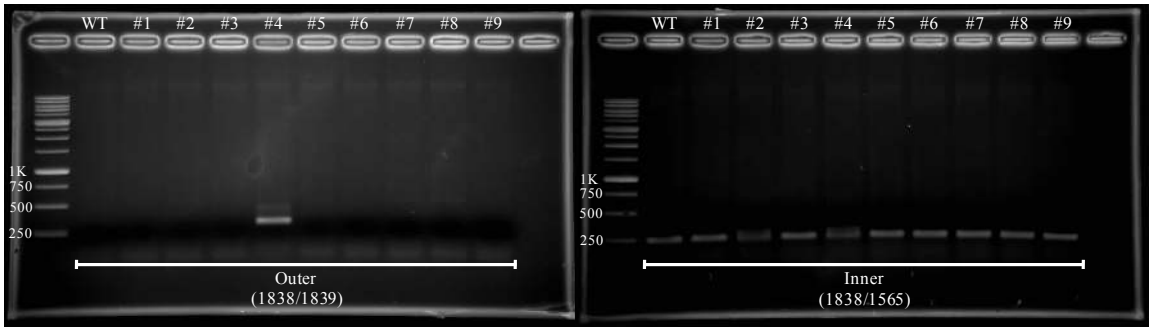
WT #1 #2 #3 #4 #5 #6 #7 #8 #9
1K
750
500
250
Outer
(1838/1839)
WT #1 #2 #3 #4 #5 #6 #7 #8 #9
1K
750
500
250
Inner
(1838/1565)

D)

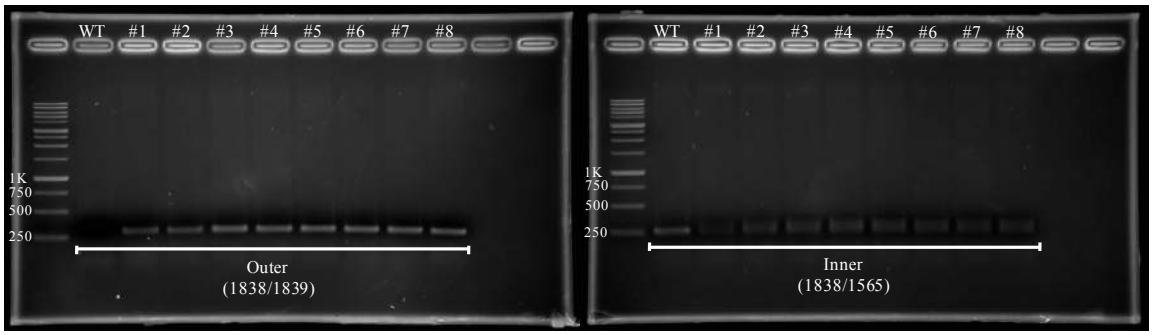
WT
#1
#2
#3
#4
#5
#6
#7
#8
1K
750
500
250
Outer
(1838/1839)
WT
#1
#2
#3
#4
#5
#6
#7
#8
1K
750
500
250
Inner
(1838/1565)

Figure 3.10. Monoallelic deletion of the putative regulatory element compromises the productions of eRNAs and IL-1β mRNA. A and B) PU.1 (0.7 μg) was transfected in wild-type and B16-BL6 cells with the monoallelic regulatory element with the transfection reagent Polyjet for 48 hours, then stimulated with LPS (100 ng/mL) for 6 hours. Cells were harvested and cDNA was prepared with RT-PCR. The qPCR amplicons of the eRNAs (A) using 11743, 10841, 10368, and 9486 primer sets and IL-1β mRNA (B) were analyzed. Data are expressed as means ± S.D. (n=3); *,$p < 0.05$,**,$p < 0.05$, ****,$p < 0.05$, Student's *t* test.

A)

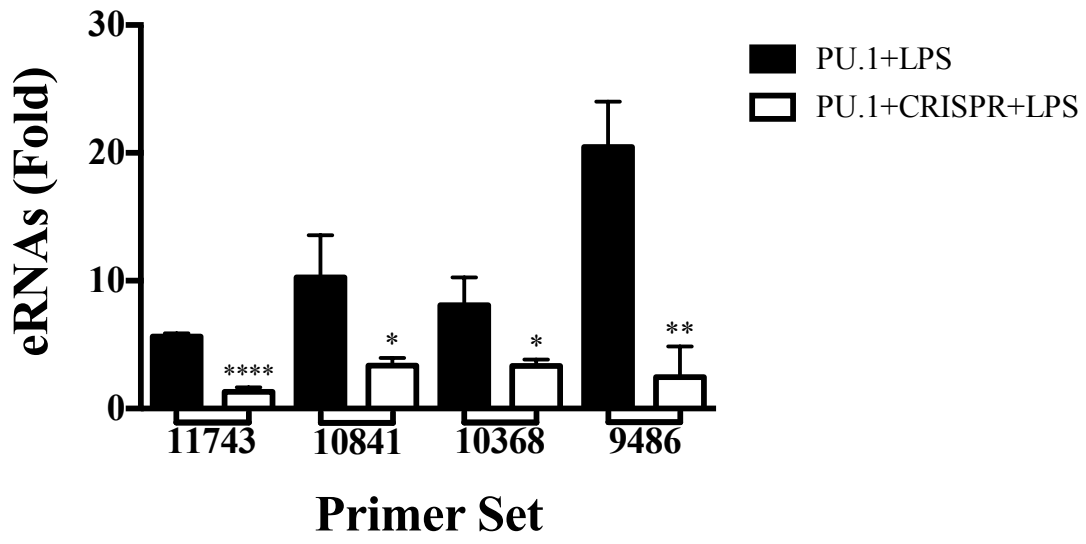
30
20
10
0
eRNAs (Fold)
PU.1+LPS
PU.1+CRISPR+LPS
****
*
*
**
11743
10841
10368
9486
Primer Set

B)

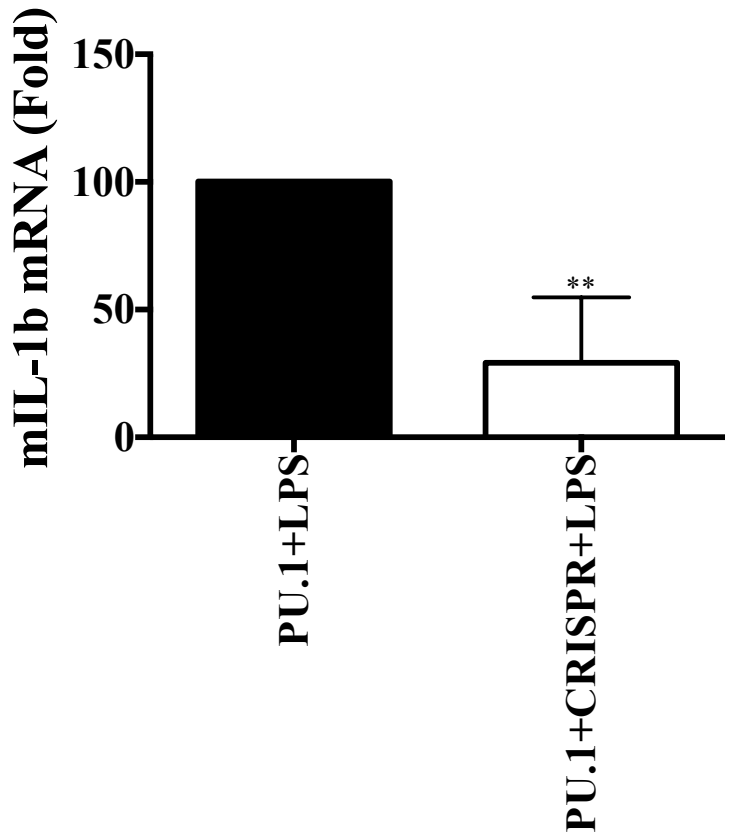
150
100
50
0
mIL-1b mRNA (Fold)
**
PU.1+LPS
PU.1+CRISPR+LPS

3.2.4 Knocking-down the putative eRNA suppresses IL-1β mRNA expression

To further examine the role of the eRNA produced in B16-BL6 cells, I first knocked down the eRNA using the ASO as described in Section 3.1.4. In line with previous results, LPS stimulation induced eRNA transcription by approximately 5-20 fold in PU.1-overexpressing B16-BL6 cells, and eRNA-ASO suppressed the production of eRNAs based on primer sets 10841, 10368, and 9486 by approximately 71%, 76.5%, and 76%, respectively (Fig. 3.11A). Also, IL-1β mRNA production in LPS-stimulated cells with the eRNA knocked-down was almost fully abolished (Fig. 3.11B), suggesting that the eRNAs also play a critical role in IL-1β mRNA expression in B16-BL6 cells expressing PU.1.

Figure 3.11. eRNAs regulate LPS-induced IL-1β response in PU.1-overexpressed melanoma cells. A and B) B16-BL6 cells were overexpressed with PU.1 (0.7 μg) for 48 hours, then re-transfected with scrambled- or eRNA-ASO (250 pmole) for 24 hours. Upon completion of transfection, PU.1-overexpressed B16-BL6 cells were exposed to LPS (100 ng/mL) for 6 hours. Expression levels of eRNAs (A) and IL-1β mRNA (B) were analyzed by qPCR. Data are expressed as means ± S.D. (n=3); *, $P < 0.05$, **, $P < 0.05$, ***, $P < 0.05$, Student's *t* test.

A)

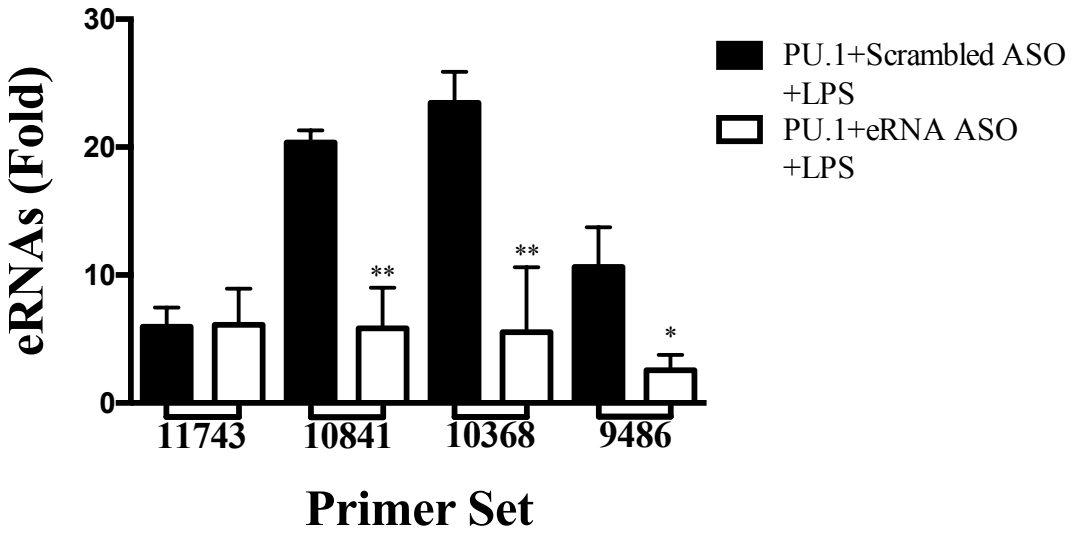
30
20
10
0
eRNAs (Fold)
**
**
*
11743
10841
10368
9486
Primer Set
PU.1+Scrambled ASO +LPS
PU.1+eRNA ASO +LPS

B)

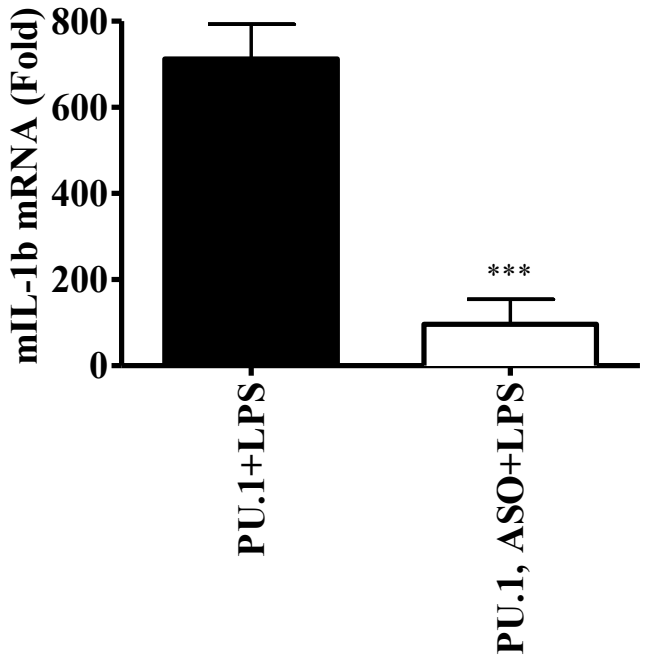
800
600
400
200
0
mIL-1b mRNA (Fold)
***
PU.1+LPS
PU.1, ASO+LPS

3.2.5 PU.1 orchestrates the interaction between the putative IL-1β regulatory element (enhancer) and promoter independent of stimulatory signal

We identified that our proposed genomic region serves as an enhancer of IL-1β by examining the characteristics that are required to define an enhancer. Specifically, PU.1-dependent activation of the enhancer induces the production of eRNAs, which contribute in the regulation of IL-1β. The ability of PU.1 to control the expression level of IL-1β piqued our interest in other potential methods of gene regulation. Hence, enhancer-promoter interactions were measured via 3C-TaqMan qPCR analysis to determine whether or not local chromatin landscape of IL-1β is altered as a consequence of PU.1 overexpression. To begin with, Fig. 3.12A shows that we detected basal level ligation between proximal fragments and the promoter of IL-1β in wild-type B16-BL6 cells, which likely occurred due to chance. Interestingly, we were also able to detect the interaction between the IL-1β promoter with a fragment ~15 kbs away, indicating that these regions are closely situated in the nuclear space. We then explored the role of PU.1 in promoting the formation of enhancer-promoter interactions (Fig. 3.12B). It is noteworthy that diagrams for LDTF-overexpressed cells only displays additional interactions that we detected on top of the interactions that occurred in the wild-type cells. Dissimilar to the case in wild-type melanoma cells, abundance of PU.1 induced chromatin looping between the enhancer and the promoter. Like macrophages, LPS stimulation of PU.1-overexpressed cells also enhanced the ligation frequency between the regulatory elements (Fig. 3.12C), suggesting that re-organization of the chromatin landscape is stimulus-dependent. Furthermore, ectopic expression of C/EBPα in B16-BL6 cells caused minimal ligation between the enhancer and the promoter (Fig. 3.12D). Since C/EBPα is not involved in promoting the generation of IL-1β mRNA and eRNAs, we speculated that the chromatin structure between unstimulated and stimulated C/EBPα-overexpressed cells would not differ; thus, 3C sample of stimulated cells was omitted and not prepared.

Next, we also quantitatively analyzed the effect of LPS treatment in promoting the interaction between the enhancer and the promoter in B16-BL6 cells overexpressed with both LDTFs. In agreement with cells that were solely transfected with PU.1, concomitant

expression of PU.1 and C/EBPα caused greater number of enhancer fragments to associate with the promoter of IL-1β upon LPS exposure (Fig. 3.12E, F). Finally, we examined the interaction between the regulatory elements in our CRISPR cell line (PU.1-overexpressed) with partial knock-out of the enhancer region. Although we expected reduced occurrence of enhancer-promoter interactions in CRISPR cells, we were still able to observe that the intact enhancer region physically associated with the IL-1β promoter via PU.1-mediated chromatin re-organization (Fig. 3.12G).

Figure 3.12. Overexpression of PU.1 induces physical interaction between the IL-1β enhancer and promoter. A-G) 3C-Taqman qPCR using the same combinations of primers as described in Fig. 3.6 was used to examine the enhancer-promoter interaction frequencies in wild-type, LDTF-overexpressing, and genome edited B16-BL6 cells. Wild-type B16-BL6 melanoma cells (A), cells that were transfected with PU.1 and/or C/EBPα (0.7 μg each; B-F), and cells with monoallelic regulatory element transfected with PU.1 (0.7 μg; G) were either unstimulated or stimulated with LPS (100 ng/mL) for 6 hours. The cells were harvested, underwent formaldehyde crosslinking, and lysed. The extracted nuclei were digested with 400 U of DpnII for 24 hours and subsequently ligated for 72 hours. The overarching arrows in (B-G) represent additional interactions between fragments with the IL-1β promoter that were detected on top of the background interactions shown in wild-type B16-BL6 cells (A). The bars in each diagram represent the frequencies of interaction between the promoter region targeted by the universal forward primer and any DNA regions that localize with the promoter in the nuclear space.

A)

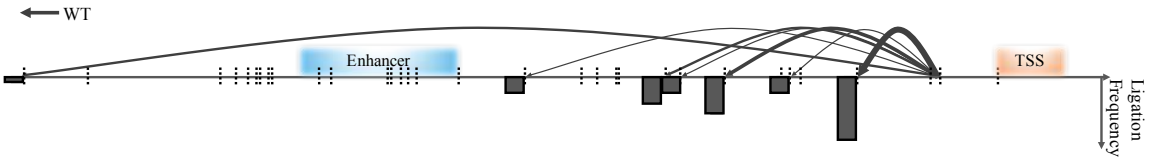
WT
Enhancer
TSS
Ligation Frequency

B)

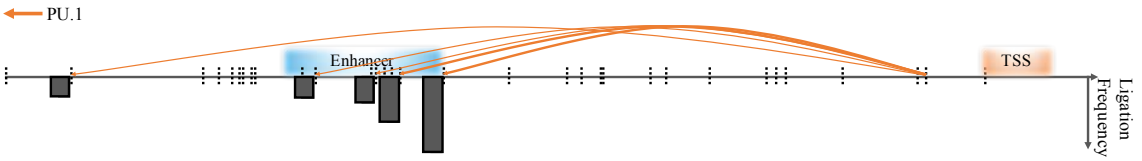
PU.1
Enhancer
TSS
Ligation Frequency

C)

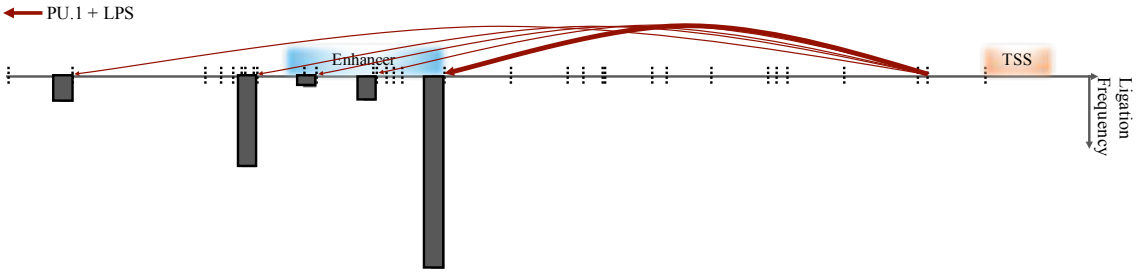
PU.1 + LPS
Enhancer
TSS
Ligation Frequency

D)

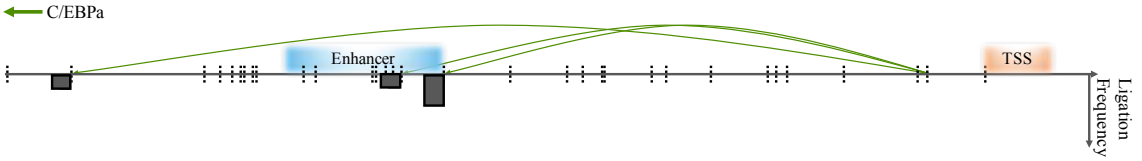
C/EBPa
Enhancer
TSS
Ligation Frequency

E)

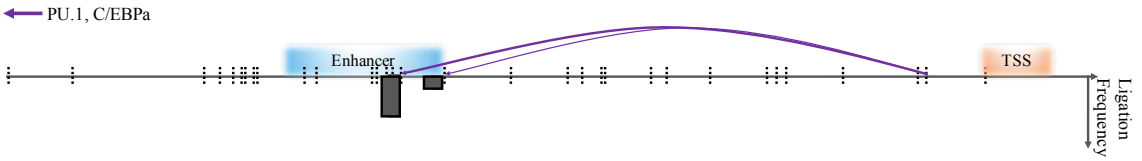
PU.1, C/EBPa
Enhancer
TSS
Ligation Frequency

F)

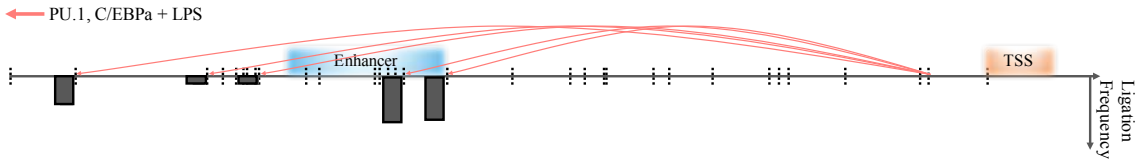
PU.1, C/EBPa + LPS
Enhancer
TSS
Ligation Frequency

G)

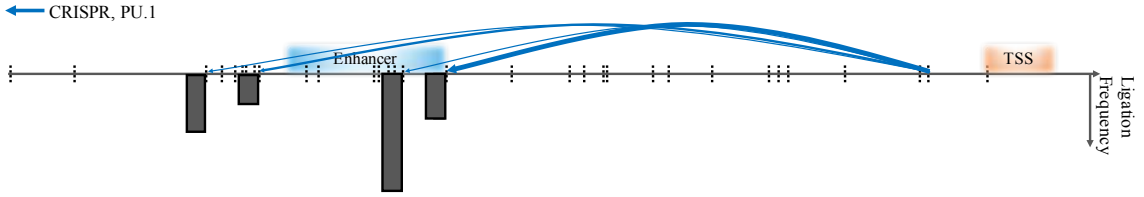
CRISPR, PU.1
Enhancer
TSS
Ligation Frequency

3.3 Elucidating the role of PU.1 domains in the IL-1β regulatory network

3.3.1 Examining the role of PU.1 domains in IL-1β eRNA and mRNA expression

It has been shown that PU.1 has four distinct domains: acidic, Gln-rich, PEST, and Ets (DNA binding) [99,135]. Fig. 3.13A illustrates the locations of these domains and constructs of PU.1 mutant plasmids obtained from Dr. Dekoter at UWO. To examine the role of each domain, wild-type PU.1 and its mutants were transfected in B16-BL6 cells, and production of IL-1β mRNA and the putative eRNA were analyzed. Cells transfected with PU.1 mutant plasmids lacking either the acidic (Δ2-30, Δ33-74) or the Gln-rich (Δ75-100) domain or with the mutated Ets domain ($PU.1^{R230, 233A}$: 230^{th} and 233^{rd} arginine residues have been replaced with alanine) failed to produce IL-1β mRNA in response to LPS, whereas cells transfected with the mutant lacking the PEST domain (Δ118-167) produced IL-1β mRNA to the same extent as cells transfected with wild-type PU.1 (Fig. 3.13B). Although changes in eRNA production was not as drastic as those of mRNA, a similar trend was observed where the levels of eRNA expression induced remained consistent in cells transfected with $PU.1^{WT}$ and $PU.1^{\Delta 118\text{-}167}$, but the levels were substantially reduced in cells transfected with $PU.1^{\Delta 2\text{-}30}$, $PU.1^{\Delta 33\text{-}74}$, $PU.1^{\Delta 75\text{-}100}$ and $PU.1^{R230, 233A}$ (Fig. 3.13C). These results suggest that the acidic, Gln-rich and Ets domains of PU.1 are required by the cells to generate IL-1β in response to LPS.

Figure 3.13. LPS-induced production of IL-1β is dependent on the acidic, Gln-rich, and Ets domains of PU.1. A) A schematic of PU.1 domains and the constructs of PU.1 mutant plasmids. Domains are represented by each coloured block; acidic (blue), Gln-rich (green), PEST (yellow), and Ets (red). B and C) B16-BL6 cells were transfected with PU.1 WT (1 μg) or PU.1 mutant ($PU.1^{\Delta 2\text{-}30}$, $PU.1^{\Delta 33\text{-}74}$, $PU.1^{\Delta 75\text{-}100}$, $PU.1^{\Delta 100}$, $PU.1^{\Delta 118\text{-}167}$, $PU.1^{R230,\ 233A}$) plasmids for 48 hours, then stimulated with LPS (100 ng/mL) for 6 hours. The production of IL-1β mRNA (A) and eRNAs (B) were analyzed by qPCR. Data are expressed as means ± S.D. (n=2); *, $P < 0.05$, **, $P < 0.05$, ***, $P < 0.05$ ANOVA.

A)

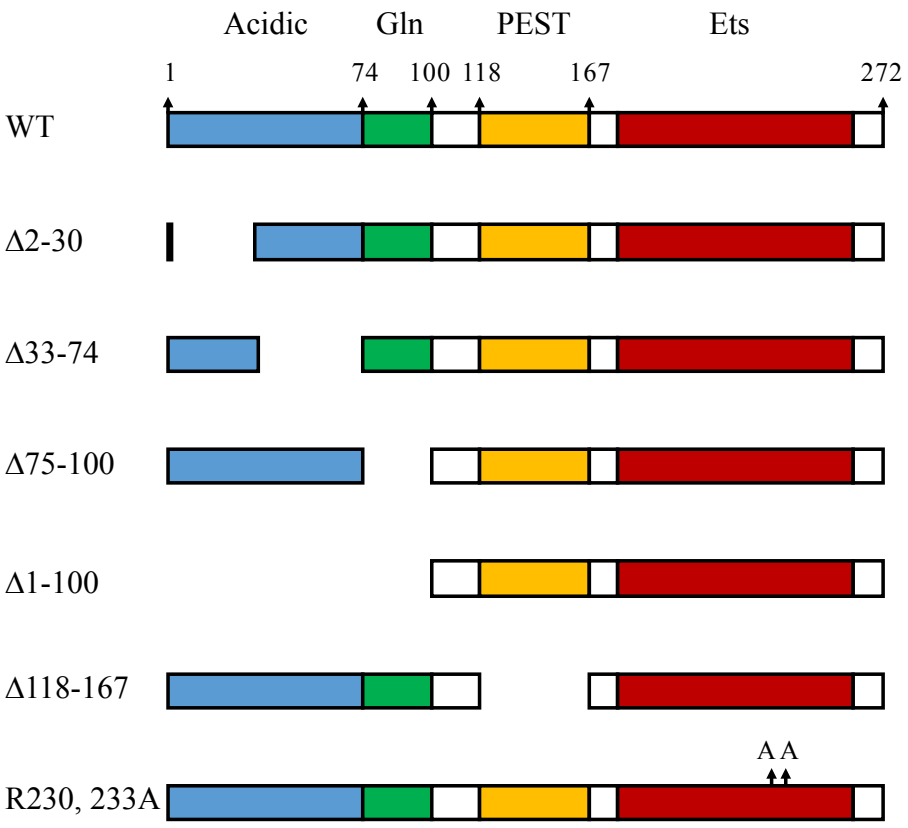
Acidic
Gln
PEST
Ets
1
74
100
118
167
272
WT
Δ2-30
Δ33-74
Δ75-100
Δ1-100
Δ118-167
A A
R230, 233A

B)

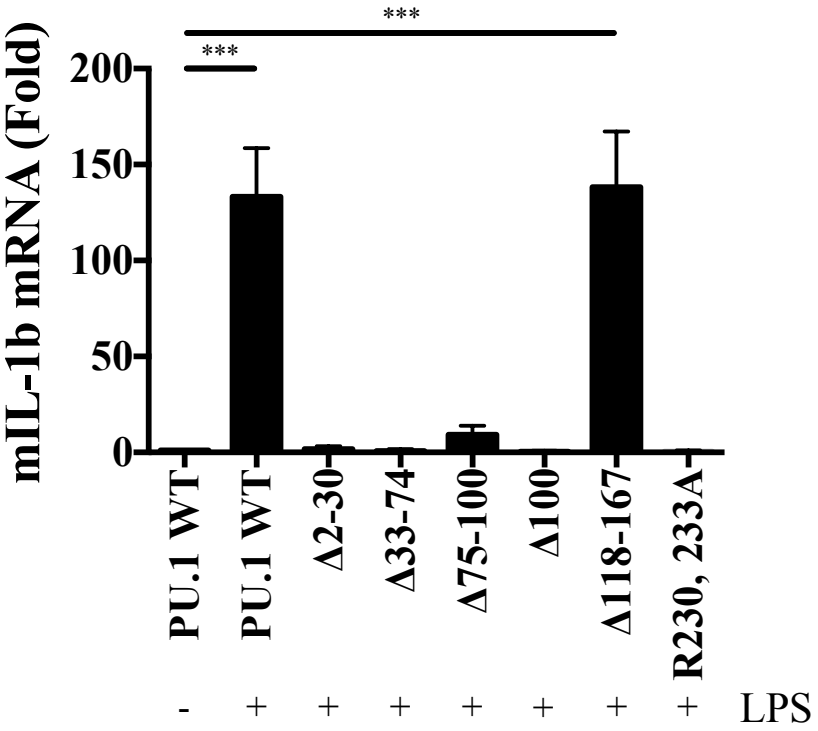
***
***
mIL-1b mRNA (Fold)
200
150
100
50
0
PU.1 WT
PU.1 WT
Δ2-30
Δ33-74
Δ75-100
Δ100
Δ118-167
R230, 233A
- + + + + + + + LPS

C)

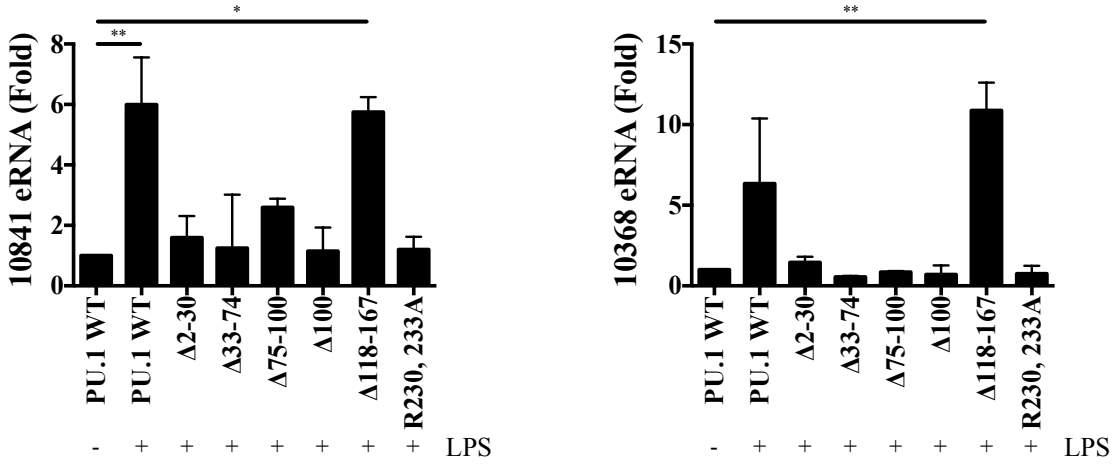
*
**
10841 eRNA (Fold)
8
6
4
2
0
PU.1 WT
PU.1 WT
Δ2-30
Δ33-74
Δ75-100
Δ100
Δ118-167
R230, 233A
- + + + + + + + LPS
**
10368 eRNA (Fold)
15
10
5
0
PU.1 WT
PU.1 WT
Δ2-30
Δ33-74
Δ75-100
Δ100
Δ118-167
R230, 233A
- + + + + + + + LPS

3.3.2 Examining the involvement of PU.1 domains in the IL-1β enhancer-promoter interaction

In section 3.2.5, I showed that overexpression of PU.1 promoted the interaction between the enhancer and the promoter. To further examine the involvement of each PU.1 domain in the IL-1β enhancer-promoter interaction, B16-BL6 cells were transfected with wild-type and various mutants ($PU.1^{\Delta 33\text{-}74}$, $PU.1^{\Delta 75\text{-}100}$, $PU.1^{\Delta 100}$, $PU.1^{\Delta 118\text{-}167}$, and $PU.1^{R230,\ 233A}$) of PU.1. The interaction between the enhancer and the promoter in the reprogrammed B16-BL6 cells was analyzed via 3C-TaqMan qPCR only using the primers that target the five fragments within the putative enhancer. Expectedly, overexpression of $PU.1^{WT}$ in B16-BL6 cells restructured the genome to cause the enhancer and the promoter of IL-1β to interact (Fig. 3.14A). Similar to $PU.1^{WT}$-transfected cells, the enhancer-promoter interaction in melanoma cells ectopically expressed with PU.1 mutants remained intact (Fig. 3.14B-F), as majority of the fragments that spanned the enhancer ligated with the IL-1β promoter. Although only the $PU.1^{\Delta 118\text{-}167}$ mutant induced the IL-1β eRNA and mRNA (Fig. 3.13) while all other PU.1 mutants were unable to do so, the extent of the enhancer-promoter interaction in $PU.1^{\Delta 33\text{-}74}$-, $PU.1^{\Delta 75\text{-}100}$-, and $PU.1^{\Delta 118\text{-}167}$-overexpressed cells did not change when compared to that of cells transfected with wild-type PU.1 (Fig. 3.14B, C, E). Interestingly, simultaneous knock-out of the acidic and Gln-rich domains ($PU.1^{\Delta 100}$) resulted in decreased enhancer-promoter interaction frequency. These data suggest that both the acidic and Gln-rich domains of PU.1 act in concert to reorganize the chromatin while the PEST domain is dispensable for the enhancer-promoter interaction. Similar to the $PU.1^{\Delta 100}$ mutant, mutation in the DNA binding domain ($PU.1^{R230,\ 233A}$) also disrupted the interaction between the regulatory elements; which was an expected finding, as such mutation can inhibit PU.1 binding to the DNA. Furthermore, in order to compare the enhancer-promoter interaction frequencies between samples from Fig. 3.14, the ligation frequencies between individual fragments in the putative enhancer with the IL-1β promoter were summed. As illustrated in Fig. 3.14G, the interaction between the enhancer and the promoter of IL-1β were significantly reduced in melanoma cells ectopically expressed with $PU.1^{\Delta 100}$ and $PU.1^{R230,\ 233A}$; indicating that not only do acidic/Gln-rich and DNA binding domains have roles in gene transactivation and DNA binding capacity of PU.1, respectively, but also partake in chromatin organization.

Figure 3.14. The acidic, Gln-rich, and DNA binding domains of PU.1 mediate IL-1β enhancer-promoter interaction. A-F) PU.1 (A) or PU.1 mutant (domains deleted: acidic – B, Gln-rich – C, acidic & Gln-rich – D, PEST – E, domain mutated: DNA binding – F) was overexpressed in B16-BL6 melanoma cells. Upon completion of the 48 hour transfection period, 3C library was prepared from cells that underwent a cycle of crosslinking, restriction enzyme digestion (400 U DpnII) and ligation. The physical association of the enhancer and the promoter was quantified via TaqMan qPCR. The black arrows in (A-F) represent the occurrence of ligation between fragments positioned within the putative enhancer with the IL-1β promoter. The upright grey bars in each diagram represent the frequencies of interaction between the promoter region and the distal enhancer fragments. G) The quantitative values of ligation frequencies represented as bars in (A-F) were totaled and compared. The ligation frequency between the enhancer and the promoter of IL-1β in B16-BL6 cells overexpressed with wild-type PU.1 was used as the control. Data are expressed as means ± S.D. (n=2); *, $P < 0.05$, **, $P < 0.05$, ANOVA.

A)

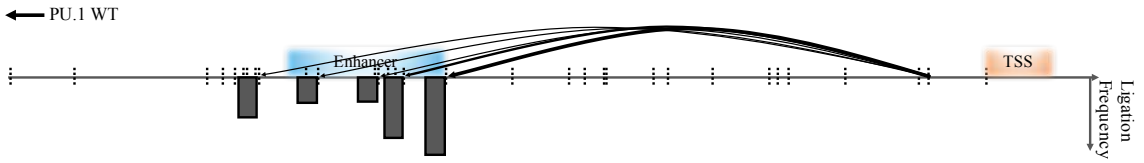
PU.1 WT
Enhancer
TSS
Ligation Frequency

B)

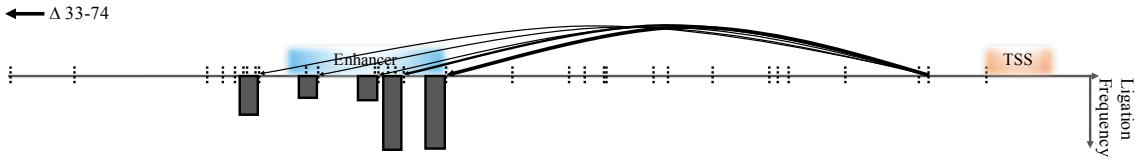
Δ 33-74
Enhancer
TSS
Ligation Frequency

C)

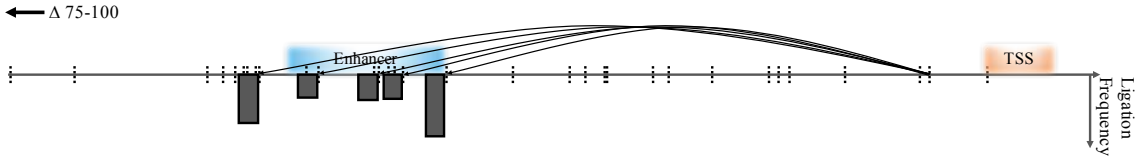
Δ 75-100
Enhancer
TSS
Ligation Frequency

D)

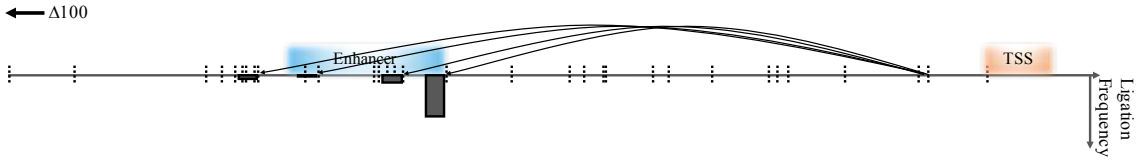
Δ100
Enhancer
TSS
Ligation Frequency

E)

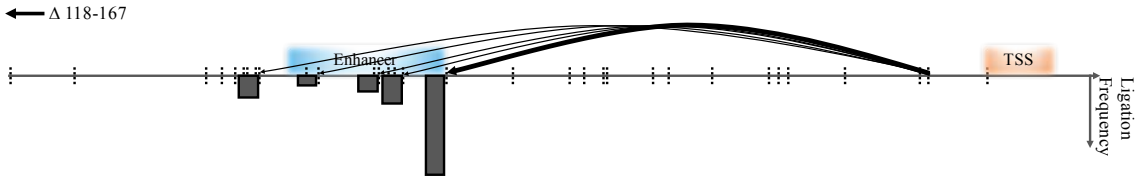
Δ 118-167
Enhancer
TSS
Ligation Frequency

F)

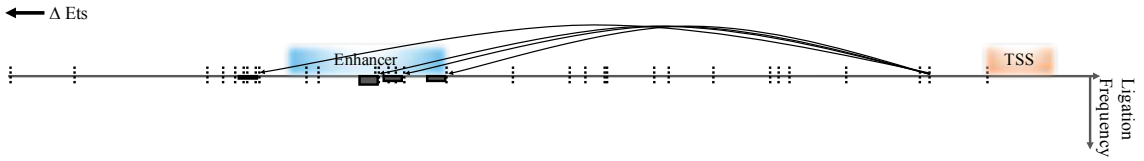
Δ Ets
Enhancer
TSS
Ligation Frequency

G)

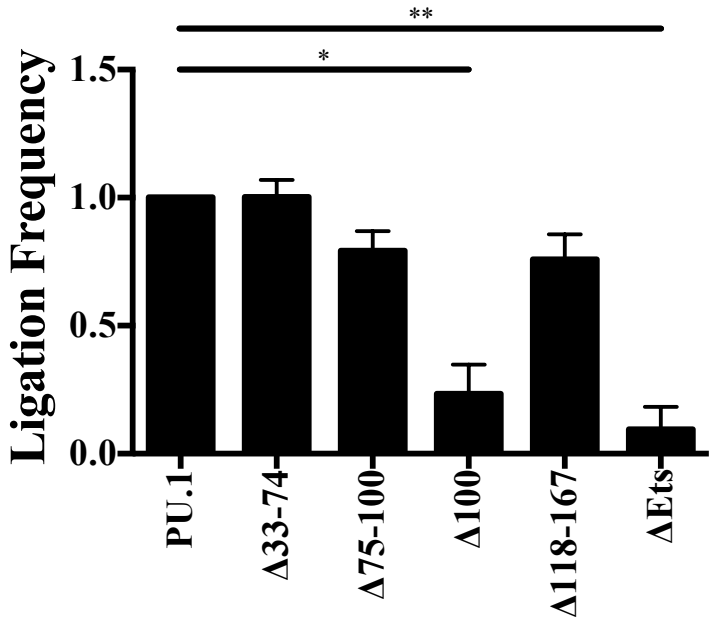
**
*
Ligation Frequency
1.5
1.0
0.5
0.0
PU.1
Δ33-74
Δ75-100
Δ100
Δ118-167
ΔEts

Chapter 4

4 Discussion

In this study, I proposed that the genomic region located ~10 kbs upstream of the IL-1β TSS is an enhancer regulating the expression of IL-1β, based on histone modification markers: H3K27Ac^{hi}, H3K4me1^{hi}, and H3K4me3^{low} (Fig. 3.1). It has been suggested that eRNAs are dynamically transcribed as a consequence of enhancer activation [136]. Therefore, I first examined whether the genomic region produced eRNAs in response to LPS in RAW264.7 cells (Fig. 3.2B, C). Upon LPS treatment, eRNA(s) was rapidly generated and reached a peak level in 90 mins, which was earlier than that of IL-1β mRNA that reached maximal production at 180 mins post LPS stimulation (Fig. 3.2D). These results were consistent with previous studies showing that transcription of enhancers precede production of mRNAs [137-139]. Specifically, de Santa *et al*. demonstrated that transcripts generated from genomic regions with enhancer-specific chromatin signatures (H3K4me1^{hi} and H3K4me3^{low}) upstream of the chemokines, chemokine ligand 5 (Ccl5) and C-X-C motif chemokine 11 (Cxcl11), were detected at an earlier time point than mRNAs in LPS-stimulated macrophages [138]. They employed ChIP-seq to show that the production of these transcripts was the result of LPS-induced binding of Ser5P (phosphorylated Serine 5 of CTD) RNAPII at the genomic regions [138]. Furthermore, another study demonstrated that transcription of enhancers preceded their proximal promoters in various cell types including stem cells, differentiating committed progenitor cells, and terminally differentiated primary cells [137]; suggesting that early transcription of eRNAs is a general phenomenon and can be a necessity for upregulation of target genes. Thus, the rapid production of the putative eRNA before the advent of IL-1β mRNA may suggest a role of the eRNA in IL-1β mRNA expression. I examined the role of the putative eRNA in IL-1β mRNA expression using the anti-sense eRNA targeting ASO (Fig. 3.4). Through successful knock-down of the eRNA, the expression of IL-1β mRNA was also suppressed; inferring that the eRNA is not just a by-product of enhancer transcription, but is a functionally important molecule involved in the regulation of IL-1β. My results were in line with several other studies that also showed that suppression of eRNAs by short hairpin (sh) RNA, siRNA, and ASO reduced

their cognate gene transcription [80,140,141]. In particular, Lam *et al*. demonstrated that the expression levels of matrix metallopeptidase 9 (*Mmp9*) and CX3C chemokine receptor 1 (*Cx3cr1*) genes were attenuated upon ASO-mediated inhibition of *Mmp9* and *Cx3cr1* eRNAs, respectively, in BMDMs [115]. Furthermore, they engineered a reporter plasmid that comprised the *Mmp9* enhancer upstream of the *Mmp9* promoter, which controlled the *Luc* expression [115]. When the sequence of the sense eRNA was removed from the *Mmp9* enhancer, Lam *et al*. reported that the *Luc* expression decreased, whereas the presence or the absence of the antisense eRNA sequence did not affect the activity of the *Mmp9* promoter [115]; concluding that the *Mmp9* enhancer regulates the transcription of *Mmp9* gene via eRNAs in a strand- and orientation-dependent manner. Considering that eRNAs can be transcribed bi-directionally, knock-down of the sense eRNA transcribed from the IL-1β enhancer can address whether or not eRNA-mediated regulation of IL-1β is orientation-specific. Moreover, through ddPCR experiments I showed that high levels of eRNA production were detected in the central region (between primer sets 8453-10841) of the enhancer (Fig. 3.3B). In addition, eRNA detected by 9013 and 11743 primer sets did not increase to the same extent as shown in the qPCR data, suggesting that the actual eRNA produced from the putative regulatory element could be an uni-directional long non-coding RNA approximately 2500 bps in size. However, this speculation is inconsistent with the current notion that the median length of eRNAs is ~350 bps [94]. Not only that, ChIP-seq analysis of RNAPII in Fig. 3.1 illustrates that RNAPII is dispersed (mainly enriched at two distinct regions) within the H3K27Ac-enriched enhancer region. Taking into account that LPS exposure of macrophages resulted in the enrichment of Ser5P RNAPII at enhancers, it is highly probable that the pre-docked RNAPII at the enhancer are paused, which are eventually converted into the elongation phase upon cell activation. Therefore, I surmise that the transcripts generated from the enhancer are not uni-directional, but are rather bi-directional transcripts that vary in size and orientation (sense and antisense).

Another checkpoint that needed to be fulfilled in order to label the proposed genomic region as an enhancer was that the distal enhancer and the promoter must be in the vicinity of one another irrespective of any intervening DNA [129,142,143]. Here, I found that the local chromatin landscape of IL-1β was altered, and the enhancer-promoter

interaction was established in a stimulus (LPS)-dependent manner in macrophages (Fig. 3.6C). This observation is in line with a previous study that demonstrated the communication between the IL-1β promoter with another potential enhancer (~3 kbs upstream of TSS) in LPS-exposed macrophages [144], suggesting that an extracellular stimulus is required and necessary to remodel the chromatin architecture of IL-1β. Despite the fact that low levels of IL-1β are constitutively expressed in macrophages, remodeling of the chromatin architecture, which brings distal regulatory elements into proximity, is absolutely necessary for rapid induction of IL-1β. There are multiple factors that are involved in the formation of enhancer-promoter interactions. For example, Lai *et al*. reported that shRNA-mediated knock-down of MED1 and MED12 subunits abolished the interaction between the zinc finger protein *SNAI1* gene and its enhancer in HEK293 cells [110]. Another group has highlighted the role of cohesin in establishing enhancer-promoter interactions by depleting the cohesin subunit, double-strand-break repair protein (RAD21), in MCF-7 cells stimulated with 17β oestradiol; essentially abrogating the interaction between the regulatory elements of the nuclear receptor-interacting protein 1 (*NRIP1*) gene [80]. Intriguingly, the mediator complex and cohesin tend to co-occupy enhancers and promoters, and it has been shown that the recruitment of these protein complexes is mediated by eRNAs [80,110,119]. In this study, I saw a correlation between the enhancer-promoter ligation frequency and eRNA production in LPS-stimulated macrophages, potentiating the role of eRNAs in remodeling the chromatin landscape of IL-1β via recruitment of the Mediator complex and cohesin.

It is generally believed that a cell-type specific repertoire of enhancers is chosen by various LDTFs [145]. It has been shown that nucleosome depletion and subsequent recruitment of LDTFs to putative enhancers are events that occur prior to the deposition of unique chromatin signatures like H3K4me1^{hi} and H3K4me3^{low} [145,146]. Specifically, PU.1 is a LDTF that has the ability to select macrophage-specific enhancers [146], which induce the upregulation of genes essential for macrophage differentiation and function. Previously, it was shown that overexpression of PU.1 and C/EBPα transdifferentiated the NIH 3T3 murine fibroblast cells into macrophage-like cells that displayed macrophage morphology, and acquired the ability to produce cytokines and phagocytose bacteria [147]. This led me to hypothesize that enhancers of IL-1β are recognized and activated by

PU.1. In order to determine whether or not activation of the enhancer is PU.1-dependent, I took an alternative approach and used non-myeloid B16-BL6 cells that do not produce IL-1β mRNA but respond to LPS (Appendix A, Fig. 3.7B). I found that ectopic expression of PU.1 in the B16-BL6 cells induced eRNA and IL-1β mRNA transcription upon exposure to LPS (Fig. 3.8B, 3.7B). Additionally, through CRISPR-Cas9-mediated knock-out of the enhancer followed by PU.1 overexpression, I observed reduced expression of eRNAs and IL-1β mRNA (Fig. 3.10), suggesting that the genomic region serves as the enhancer of IL-1β. Moreover, ASO-mediated knock-down of the eRNA inhibited IL-1β expression (Fig. 3.11). These results indicate that PU.1, which drives macrophage differentiation at high concentrations [102], recognized and opened up the macrophage-specific IL-1β enhancer in B16-BL6 cells. It has been reported that PU.1 promotes the deposition of H3K4me1 and recruitment of p300 at enhancers in macrophages [103,104]. Furthermore, stimulation of macrophages induces the binding of p65 (active subunit of NF-κB) at PU.1/p300 co-occupied, and H3K4me1-enriched enhancer regions [65]; suggesting that LPS-induced production of eRNAs in PU.1-overexpressed B16-BL6 cells is the result of these sequence of intracellular events. Conversely, C/EBPα had minimal impact on the production of both transcripts, which is expected as abundance of C/EBPα is associated with the development of granulocytes and neutrophils [107,108]. However, the role of C/EBPα should not be neglected as low level of endogenous C/EBPα mRNA was detected in B16-BL6 cells (data not shown). Since majority of macrophage-specific enhancers tend to be co-occupied by PU.1 and C/EBP family of proteins [86,148,149], which recruit p65 most efficiently [129], it is likely that both LDTFs are required for the activation of the IL-1β enhancer.

Moreover, I utilized 3C analysis to investigate the role of LDTFs in reorganizing the chromatin landscape, specifically resulting in the formation of IL-1β enhancer-promoter interactions, whether it be solely under the influence of PU.1, C/EBPα or the combination of the two LDTFs. It has previously been shown that PU.1 has the capacity to remodel the chromatin architecture and mediate enhancer-promoter interactions [130,150]. For example, PU.1 is able to autoregulate itself by binding to a distal enhancer (~14 kbs upstream of the PU.1 TSS) and bridging its physical association with the PU.1 promoter in hematopoietic stem cells and macrophages [150]. Likewise, as presented in Fig. 3.12B,

I found that the physical association of the IL-1β enhancer and promoter occurred upon ectopic expression of PU.1 in B16-BL6 cells. The PU.1-dependent association of the regulatory elements was absent in RAW264.7 macrophages, indicating that higher concentration of PU.1 may be required for the enhancer-promoter interaction to be pre-formed. Furthermore, C/EBPα also had the capacity to bridge the interaction between the enhancer and the promoter (Fig. 3.12D), which was an unexpected finding because this TF did not render the B16-BL6 cells to express IL-1β (Fig. 3.7B). Enhancer-promoter interactions in C/EBPα-overexpressed cells could have emerged due to low levels endogenous PU.1 in the cells, which could be generated by C/EBPα-mediated activation of the PU.1 promoter and distal enhancer [151,152]. These results indicate that both LDTFs, whether directly or indirectly, partake in the formation of enhancer-promoter interactions prior to LPS challenge. Moreover, similar to macrophages, LPS stimulation of the reprogrammed melanoma cells increased the interaction frequency between the IL-1β regulatory elements. This observation signifies that the the enhancer-promoter interaction in the IL-1β regulatory network is stimulus-dependent, and supports the potential involvement of eRNAs is mediating the communication between the regulatory elements.

PU.1 is a 271 amino acid long protein with four distinct domains. Since PU.1 is deemed the master regulator of IL-1β transcription in the reprogrammed B16-BL6 cells, I was interested in examining the role of each PU.1 domain in promoting the expression of IL-1β eRNAs and mRNA, as well as enhancer-promoter interactions. As the PU.1 mutants had contrasting effects on the overall production of IL-1β mRNA and eRNAs (Fig. 3.13B, C), we predicted that the frequency of enhancer-promoter interactions orchestrated by these PU.1 variants would also differ. To our surprise, there was no significant change in how frequently the regulatory elements of IL-1β ligated in cells overexpressed with the PU.1 variants, despite complete abrogation of IL-1β mRNA and eRNAs in PU.1$^{\Delta 33\text{-}74}$- and PU.1$^{\Delta 75\text{-}100}$-transfected cells (Fig. 3.14). Most interestingly, concomitant knock-out of the acidic and Gln-rich domains of PU.1 (PU.1$^{\Delta 100}$) attenuated the interaction between the enhancer and the promoter of IL-1β. Thus, these findings lead to the conclusion that single domains of PU.1 are not responsible for the establishment of

chromatin looping between the enhancer and the promoter, but are dictated by the cooperation of two domains in the N-terminus of PU.1. Reorganization of the chromatin landscape mediated by the acidic and Gln-rich domains could potentially be an underlying mechanism of their ability to transactivate genes. Furthermore, there are other potential candidates that could collaborate with PU.1 to rearrange the chromatin. The first group of candidates is HATs such as CBP and p300, which directly interact with the Gln-rich domain of PU.1 [153,154]. Although the role of HATs in enhancer-promoter interactions has not yet been demonstrated, they are transcription co-factors that co-localize with pioneer factors and acetylate unique residues of histones [47,81]. Specifically, Whalen *et al.* exemplified the enrichment of H3K27Ac at interacting regulatory elements [155], which extends the possibility that the proteins responsible for the deposition of such chromatin signature may be essential for the interaction to occur. Brd4, a protein that contains 2 bromodomains, is the other candidate that could bring the regulatory elements into vicinity. It has been postulated that Brd4 binds enhancers (co-occupied by PU.1) and promoters to promote transcription [156,157]. The Brd-4-specific inhibitor, JQ1, could be used to suppress Brd-4 mediated generation of the putative eRNA to study its role in chromatin remodeling. Lastly, it has been demonstrated that 5hmC, the oxidized metabolite of 5mC, accumulates at enhancers and is associated with enhancer activity [158,159]. Hon *et al*. has previously shown that Tet2-mediated conversion of 5mC to 5hmC at enhancers correlated with binding of various TFs such as Oct4 and Sox2 in mouse embryonic stem cells [158]. Interestingly, PU.1 is able to physically interact and recruit Tet2, possibly suggesting that hypomethylated state of regulatory elements may contribute in chromatin reorganization [160].

In summary, I identified an enhancer of IL-1β that lies ~10 kbs upstream of the TSS. This particular enhancer was activated by PU.1, which serves as the pioneer transcription factor that recruits other necessary components to initiate transcription of the putative eRNA in response to LPS stimulation. Most notably, in the presence of abundant PU.1, intra-chromosomal interaction between the enhancer and the promoter was formed, which was further enhanced upon stimulation of the cells with LPS. Fig. 4.1 illustrates my working model of PU.1 and IL-1β enhancer-promoter looping formation. This study

unraveled the mechanisms by which PU.1 regulates the expression of IL-1β in response to LPS stimulation.

4.1 Clinical significance and therapeutic treatment

The concept of chromatin architecture has recently garnered attention as it adds a layer of complexity in gene regulation. Thorough analysis of how the chromatins are organized can be used to define the overall state or identity of cells. For example, taking into account that a repertoire of enhancers is cell-type specific, malignant cells with unique gene expression profiles will display enhanced physical association between the regulatory elements of highly active genes; thus, our knowledge of chromatin architecture can be considered as a preventive measure. This is also applicable in our attempt to regulate the expression of IL-1β. In many IL-1β-induced diseases, we can analyze whether or not the uncontrolled expression of the cytokine is caused by high interaction frequency between our proposed enhancer and the promoter. If so, considering that eRNAs are one of the determinants of enhancer-promoter interactions [80,110,111], sequence-specific ASO can be employed to target the eRNAs and disrupt their activity.

Figure 4.1. Schematic representation of how the IL-1β regulatory network is modulated by PU.1. Enhancer-promoter interactions are pre-formed at high concentrations of PU.1. PU.1 has an additional role of recruiting p300/CBP and Tet that can deposit epigenetic marks such as H3K27Ac and 5hmC on histones and cytosine, respectively. Acetylated lysines of histone H3 are recognized by Brd4, which activates P-TEFb to initiate transcription of IL-1β eRNA and mRNA.

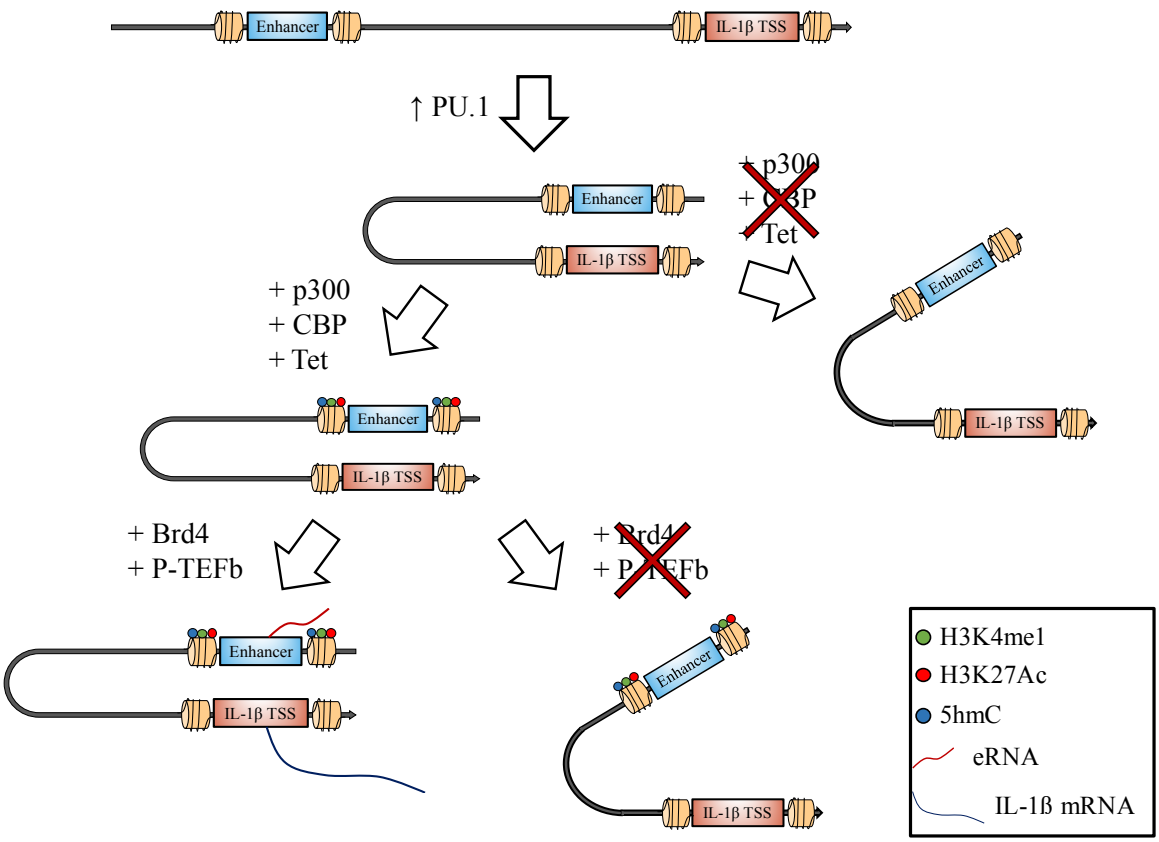
Enhancer
IL-1β TSS
↑ PU.1
+ p300
+ CBP
+ Tet
+ Brd4
+ P-TEFb
H3K4me1
H3K27Ac
5hmC
eRNA
IL-1ß mRNA

4.2 Future studies

4.2.1 Identifying other active enhancers of IL-1β via 3C-derivative experiments

It is widely accepted that multiple enhancers work in concert to trigger transcription of genes. However, the ability of enhancers to function over long distances makes it challenging for investigators to pinpoint their cognate genes. This study used 3C-TaqMan qPCR to quantitatively analyze the physical association between the IL-1β enhancer and promoter. A disadvantage of 3C analysis is that only known sequences of the captured fragment (enhancer) and the bait (promoter) are examined [161]; thus, this particular technique cannot be utilized for genome-wide studies. In order to overcome the limit, 3C-derivative experiments such as 4C (3C-seq; 3C followed by next generation sequencing) has gained popularity in recent years. Therefore, 3C is often described as a one-to-one approach and 4C is a one-to-all approach [162]. In contrast to using a single 4-cutter restriction enzyme in 3C, two rounds of digestion are performed in 4C [163]. The primary digestion step, which involves digestion of the crosslinked DNA with a 6-cutter restriction enzyme and a subsequent ligation step, is followed by a secondary digestion/ligation step to generate small circular DNA [162,163]. The ligated captured-bait fragments are then amplified with bait-specific primers via PCR, and the resulting products are sequenced through NGS [162,163]. Our lab has performed 4C analysis using IL-1β promoter as the bait and identified 5 other genomic locations that formed intra-chromosomal interactions (Appendix B). These interactions now can be confirmed by 3C analysis or reverse 4C (using the candidate enhancers as the bait).

4.2.2 Elucidating the role of epigenetic modifiers in IL-1β regulation

The level of histone acetylation is determined by the interplay between HATs and HDACs [164-166]. Histone acetylation initiates depletion of nucleosomes, rendering DNA accessibility to various transcription factors [167]. For example, Frank *et al.* showed that inhibition of HDACs results in remarkable changes in chromatin accessibility and PU.1 preferentially associated with euchromatin [168]. Although the dynamic switch from euchromatin to heterochromatin is dictated by HDACs, the ability of these histone modifiers to remodel the chromatin architecture on a genome-wide scale

has not yet been determined. Our lab showed that HDAC8, a member of class I HDACs, selectively deacetylates H3K27Ac [169]. In addition, the diminished levels of H3K27Ac are in line with reduced eRNA and IL-1β mRNA production [169]. Considering that H3K27Ac is a unique marker of active enhancers, I speculate that the mechanism of HDAC8 in regulating IL-1β expression is likely through enhancing the enhancer-promoter interaction. Since I identified the IL-1β enhancer, it will be interesting to examine whether HDAC8 is involved in the enhancer-promoter interaction through 3C analysis in macrophages. We expect that overexpression of HDAC8 will abolish the enhancer-promoter interaction; whereas, HDAC8 inhibition will result in higher frequency of the interaction.

4.2.3 Examining the mechanism of macrophage tolerance

As previously mentioned, plasticity and heterogeneity are hallmarks of macrophages. Tissue-resident macrophages are scattered throughout the body, and have the capacity to generate appropriate responses according to the environmental cues [170,171]. Amongst many stimuli that foster cell-type specific responses, prolonged exposure to LPS can result in the development of a phenomenon known as LPS tolerance [172,173]. In this hyporesponsive state, macrophages become refractory to a secondary LPS challenge [173,174]. Another notable environmental stimulus that suppresses macrophage activation is the probiotic strain such as *Lactobacillus rhamnosus* GR-1 [175]. Similar to LPS-tolerated macrophages, pre-exposure of macrophages to *L. rhamnosus* GR-1 abrogated expression of IL-1β. Granulocyte colony stimulating factor (G-CSF), which is well-known for its involvement in the generation of neutrophils, is an immunoregulatory cytokine that leads macrophages to immunomodulatory cells [176,177]. Contrastingly, recent discoveries documented that macrophages can be converted into nonspecific innate memory cells upon initial exposure to β-glucan [178]. In this trained state, macrophages have acquired the ability to generate a stronger response to secondary stimuli [178,179]. Interestingly, increased responsiveness of trained macrophages is the product of elevated H3K27Ac and H3K4me3 levels at distal enhancers and promoters, respectively [178,180]. Epigenetic reprogramming of innate memory cells raises the possibility that macrophage tolerance is regulated via similar epigenetic mechanisms. Furthermore, such

phenotypic variance of macrophages prompts us to investigate if different activity states, particularly in regards to IL-1β production, are affected by enhancer-promoter interactions; which can be determined through 3C-Taqman qPCR. We speculate that macrophage training is largely associated with enhanced interaction between the regulatory elements while LPS-, GR-1-, and G-CSF-mediated tolerance will show opposing results. These findings could be directly linked to epigenetic reprogramming of the genome, and various histone modifiers can be targeted to modulate chromatin reorganization.

References

1. Mosser, D. M. & Edwards, J. P. Exploring the full spectrum of macrophage activation. *Nat. Rev. Immunol.* **8,** 958–969 (2008).

2. Wynn, T. A., Chawla, A. & Pollard, J. W. Macrophage biology in development, homeostasis and disease. *Nature* **496,** 445–455 (2013).

3. Aderem, A. Phagocytosis and the Inflammatory Response. *J. Infect. Dis.* **187,** S340–S345 (2003).

4. Murray, R. Z. & Stow, J. L. Cytokine secretion in macrophages: SNAREs, Rabs, and membrane trafficking. *Front. Immunol.* **5,** 1–9 (2014).

5. Mantovani, A., Sica, A. & Locati, M. New vistas on macrophage differentiation and activation. *Eur. J. Immunol.* **37,** 14–16 (2007).

6. Chow, A., Brown, B. D. & Merad, M. Studying the mononuclear phagocyte system in the molecular age. *Nat. Rev. Immunol.* **11,** 788–798 (2011).

7. Gordon, S. & Taylor, P. R. Monocyte and macrophage heterogeneity. *Nat. Rev. Immunol.* **5,** 953–964 (2005).

8. Gautiar, E. L. *et al.* Gene-expression profiles and transcriptional regulatory pathways that underlie the identity and diversity of mouse tissue macrophages. *Nat. Immunol.* **13,** 1118–1128 (2012).

9. Taylor, P. R. *et al.* Macrophage Receptors and Immune Recognition. *Annu. Rev. Immunol.* **23,** 901–944 (2005).

10. Martinez, F. O. & Gordon, S. The M1 and M2 paradigm of macrophage activation: time for reassessment. *F1000Prime Rep.* **6,** 1–13 (2014).

11. Jablonski, K. A. *et al.* Novel markers to delineate murine M1 and M2 macrophages. *PLoS One* **10,** 5–11 (2015).

12. Gabet, Y. *et al.* Krox20/EGR2 deficiency accelerates cell growth and differentiation in the monocytic lineage and decreases bone mass. *Blood* **116,** 3964–3971 (2010).

13. Fleetwood, A. J., Lawrence, T., Hamilton, J. A. & Cook, A. D. Granulocyte-Macrophage Colony-Stimulating Factor (CSF) and Macrophage CSF-Dependent Macrophage Phenotypes Display Differences in Cytokine Profiles and Transcription Factor Activities: Implications for CSF Blockade in Inflammation. *J. Immunol.* **178,** 5245–5252 (2007).

14. Akira, S. & Takeda, K. Toll-like receptor signalling. *Nat. Rev. Immunol.* **4,** 499–511 (2004).

15. Tobias, P. S., Soldau, K. & Ulevitch, R. J. ISOLATION OF A LIPOPOLYSACCHARIDE-BINDING ACUTE PHASE REACTANT FROM RABBIT SERUM. *J. Exp. Med.* **164,** 777–793 (1986).

16. Wright, S. D. *et al.* CD14 , a Receptor for Complexes of Lipopolysaccharide (LPS) and LPS Binding Protein. *Science (80-.).* **249,** 1431–1433 (1990).

17. Lu, Y. C., Yeh, W. C. & Ohashi, P. S. LPS/TLR4 signal transduction pathway. *Cytokine* **42,** 145–151 (2008).

18. Ohnishi, H. *et al.* Structural basis for the multiple interactions of the MyD88 TIR domain in TLR4 signaling. *Proc. Natl. Acad. Sci.* **106,** 10260–10265 (2009).

19. Yamamoto, Y. & Gaynor, R. B. IκB kinases: Key regulators of the NF-κB pathway. *Trends Biochem. Sci.* **29,** 72–79 (2004).

20. Viganò, E. & Mortellaro, A. Caspase-11: The driving factor for noncanonical inflammasomes. *Eur. J. Immunol.* **43,** 2240–2245 (2013).

21. Pellegrini, C., Antonioli, L., Lopez-Castejon, G., Blandizzi, C. & Fornai, M. Canonical and non-canonical activation of NLRP3 inflammasome at the crossroad between immune tolerance and intestinal inflammation. *Front. Immunol.* **8,** (2017).

22. Dinarello, C. A. Immunological and Inflammatory Functions of the Interleukin-1 Family. *Annu. Rev. Immunol.* **27,** 519–550 (2009).

23. Dinarello, C. A. Overview of the interleukin-1 family of ligands and receptors. *Semin. Immunol.* **25,** 389–393 (2013).

24. Mailer, R. K. W. *et al.* IL-1β promotes Th17 differentiation by inducing alternative splicing of FOXP3. *Sci. Rep.* **5,** 1–9 (2015).

25. Xu, B. *et al.* Interleukin-1β induces autophagy by affecting calcium homeostasis and trypsinogen activation in pancreatic acinar cells. *Int. J. Clin. Exp. Pathol.* **7,** 3620–3631 (2014).

26. Wang, Q., Zhang, H., Zhao, B. & Fei, H. IL-1beta caused pancreatic beta-cells apoptosis is mediated in part by endoplasmic reticulum stress via the induction of endoplasmic reticulum Ca2+ release through the c-Jun N-terminal kinase pathway. *Mol. Cell. Biochem.* **324,** 183–90 (2009).

27. Nambu, A., Nakae, S. & Iwakura, Y. IL-1β, but not IL-1α, is required for antigen-specific T cell activation and the induction of local inflammation in the delayed-type hypersensitivity responses. *Int. Immunol.* **18,** 701–712 (2006).

28. Kozak, W. *et al.* IL-6 and IL-1 beta in fever. Studies using cytokine-deficient (knockout) mice. *Ann. N. Y. Acad. Sci.* **856,** 33–47 (1998).

29. Ciccarelli, F., Martinis, M. & Ginaldi, L. An Update on Autoinflammatory Diseases. *Curr. Med. Chem.* **21,** 261–269 (2013).

30. Libby, P. Interleukin-1 Beta as a Target for Atherosclerosis Therapy: Biological Basis of CANTOS and Beyond. *J. Am. Coll. Cardiol.* **70,** 2278–2289 (2017).

31. Maedler, K., Dharmadhikari, G., Schumann, D. M. & Storling, J. Interleukin-1 beta targeted therapy for type 2 diabetes. *Expert Opin. Biol. Ther* **9,** 1177–1188 (2009).

32. Klimek, M. E. B., Sali, A., Rayavarapu, S. & Nagaraju, K. Effect of the IL-1 Receptor Antagonist Kineret® on Disease Phenotype in mdx Mice. *PLoS One* **11,** 1–12 (2016).

33. Maston, G. A., Evans, S. K. & Green, M. R. Transcriptional Regulatory Elements in the Human Genome. *Annu. Rev. Genomics Hum. Genet.* **7,** 29–59 (2006).

34. Danino, Y. M., Even, D., Ideses, D. & Juven-Gershon, T. The core promoter: At the heart of gene expression. *Biochim. Biophys. Acta - Gene Regul. Mech.* **1849,** 1116–1131 (2015).

35. Andersson, R., Sandelin, A. & Danko, C. G. A unified architecture of transcriptional regulatory elements. *Trends Genet.* **31,** 426–433 (2015).

36. Heintzman, N. D. & Ren, B. Finding distal regulatory elements in the human genome. *Curr. Opin. Genet. Dev.* **19,** 541–549 (2009).

37. Lam, M. T. Y., Li, W., Rosenfeld, M. G. & Glass, C. K. Enhancer RNAs and regulated transcriptional programs. *Trends Biochem. Sci.* **39,** 170–182 (2014).

38. Wallace, J. A. & Felsenfeld, G. We gather together: insulators and genome organization. *Curr. Opin. Genet. Dev.* **17,** 400–407 (2007).

39. Gibney, E. R. & Nolan, C. M. Epigenetics and gene expression. *Heredity (Edinb).* **105,** 4–13 (2010).

40. Thurman, R. E. *et al.* The accessible chromatin landscape of the human genome. *Nature* **489,** 75–82 (2012).

41. Pfeifer, G. P., Kadam, S. & Jin, S.-G. 5-Hydroxymethylcytosine and Its Potential Roles in Development and Cancer. *Epigenetics Chromatin* **6,** 10 (2013).

42. Calo, E. & Wysocka, J. Modification of Enhancer Chromatin: What, How, and Why? *Mol. Cell* **49,** 825–837 (2013).

43. Hashimoto, K., Oreffo, R. O. C., Gibson, M. B., Goldring, M. B. & Roach, H. I. DNA De-methylation at Specific CpG Sites in the IL1B Promoter in Response to Inflammatory Cytokines in Human Articular Chondrocytes. *Arthritis Rheum*. **60**, 3303-3313 (2009).

44. Bae, M. G., Kim, J. Y. & Choi, J. K. Frequent hypermethylation of orphan CpG islands with enhancer activity in cancer. BMC Med. *Genomics* **9**, (2016).

45. Sharifi-Zarchi, A. et al. DNA methylation regulates discrimination of enhancers from promoters through a H3K4me1-H3K4me3 seesaw mechanism. BMC *Genomics* **18**, 1–21 (2017).

46. Charlet, J. *et al*. "Bivalent" regions of cytosine methylation and H3K27 acetylation suggest an active role for DNA methylation at enhancers. *Mol. Cell.* **62**, 422-431 (2016).

47. Schmidl, C. et al. Lineage-specific DNA methylation in T cells correlates with histone methylation and enhancer activity. *Genome Res.* **19**, 1165–1174 (2009).

48. Kohli, R. M. & Zhang, Y. TET enzymes, TDG and the dynamics of DNA demethylation. *Nature* **502,** 472–479 (2013).

49. Yu, M. *et al.* Base-resolution analysis of 5-hydroxymethylcytosine in the mammalian genome. *Cell* **149,** 1368–1380 (2012).

50. Kolendowski, B. *et al*. Genome-wide analysis reveals a role for TDG in estrogen receptor-mediated enhancer RNA transcription and 3-dimensional reorganization. *Epigenetics and Chromatin* **11**, 1–19 (2018).

51. Jin, B., Li, Y. & Robertson, K. D. DNA methylation: Superior or subordinate in the epigenetic hierarchy? *Genes and Cancer* **2,** 607–617 (2011).

52. Ito, S. *et al*. Tet proteins can convert 5-methylcytosine to 5-formylcytosine and 5-carboxylcytosine. *Science* (80-.). **333**, 1300–1303 (2011).

53. Ramakrishnan, V. Histone Structure and the Organization of the Nucleosome. *Annu. Rev. Biophys. Biomol. Struct.* **26,** 83–112 (1997).

54. Fraser, J., Williamson, I., Bickmore, W. A. & Dostie, J. An Overview of Genome Organization and How We Got There: from FISH to Hi-C. *Microbiol. Mol. Biol. Rev.* **79,** 347–372 (2015).

55. Erler, J. *et al.* The Role of Histone Tails in the Nucleosome: A Computational Study. *Biophys. J.* **107,** 2911–2922 (2014).

56. Bannister, A. J. & Kouzarides, T. Regulation of chromatin by histone modifications. *Cell Res.* **21,** 381–395 (2011).

57. Zhang, Y. & Reinberg, D. Transcription regulation by histone methylation: Interplay between different covalent modifications of the core histone tails. *Genes Dev.* **15,** 2343–2360 (2001).

58. Upadhyay, A. K. & Cheng, X. Dynamics of histone lysine methylation: Structures of methyl writers and erasers. *Prog. Drug Res.* **67,** 107–124 (2011).

59. Zhang, X., Wen, H. & Shi, X. Lysine methylation: beyond histones. *Acta Biochim Biophys Sin* **44,** 14–27 (2012).

60. Heintzman, N. D. *et al.* Histone modifications at human enhancers reflect global cell-type-specific gene expression. *Nature* **459,** 108–112 (2009).

61. Djebali, S. *et al.* Landscape of transcription in human cells. *Nature* **489,** 101–108 (2012).

62. Eberharter, A. & Becker, P. B. Histone acetylation: A switch between repressive and permissive chromatin. Second in review on chromatin dynamics. *EMBO Rep.* **3,** 224–229 (2002).

63. Javaid, N. & Choi, S. Acetylation- and methylation-related epigenetic proteins in the context of their targets. *Genes (Basel).* **8,** (2017).

64. Carrozza, M. J., Utley, R. T., Workman, J. L. & Côté, J. The diverse functions of histone acetyltransferase complexes. *Trends Genet.* **19,** 321–329 (2003).

65. Ogryzko, V. V., Schiltz, R. L., Russanova, V., Howard, B. H. & Nakatani, Y. The transcriptional coactivators p300 and CBP are histone acetyltransferases. *Cell* **87,** 953–959 (1996).

66. Tie, F. *et al.* CBP-mediated acetylation of histone H3 lysine 27 antagonizes Drosophila Polycomb silencing. *Development* **136,** 3131–3141 (2009).

67. Pasini, D. *et al.* Characterization of an antagonistic switch between histone H3 lysine 27 methylation and acetylation in the transcriptional regulation of Polycomb group target genes. *Nucleic Acids Res.* **38,** 4958–4969 (2010).

68. Seto, E. & Yoshida, M. Erasers of histone acetylation: The histone deacetylase enzymes. *Cold Spring Harb. Perspect. Biol.* **6,** 1–26 (2014).

69. Fritz, A. *et al.* Chromosomes at Work: Organization of Chromosome Territories in the Interphase Nucleus. *J Cell Biochem.* **117,** 9–19 (2017).

70. Dekker, J. & Heard, E. Structural and functional diversity of Topologically Associating Domains. *FEBS Lett.* **589,** 2877–2884 (2015).

71. Dixon, J. R. *et al.* Topological domains in mammalian genomes identified by analysis of chromatin interactions. *Nature* **485,** 376–379 (2012).

72. Rao, S. S. P. *et al.* A 3D map of the human genome at kilobase resolution reveals principles of chromatin looping. *Cell* **159,** 1665–1680 (2014).

73. Kim, T. K. *et al.* Widespread transcription at neuronal activity-regulated enhancers. *Nature* **465,** 182–187 (2010).

74. Marsman, J. & Horsfield, J. A. Long distance relationships: Enhancer-promoter communication and dynamic gene transcription. *Biochim. Biophys. Acta - Gene Regul. Mech.* **1819,** 1217–1227 (2012).

75. Xie, W. & Ren, B. Enhancing pluripotency and lineage specification. *Science (80-.).* **341,** 245–247 (2013).

76. Buecker, C. & Wysocka, J. Enhancers as information integration hubs in development: Lessons from genomics. *Trends Genet.* **28,** 276–284 (2012).

77. Denisenko, E. *et al.* Genome-wide profiling of transcribed enhancers during macrophage activation. *Epigenetics and Chromatin* **10,** 1–17 (2017).

78. Léveillé, N., Melo, C. A. & Agami, R. Enhancer-associated RNAs as therapeutic targets. *Expert Opin. Biol. Ther.* **15,** 723–734 (2015).

79. Li, W., Notani, D. & Rosenfeld, M. G. Enhancers as non-coding RNA transcription units: Recent insights and future perspectives. *Nat. Rev. Genet.* **17,** 207–223 (2016).

80. Li, W. *et al.* Functional roles of enhancer RNAs for oestrogen-dependent transcriptional activation. *Nature* **498,** 516–520 (2013).

81. Szerlong, H. J., Prenni, J. E., Nyborg, J. K. & Hansen, J. C. Activator-dependent p300 acetylation of chromatin in vitro: Enhancement of transcription by disruption of repressive nucleosome-nucleosome interactions. *J. Biol. Chem.* **285,** 31954–31964 (2010).

82. Creyghton, M. P. *et al.* Histone H3K27ac separates active from poised enhancers and predicts developmental state. *Proc. Natl. Acad. Sci.* **107,** 21931–21936 (2010).

83. Xi, H. *et al.* Identification and Characterization of Cell Type–Specific and Ubiquitous Chromatin Regulatory Structures in the Human Genome. *PLoS Genet.* **3,** e136 (2007).

84. Iglesias, A. R. *et al.* A unique chromatin signature uncovers early developmental enhancers in humans. *Nature* **470,** 279–283 (2011).

85. Zentner, G. E. *et al.* Epigenetic signatures distinguish multiple classes of enhancers with distinct cellular functions. *Genome Res.* **21,** 1273–1283 (2011).

86. Visel, A. *et al.* ChIP-seq accurately predicts tissue-specific activity of enhancers. *Nature* **457,** 854–858 (2009).

87. Jin, Q. *et al.* Distinct roles of GCN5/PCAF-mediated H3K9ac and CBP/p300-mediated H3K18/27ac in nuclear receptor transactivation. *EMBO J.* **30,** 249–262 (2011).

88. Moon, K. J. *et al.* The bromodomain protein Brd4 is a positive regulatory component of P-TEFb and stimulates RNA polymerase II-dependent transcription. *Mol. Cell* **19,** 523–534 (2005).

89. Dey, A., Chitsaz, F., Abbasi, A., Misteli, T. & Ozato, K. The double bromodomain protein Brd4 binds to acetylated chromatin during interphase and mitosis. *Proc. Natl. Acad. Sci.* **100,** 8758–8763 (2003).

90. Yang, Z. *et al.* Recruitment of P-TEFb for stimulation of transcriptional elongation by the bromodomain protein Brd4. *Mol. Cell* **19,** 535–545 (2005).

91. Kaikkonen, M. U. *et al.* Remodeling of the enhancer landscape during macrophage activation is coupled to enhancer transcription. *Mol. Cell* **51,** 310–325 (2013).

92. Plosky, B. S. ERNAs lure NELF from paused polymerases. *Mol. Cell* **56,** 3–4 (2014).

93. Bowman, E. A. & Kelly, W. G. RNA Polymerase II transcription elongation and Pol II CTD Ser2 phosphorylation. A tail of two kinases. *Nucleus* **5,** 224–236 (2014).

94. Andersson, R. *et al.* An atlas of active enhancers across human cell types and tissues. *Nature* **507,** 455–460 (2014).

95. Monticelli, S. & Natoli, G. Transcriptional determination and functional specificity of myeloid cells: Making sense of diversity. *Nat. Rev. Immunol.* **17,** 595–607 (2017).

96. Fisher, R. C. & Scott, E. W. Role of PU.1 in Hematopoiesis. *Stem Cells* **16,** 25–37 (1998).

97. Klemsz, M. J. *et al.* The macrophage and B cell-specific transcription factor PU.1 is related to the ets oncogene. *Cell* **61,** 113–124 (1990).

98. Lloberas, J., Soler, C. & Celada, A. The key role of PU.1/SPI-1 in B cells, myeloid cells and macrophages. *Immunol. Today* **20,** 184–189 (1999).

99. Nishiyama, C. *et al.* Functional analysis of PU.1 domains in monocyte-specific gene regulation. *FEBS Lett.* **561,** 63–68 (2004).

100. Klemsz, M. J. & Maki, R. a. Activation of transcription by PU.1 requires both acidic and glutamine domains. *Mol. Cell. Biol.* **16,** 390–397 (1996).

101. Fisher, R. C. *et al.* Normal myeloid development requires both the glutamine-rich transactivation domain and the PEST region of transcription factor PU.1 but not the potent acidic transactivation domain. *Mol. Cell. Biol.* **18,** 4347–57 (1998).

102. DeKoter, R. P. & Singh, H. Regulation of B lymphocyte and macrophage development by graded expression of PU.1. *Science (80-.).* **288,** 1439–1442 (2000).

103. Ghisletti, S. *et al.* Identification and Characterization of Enhancers Controlling the Inflammatory Gene Expression Program in Macrophages. *Immunity* **32,** 317–328 (2010).

104. Heinz, S. *et al.* Simple Combinations of Lineage-Determining Transcription Factors Prime cis-Regulatory Elements Required for Macrophage and B Cell Identities. *Mol. Cell* **38,** 576–589 (2010).

105. Monticelli, S. & Natoli, G. Transcriptional determination and functional specificity of myeloid cells: Making sense of diversity. *Nat. Rev. Immunol.* **17,** 595–607 (2017).

106. Gosselin, D. *et al.* Environment drives selection and function of enhancers controlling tissue-specific macrophage identities. *Cell.* **159,** 1327–1340 (2015).

107. Gupta, P., Gurudutta, G. U., Saluja, D. & Tripathi, R. P. PU.1 and partners: Regulation of haematopoietic stem cell fate in normal and malignant haematopoiesis. *J. Cell. Mol. Med.* **13,** 4349–4363 (2009).

108. Dahl, R. *et al.* Regulation of macrophage and neutrophil cell fates by the PU.1:C/EBPα ratio and granulocyte colony-stimulating factor. *Nat. Immunol.* **4,** 1029–1036 (2003).

109. Schaukowitch, K. *et al.* Enhancer RNA facilitates NELF release from immediate early genes. *Mol. Cell* **56,** 29–42 (2014).

110. Lai, F. *et al.* Activating RNAs associate with Mediator to enhance chromatin architecture and transcription. *Nature* **494,** 497–501 (2013).

111. Hsieh, C.-L. *et al.* Enhancer RNAs participate in androgen receptor-driven looping that selectively enhances gene activation. *Proc. Natl. Acad. Sci.* **111,** 7319–7324 (2014).

112. Yang, J. & Corces, V. G. Insulators, long-range interactions, and genome function. *Curr. Opin. Genet. Dev.* **22,** 86–92 (2012).

113. Hou, C., Zhao, H., Tanimoto, K. & Dean, A. CTCF-dependent enhancer-blocking by alternative chromatin loop formation. *Proc. Natl. Acad. Sci.* **105,** 20398–20403 (2008).

114. Kim, S., Yu, N. K. & Kaang, B. K. CTCF as a multifunctional protein in genome regulation and gene expression. *Exp. Mol. Med.* **47,** e166 (2015).

115. Lam, M. T. Y. *et al.* Rev-Erbs repress macrophage gene expression by inhibiting enhancer-directed transcription. *Nature* **498,** 511–514 (2013).

116. Krivega, I. & Dean, A. Enhancer and promoter interactions-long distance calls. *Curr. Opin. Genet. Dev.* **22,** 79–85 (2012).

117. Holwerda, S. & de Laat, W. Chromatin loops, gene positioning, and gene expression. *Front. Genet.* **3,** 1–13 (2012).

118. Peters, J. M., Tedeschi, A. & Schmitz, J. The cohesin complex and its roles in chromosome biology. *Genes Dev.* **22,** 3089–3114 (2008).

119. Kagey, M. H. *et al.* Mediator and cohesin connect gene expression and chromatin architecture. *Nature* **467,** 430–435 (2010).

120. Wit, E. De & Laat, W. De. A decade of 3C technologies: insights into nuclear organization. *Genes Dev.* **26,** 11–24 (2012).

121. Dekker, J., Rippe, K., Dekker, M. & Kleckner, N. Capturing chromosome conformation. *Science.* **295,** 1306–1311 (2002).

122. Hagege, H. *et al.* Quantitative analysis of chromosome conformation capture assays (3C-qPCR). *Nat. Protoc.* **2,** 1722–1733 (2007).

123. Simonis, M., Kooren, J. & de Laat, W. An evaluation of 3C-based methods to capture DNA interactions. *Nat. Methods.* **4,** 895–901 (2007).

124. Pinheiro, L. B. *et al.* Evaluation of a droplet digital polymerase chain reaction format for DNA copy number quantification. *Anal. Chem.* **84,** 1003–1011 (2012).

125. Taylor, S. C., Laperriere, G. & Germain, H. Droplet Digital PCR versus qPCR for gene expression analysis with low abundant targets: From variable nonsense to publication quality data. *Sci. Rep.* **7,** 1–8 (2017).

126. Mazaika, E. & Homsy, J. Digital Droplet PCR: CNV Analysis and Other Applications. *Curr. Protoc. Hum. Genet.* **82,** 7.24.1-7.24.13 (2014).

127. Orom, U. A. Enhancer RNAs. *Methods Mol Biol* **1468,** 11–18 (2017).

128. Bartkuhn, M. & Renkawitz, R. Long range chromatin interactions involved in gene regulation. *Biochim. Biophys. Acta - Mol. Cell Res.* **1783,** 2161–2166 (2008).

129. Mora, A., Sandve, G. K., Gabrielsen, O. S. & Eskeland, R. In the loop: promoter–enhancer interactions and bioinformatics. *Brief. Bioinform.* **17**, bbv097 (2015).

130. Krivega, I. & Dean, A. Enhancer and promoter interactions-long distance calls. *Curr. Opin. Genet. Dev.* **22**, 79–85 (2012).

131. Kadauke, S. & Blobel, G. A. Chromatin loops in gene regulation. *Biochim. Biophys. Acta - Gene Regul. Mech.* **1789,** 17–25 (2009).

132. Orom, U. A. & Shiekhattar, R. Long noncoding RNAs usher in a new era in the biology of enhancers. *Cell* **154,** 1190–1193 (2013).

133. Duan, Z. *et al.* A genome-wide 3C-method for characterizing the three-dimensional architectures of genomes. *Methods* **58,** 277–288 (2013).

134. Naumova, N., Smith, E. M., Zhan, Y., & Dekker, J. Analysis of long-range chromatin interactions using Chromosome Conformation Capture. *Methods* **58,** 1–27 (2012).

135. Pongubala, J. M. & Atchison, M. L. PU.1 can participate in an active enhancer complex without its transcriptional activation domain. *Proc. Natl. Acad. Sci. U. S. A.* **94,** 127–132 (1997).

136. Rahman, S. *et al.* Single-cell profiling reveals that eRNA accumulation at enhancer-promoter loops is not required to sustain transcription. *Nucleic Acids Res.* **45,** 3017–3030 (2016).

137. Arner. E. *et al.* Transcribed enhancers lead waves of coordinated transcription in transitioning mammalian cells. *Science (80-.).* **347,** 101–1014 (2015).

138. de Santa, F. *et al.* A large fraction of extragenic RNA Pol II transcription sites overlap enhancers. *PLoS Biol.* **8,** 1–17 (2010).

139. Kim, Y. W., Lee, S., Yun, J. & Kim, A. Chromatin looping and eRNA transcription precede the transcriptional activation of gene in the β-globin locus. *Biosci. Rep.* **35,** 1–8 (2015).

140. Pnueli, L., Rudnizky, S., Yosefzon, Y. & Melamed, P. RNA transcribed from a distal enhancer is required for activating the chromatin at the promoter of the gonadotropin α-subunit gene. *Proc. Natl. Acad. Sci.* **112,** 4369–4374 (2015).

141. Mousavi, K. *et al.* ERNAs Promote Transcription by Establishing Chromatin Accessibility at Defined Genomic Loci. *Mol. Cell* **51,** 606–617 (2013).

142. Ron, G., Globerson, Y., Moran, D. & Kaplan, T. Promoter-enhancer interactions identified from Hi-C data using probabilistic models and hierarchical topological domains. *Nat. Commun.* **8,** 1–12 (2017).

143. Nolis, I. K. *et al.* Transcription factors mediate long-range enhancer-promoter interactions. *Proc. Natl. Acad. Sci.* **106,** 20222–20227 (2009).

144. Adamik, J. *et al.* Distinct Mechanisms for Induction and Tolerance Regulate the Immediate Early Genes Encoding Interleukin 1β and Tumor Necrosis Factor α. *PLoS One* **8,** e70622 (2013).

145. Aktories, K. *et al.* Epigenetic Regulation of Lymphocyte Development. *Current Topics in Microbiology and Immunology Series Editors*. **386,** (2012).

146. Iwafuchi-Doi, M. & Zaret, K. S. Pioneer transcription factors in cell reprogramming. *Genes Dev.* **28,** 2679–2692 (2014).

147. Feng, R. *et al.* PU.1 and C/EBPα/β convert fibroblasts into macrophage-like cells. *Proc. Natl. Acad. Sci. U. S. A.* **105,** 6057–6062 (2008).

148. Link, V. M., Gosselin, D. & Glass, C. K. Mechanisms underlying the selection and function of macrophage-specific enhancers. *Cold Spring Harb Symp Quant Biol.* **80,** 213–221 (2015).

149. Rojo, R., Pridans, C., Langlais, D. & Hume, D. A. Transcriptional mechanisms that control expression of the macrophage colony-stimulating factor receptor locus. *Clin. Sci.* **131,** 2161–2182 (2017).

150. Staber, P. B. *et al.* Sustained PU.1 Levels Balance Cell-Cycle Regulators to Prevent Exhaustion of Adult Hematopoietic Stem Cells. *Mol Cell* **49,** 934–946 (2013).

151. Friedman, A. D. Transcriptional control of granulocyte and monocyte development. *Oncogene* **26,** 6816–6828 (2007).

152. Yeamans, C. *et al.* C/EBPα binds and activates the PU.1 distal enhancer to induce monocyte lineage commitment. *Blood* **110,** 3136–3142 (2007).

153. Yamamoto, H. *et al.* Physical and functional interactions between the transcription factor PU.1 and the coactivator CBP. *Oncogene* **18,** 1495–1501 (1999).

154. Listman, J. A. *et al.* Conserved ETS Domain Arginines Mediate DNA Binding, Nuclear Localization, and a Novel Mode of bZIP Interaction. *J. Biol. Chem.* **280,** 41421–41428 (2005).

155. Whalen, S., Truty, R. M. & Pollard, K. S. Enhancer-promoter interactions are encoded by complex genomic signatures on looping chromatin. *Nature Genet* **48,** 488–496 (2016).

156. Roe, J. S., Mercan, F., Rivera, K., Pappin, D. J. & Vakoc, C. R. BET Bromodomain Inhibition Suppresses the Function of Hematopoietic Transcription Factors in Acute Myeloid Leukemia. *Mol. Cell* **58,** 1028–1039 (2015).

157. Carey, H. A. *et al.* Enhancer variants reveal a conserved transcription factor network governed by PU.1 during osteoclast differentiation. *Bone Res.* **6,** 1–12 (2018).

158. Hon, G. C. *et al.* 5mC oxidation by Tet2 modulates enhancer activity and timing of transcriptome reprogramming during differentiation. *Mol. Cell* **56,** 286–297 (2014).

159. Stroud, H., Feng, S., Morey Kinney, S., Pradhan, S. & Jacobsen, S. E. 5-Hydroxymethylcytosine is associated with enhancers and gene bodies in human embryonic stem cells. *Genome Biol.* **12,** (2011).

160. de la Rica, L. *et al.* PU.1 target genes undergo Tet2-coupled demethylation and DNMT3b-mediated methylation in monocyte-to-osteoclast differentiation. *Genome Biol.* **14,** 1–21 (2013).

161. Gondor, A., Rougier, C. & Ohlsson, R. High-resolution circular chromosome conformation capture assay. *Nat. Protoc.* **3,** 509–524 (2008).

162. Denker, A. & De Laat, W. The second decade of 3C technologies: Detailed insights into nuclear organization. *Genes Dev.* **30,** 1357–1382 (2016).

163. Stadhouders, R. *et al.* Multiplexed chromosome conformation capture sequencing for rapid genome-scale high-resolution detection of long-range chromatin interactions. *Nat. Protoc.* **3,** 303–313 (2013).

164. Yang, X. J. & Seto, E. HATs and HDACs: From structure, function and regulation to novel strategies for therapy and prevention. *Oncogene* **26,** 5310–5318 (2007).

165. Simone, C. & Peserico, A. Physical and functional HAT/HDAC interplay regulates protein acetylation balance. *J. Biomed. Biotechnol.* **2011,** (2011).

166. Toussirot, E. *et al.* Imbalance between HAT and HDAC Activities in the PBMCs of Patients with Ankylosing Spondylitis or Rheumatoid Arthritis and Influence of HDAC Inhibitors on TNF Alpha Production. *PLoS One* **8,** 1–10 (2013).

167. Eberharter, A. & Becker, P. B. Histone acetylation: A switch between repressive and permissive chromatin. Second in review on chromatin dynamics. *EMBO Rep.* **3,** 224–229 (2002).

168. Frank, C. L., Manandhar, D., Gordân, R. & Crawford, G. E. HDAC inhibitors cause site-specific chromatin remodeling at PU.1-bound enhancers in K562 cells. *Epigenetics and Chromatin* **9,** 1–17 (2016).

169. Ha, S. D., Reid, C., Meshkibaf, S. & Kim, S. O. Inhibition of interleukin 1 β (IL-1 β) expression by anthrax Lethal Toxin (LeTx) is reversed by histone deacetylase 8 (HDAC8) inhibition in murine macrophages. *J. Biol. Chem.* **291,** 8745–8755 (2016).

170. Gordon, S. & Martinez-Pomares, L. Physiological roles of macrophages. *Pflugers Arch. Eur. J. Physiol.* **469,** 365–374 (2017).

171. Kolattukudy, P., Sirakova, T. & Kapoor, N. The critical role of MCPIP in the chameleon's response to the microenvironment. *Macrophage* **2,** 2–5 (2015).

172. Mages, J., Dietrich, H. & Lang, R. A genome-wide analysis of LPS tolerance in macrophages. *Immunobiology* **212,** 723–737 (2008).

173. Foster, S. L., Hargreaves, D. C. & Medzhitov, R. Gene-specific control of inflammation by TLR-induced chromatin modifications. *Nature* **447,** 972–978 (2007).

174. Hoeksema, M. A. & de Winther, M. P. J. Epigenetic Regulation of Monocyte and Macrophage Function. *Antioxid. Redox Signal.* **25,** 758–774 (2016).

175. Martins, A. J., Spanton, S., Sheikh, H. I. & Kim, S. O. The anti-inflammatory role of granulocyte colony-stimulating factor in macrophage-dendritic cell crosstalk after *Lactobacillus rhamnosus* GR-1 exposure. *J. Leukoc. Biol.* **89,** 907–915 (2011).

176. Liu, F., Wu, H. Y., Wesselschmidt, R., Kornaga, T. & Link, D. C. Impaired production and increased apoptosis of neutrophils in granulocyte colony-stimulating factor receptor-deficient mice. *Immunity* **5,** 491–501 (1996).

177. Meshkibaf, S., Martins, A. J., Henry, G. T. & Kim, S. O. Protective role of G-CSF in dextran sulfate sodium-induced acute colitis through generating gut-homing macrophages. *Cytokine* **78,** 69–78 (2016).

178. Saeed, S. *et al.* Epigenetic programming of monocyte-to-macrophage differentiation and trained innate immunity. *Science (80-.).* **345,** (2014).

179. Netea, M. G. *et al.* Trained immunity: a program of innate immune memory in health and disease. *Science.* **352,** 1–23 (2017).

180. Quintin, J. *et al.* Candida albicans Infection Affords Protection against Reinfection via Functional Reprogramming of Monocytes. *Cell Host Microbe.* **12,** 1–15 (2012).

Appendices

Appendix A: LPS-stimulation induces activation of MAPKs in wild-type and PU.1-, C/EBPα-overexpressed B16-BL6 cells. Expression levels of phospho-p38, phospho-ERK, and phospho-IκB in wild-type and PU.1-, C/EBPα-overexpressed (transfected 0.7 μg of each plasmid with Polyjet for 48 hours) B16-BL6 cells untreated or treated with LPS (100 ng/mL) for 1, 2, or 3 hours were analyzed by Western blots. B-actin was used for loading controls. **Data in Appendix A were generated by Dr. Soon-Duck Ha.**

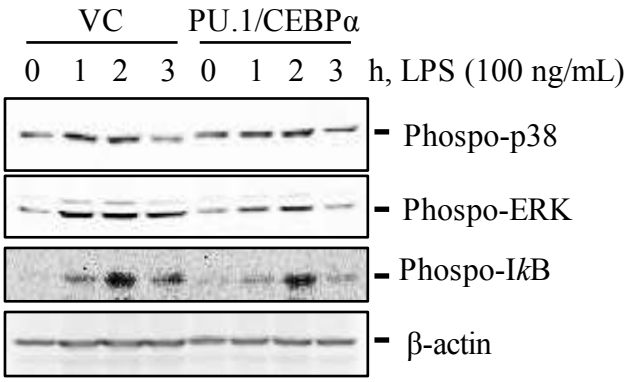
VC
PU.1/CEBPα
0 1 2 3 0 1 2 3 h, LPS (100 ng/mL)
Phospo-p38
Phospo-ERK
Phospo-IkB
β-actin

Appendix B: 4C analysis of inter- and intra-chromosomal interactions between the IL-1β promoter and potential enhancers scattered in the genome. A) Circos plot displays physical association of the IL-1β promoter with enhancers localized in different chromosomes of activated macrophages. LPS-stimulated RAW264.7 macrophages were harvested and crosslinked with formaldehyde. Two cycles of restriction enzyme digestion and ligation were performed in 4C. The extracted DNA was sequenced with Illumina sequencing. B) Computational analysis of the raw sequencing data also generated a spider plot to display the intra-chromosomal interactions detected in activated macrophages. **Data in Appendix B were generated by Dr. Soon-Duck Ha and Jeremy Wong.**

A)

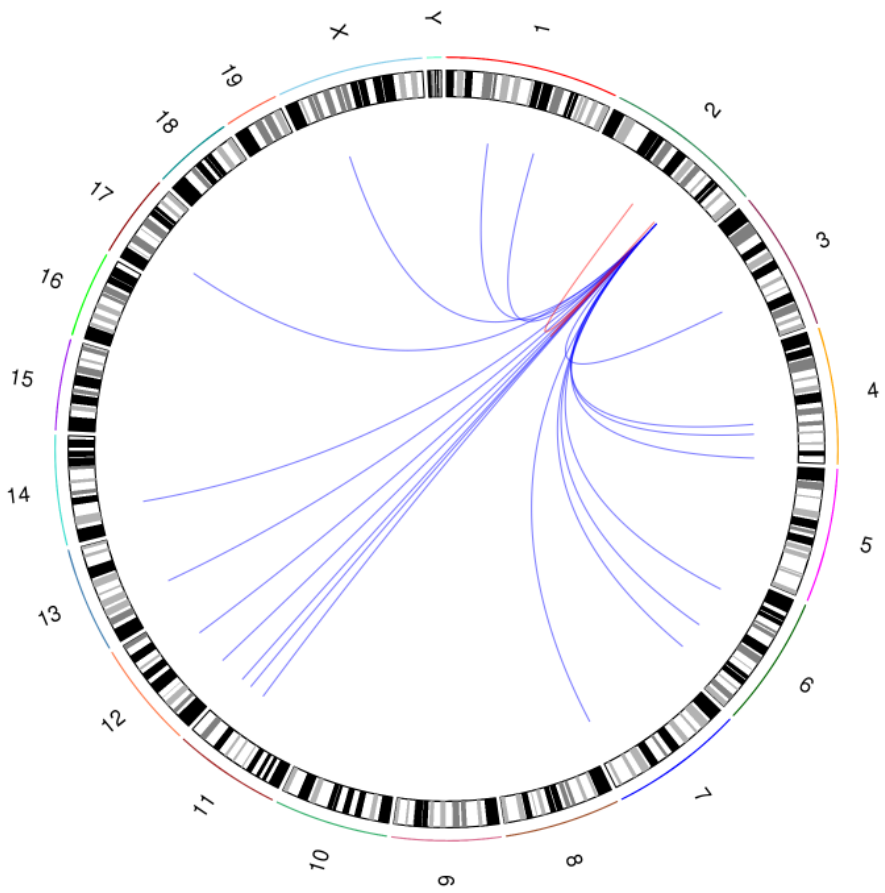
X
Y
1
2
3
4
5
6
7
8
9
10
11
12
13
14
15
16
17
18
19

B)

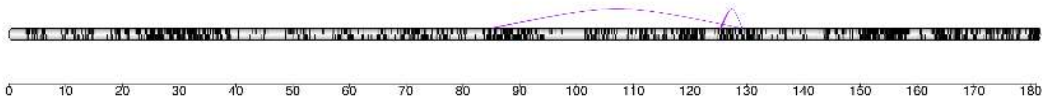
0
10
20
30
40
50
60
70
80
90
100
110
120
130
140
150
160
170
180

Curriculum Vitae

Name: Woohyun Cho

Post-secondary Education and Degrees:
University of Toronto
Toronto, Ontario, Canada
2010-2015 Honours B.Sc. in Immunology and Human Biology

The University of Western Ontario
London, Ontario, Canada
2016-2018 M.Sc. Microbiology and Immunology

Honours and Awards: Schulich Graduate & Western Graduate Research Scholarships 2016-2018

Abstracts:

Cho, W., Ha, S.D. & Kim, S. O. (Mar, 2018). Role of PU.1 and C/EBPα in Remodeling the Interleukin (IL)-1β Enhancer-Promoter Interaction, Chromatin Architecture and Chromosome Organization, Whistler, BC.

Cho, W., Ha, S.D. & Kim, S. O. (Oct, 2017). Characterization of interleukin (IL)-1β regulatory elements and chromatin conformation in murine macrophage activation, Infection and Immunity Research Forum (IIRF), London, ON.

Publications:

Ha, S. D., Cho, W. & Kim, S. O. HDAC8 prevents anthrax lethal toxin-induced cell cycle arrest through silencing PTEN in human monocytic THP-1 cells. *Toxins (Basel)*. **9,** 1–15 (2017).

Tam, L. E., Cho, W., Wang, B. Y. & De Souza, G. Effect of Bleaching Treatment on Fatigue Resistance and Flexural Strength of Bovine Dentin. *J. Esthet. Restor. Dent.* **27,** 374–382 (2015).